Australian Government

Wine Australia

THE UNIVERSITY of ADELAIDE

# Plant sensor-based precision irrigation for improved vineyard water use efficiency, grape and wine composition and quality, and vineyard profitability



FINAL REPORT TO WINE AUSTRALIA

Project Number: **UA 1803-1.3**

Principal Investigator: **Dr Vinay Pagay**

Research Organisation: **The University of Adelaide**

Date: **August 2022**

# TABLE OF CONTENTS


**ABSTRACT** ..... **4**

**1 EXECUTIVE SUMMARY** ..... **5**

**2 BACKGROUND** ..... **7**

**3 PROJECT AIMS** ..... **9**

**4 MATERIALS AND METHODS** ..... **10**

4.1 DESIGN OF IRRIGATION TRIALS ..... 10
*4.1.1 Location* ..... *10*
*4.1.2 Experimental design* ..... *11*
4.2 SCIENTIFIC EQUIPMENT AND SENSORS ..... 12
*4.2.1 Direct, proximal, and continuous sensors* ..... *12*
*4.2.2 Remote sensing equipment* ..... *16*
*4.2.3 Thresholds for irrigation scheduling* ..... *20*
4.3 DATA COLLECTION TIME POINTS ..... 20
4.4 METHODOLOGY AND PROCESSING ..... 21
*4.4.1 Ground data methodology and processing* ..... *21*
*4.4.2 Harvest, yield components, and pruning* ..... *21*
*4.4.3 Winemaking* ..... *21*
*4.4.4 Berry, juice and wine chemical analyses* ..... *22*
*4.4.5 Remote sensing data methodology and processing* ..... *22*
*4.4.6 Financial Analysis* ..... *27*
*4.4.7 Vineyard Irrigation Survey* ..... *27*

**5 RESULTS AND DISCUSSION** ..... **28**

5.1 SEASONAL IRRIGATION ..... 28
5.2 SOIL MOISTURE AND VINE PERFORMANCE MEASURED VIA PROXIMAL SENSING ..... 28
*5.2.1 Seasonal soil moisture* ..... *28*
*5.2.2 Seasonal light interception and vine vigour (Leaf area index and porosity)* ..... *32*
*5.2.3 Seasonal evapotranspiration ($ET_0$) and crop coefficient ($K_c$)* ..... *37*
*5.2.4 Seasonal plant water status and stomatal conductance* ..... *40*
*5.2.5 Seasonal net photosynthesis and intrinsic water use efficiency* ..... *44*
5.3 CONTINUOUS SENSOR-BASED DATA ..... 49
5.4 REMOTELY-SENSED CANOPY PERFORMANCE ..... 52
*5.4.1 Correlation analysis* ..... *52*
*5.4.2 High resolution prediction of soil and vine water status* ..... *52*
*5.4.3 High resolution prediction of vine crop coefficient* ..... *55*
*5.4.4 High resolution prediction of canopy gas exchange* ..... *57*
5.5 YIELD COMPONENTS AND PRUNING WEIGHTS ..... 60
5.6 WATER USE EFFICIENCY ..... 64
*5.6.1 Crop water use efficiency* ..... *64*
*5.6.2 Berry carbon isotopes* ..... *66*
5.7 BERRY AND JUICE COMPOSITION ..... 67
5.8 WINE COMPOSITION ..... 72
5.9 FINANCIAL ANALYSIS ..... 74
*5.9.1 Cabernet Sauvignon – Terra rossa* ..... *76*
*5.9.2 Cabernet Sauvignon – Rendzina* ..... *78*
*5.9.3 Shiraz – Terra rossa* ..... *79*
5.10 IRRIGATION PRACTICES SURVEY ..... 80

**6 OTHER RELATED OUTPUTS** ..... **80**

**7 CONCLUDING REMARKS ..... 81**

**8 ACKNOWLEDGEMENTS ..... 81**

**9 REFERENCES ..... 82**

**10 APPENDIX: LIMESTONE COAST VINEYARD IRRIGATION SURVEY ..... 84**

## Abstract

Prudent water management in Australian vineyards has become increasingly important in light of current energy market prices, potential oversupply of grapes and wine leading to low farm gate prices paid for grapes, as well as inefficiencies in ageing irrigation infrastructure in many vineyards. Increasing the efficiency of irrigation water use to maximise yield and/or quality is one strategy to address some of these issues, and can be done by precise monitoring of soil and vine moisture levels, and applying irrigation based on cultivar-specific thresholds relevant to each metric based on phenological stage. We evaluated the benefits associated with implementing irrigation schedules on Cabernet Sauvignon and Shiraz grapevines in Coonawarra based on non-data-driven (CONV) and data-driven metrics including crop evapotranspiration ($ET_c$), soil moisture thresholds (SWS), and two plant-based water status thresholds (PWS/PWS1, PWS2). SWS and PWS strategies were informed by remote monitoring of the respective parameters using continuous moisture sensors. Our results indicated that using data-driven approaches was generally superior to non-data-driven methods, and that water use efficiency (WUE = yield/irrigation) could be enhanced, particularly when using metrics that were associated with the vine itself i.e. ETc and PWS. Despite inter-annual variations in the results that were attributed to seasonal weather conditions, we observed three- to six-fold increases in WUE based on data-driven methods compared to the conventional (non-data driven) method in Cabernet Sauvignon, and a doubling of WUE in Shiraz. Comparing various irrigation schedules, PWS1, based on proximal thermal sensors, had the highest WUE in Shiraz during the final season, while ET had the highest WUE in Cabernet Sauvignon in the same season. The PWS group consistently outperformed the conventional group every season. Despite reductions in irrigation in the data-driven treatments, no significant impacts to yield or grape composition parameters were observed. High resolution remote sensing was utilised to generate spatial and temporal information of all three-vineyard blocks; these data were used to develop predictive models of soil and vine water status, gas exchange and crop coefficients. Financial (cost-benefit) analysis revealed that the economic water productivity (gross margin $ per ML of water applied) for Cabernet Sauvignon was four-fold higher in the ET and PWS treatments and CONV was highest in Shiraz due to the high yields obtained in the final season. Finally, an irrigation practices survey conducted in 2021 across the Limestone Coast region revealed that over 70% of growers used experience or historical schedules to irrigate and only 6% of growers used plant-based sensors to inform their irrigation decisions. The greatest barriers to adoption of new technology for irrigation decision-making were a lack of understanding of their value and high cost. This study has demonstrated the potential of several direct, proximal and remote irrigation sensors and tools to determine irrigation schedules in order to increase water use efficiency in grapevine through precision irrigation.

# 1 Executive summary

The overarching objective of this project was to assess the value of plant-sensor-based precision irrigation on grapevine performance, water use efficiency and grape and wine composition of Cabernet Sauvignon (CAS) and Shiraz (SHI) grapevines. The project was conducted in the Coonawarra viticultural region of South Australia. In the first three seasons, five irrigation strategies were investigated: conventional or grower-driven approach (CONV), 2x CONV for 'well-watered' vines (CONV+), and three data-driven (sensor-based) irrigation strategies: vine water status based on proximal thermal sensors (PWS/PWS1), soil water status (SWS), and crop evapotranspiration ($ET_c$). In the fourth season (2021/22), an additional plant sensor-based irrigation strategy based on continuous measurement of trunk water potential (PWS2) was also evaluated. Additionally, UAV-based remote sensing was used to obtain high resolution (vine-level) estimates of grapevine crop coefficients, soil and water status, and canopy gas exchange.

For measuring plant performance and water status, various instruments for direct, proximal and remote sensing were used at key phenological stages of grapevine development. The evidence- or sensor-based irrigation strategies had a clear advantage of saving irrigation water in CAS and SHI grown in Terra rossa soil and Rendzina soils (SHI in Terra rossa only). For instance, in 2020/21 season (S3) in CAS (in lighter Terra rossa soil), ET- and PWS-treated vines received only 38% and 67% of the total irrigation of CONV+ treated vines. However, despite significantly lower soil and plant water status, ET- and PWS-treated vines showed similar net carbon assimilation ($A_N$), stomatal conductance ($g_s$), leaf intrinsic water use efficiency ($WUE_i$), yield, and berry anthocyanin and phenolics concentrations relative to CONV+ vines. Reduction of irrigation by 38% in SWS treatments led to significant reductions in soil and plant water status, $g_s$ and $A_N$ however, vines maintained similar $WUE_i$ relative to CONV+ treatment. The reduction of irrigation did not result in a yield penalty, nor reduced berry and juice composition in the CAS vines on Terra rossa soils.

In the 2020/21 season in CAS on heavier Rendzina soils, sensor-based irrigation reduced water supply by 30-40% relative to CONV+. Despite significantly lower plant water status and $g_s$, all vines maintained similar $WUE_i$ to CONV+. ET and PWS treatments did not result in yield penalties, a positive result, however, yield was significantly reduced in the SWS treatment relative to CONV+ vines.

In SHI grapevines on Terra rossa soils, plant sensor-based irrigation (PWS) reduced irrigation by 40-60% compared to CONV+ treated vines. Even though reduced water supply significantly reduced plant water status and leaf gas exchange, PWS1, PWS2 and SWS treatments significantly improved $WUE_i$ relative to CONV+ vines during 2021/22 season, without yield penalties or decreases in berry/juice composition parameters.

Overall, our results suggest that both ET- and plant sensor-based irrigation scheduling are superior approaches for high-quality grape/wine production for CAS, while in SHI, the plant sensor-based irrigation scheduling approach is superior in order to increase water use efficiency without yield or quality penalties.

Using high-resolution (UAV-based) thermal and multispectral remote sensing in conjunction with machine learning modelling, we obtained spatial (vine-level) and temporal (phenology-specific) information on soil moisture ($\Psi_{pd}$) and vine physiological parameters ($\Psi_s$, $A_n$, $g_s$, $WUE_i$, $K_c$) for the entire vineyard block and beyond the trial sub-block. These predictive models can aid practitioners in implementing precision irrigation i.e. irrigating blocks at the sub-block level, based on water requirements as determined by the various sensors such as those evaluated in this project. The spatial maps can also be used to inform the placement of proximal or direct plant and soil sensors for improved decision-making at the sub-block level.

Financial analysis of the various data-driven options (PWS, SWS, ET) versus the non-data-driven option (CONV/CONV+) indicated that there was a strong dependence of gross margin and payback period on yield

and/or irrigation application rates. Hence, the ET (in CAS and SHI) and PWS (in SHI) treatments had the highest financial returns to the grower based on lower water application rates, as yields were similar across the different strategies. These differences would be even higher if growers had to pay for water, increasing the impetus for using sensors to inform irrigation decisions.

The project successfully met its objectives and delivered:

- a comprehensive evaluation of various irrigation scheduling methods available to grape growers that are based on subjective and objective assessments. Vine performance and fruit/wine level assessments were carried out for each irrigation regime.

- an evaluation of two new commercial crop water status sensors and determination of their thresholds to increase water use efficiency.

- a new high-resolution remote sensing platform for assessment of canopy performance, and spatial and temporal prediction of the same parameters.

- a financial analysis of the different irrigation scheduling strategies evaluated in this study.

- a comprehensive industry survey of current irrigation practices in the Limestone Coast.

- knowledge dissemination to the industry via seminars and scientific papers.

# 2 Background

As a perennial crop, grapevines (*Vitis vinifera* L.) are vulnerable to changing environmental conditions, both within a growing season and inter-annually. Predictions of climatic conditions across many Australian viticultural regions indicate that average growing season temperatures are likely to increase and precipitation is likely to decrease (Webb et al. 2007). In South Australia, the largest winegrape producing state in Australia (Wine Australia 2022), the annual mean maximum temperature is predicted to increase by 2.1 °C by 2050 while annual precipitation is predicted to decrease by between 6.6-15% by the same time (Green and Pannell, 2020). Superimposed on this climate background are extreme weather events such as heatwaves, which are predicted to increase in both frequency and severity, with the number of days per year above 40 °C projected to double by 2050 compared to the baseline period of 1981-2010. These conditions will result in higher rates of evapotranspiration (ET) with a consequent decrease in soil moisture and increase in soil salinity (Schultz and Stoll 2010). As grapevine phenology, grape yield, chemical composition and quality, and consequent wine quality are all intimately tied to the prevailing environmental conditions, the predicted shifts in climate across Australian viticultural regions will undoubtedly impact future winegrape production, grape/wine quality, and profitability (Webb and Jones, 2010). In this context, some vineyards within existing viticultural regions may become economically unviable (White et al., 2006), and regional cultivars and wine styles may become undesirable (Jones et al., 2005).

Several strategies exist to mitigate the negative impact of increasing temperatures and decreasing rainfall including soil management, irrigation, use of undervine and inter-row cover crops (Santos et al., 2020, Marks et al. 2022), canopy management practices (Santos et al., 2020), vineyard cooling strategies (Bayer et al., 2017; Pagay 2018), and use of heat- and drought-tolerant cultivars and rootstocks (Fraga et al. 2012). In semi-arid regions such as the Murray-Darling Basin, supplemental irrigation (i.e. irrigation in excess of rainfall; henceforth termed 'irrigation') is not only essential, but is a powerful tool to manipulate canopy development and vigour, yield, fruit composition and wine quality. Under heatwave conditions, which are becoming increasingly frequent during the grape growing season in inland Australian viticultural regions, irrigation can also help to mitigate heat stress in grapevines, and provide ancillary benefits such as maintaining soil structure, soil microbial activity and cover crop function. A critically important aspect that motivated the present work, increasing ET across Australian viticultural regions has placed increased pressure on fresh water for irrigation, which has compelled irrigators to seek approaches to increase water use efficiency (WUE) such that greater productivity is obtained from their vineyards through prudent irrigation management. Irrigation scheduling, which refers to the timing and quantum of irrigation water applied to crops, is a useful tool to increase WUE at the vine and vineyard scales. Strategies such as regulated deficit irrigation (Fereres and Soriano, 2007; Romero et al. 2022) and partial rootzone drying (Dry et al. 2001) have been shown to be useful irrigation scheduling tools to increase the WUE in vineyards.

Irrigation strategies can be broadly categorised as those based on: i) historical applications or experience; ii) evaporative demand (e.g. crop evapotranspiration, $ET_c$); iii) soil moisture (either matric potential (tension) or volumetric water content) thresholds; and iv) plant water status thresholds. A number of review papers have been published that describe each of these approaches in detail, for example, Jones, 2004; Cifre et al., 2005, Jones, 2007; Williams, 2017, Fernández, 2017, Rienth and Scholasch, 2019, Mirás-Avalos and Araujo, 2021.

Irrigation scheduling tools are typically based on the interpretation of soil moisture, with their popularity ascribed to the well-established relationship between vine physiological parameters and soil water availability (Centeno et al., 2010). Common methods for soil moisture monitoring generally include a variety of sensors and probes aimed at measuring either volumetric water content (%VWC) or soil matric potential (kPa) (Munoz-

Carpena et al., 2004). However, despite their prevalence, an accurate measure of soil moisture is limited by soil heterogeneity and uncertain rootzone depths (Lebon et al., 2003), both of which represent limitations to soil moisture-based irrigation scheduling. In contrast, plant-based methods for irrigation scheduling are thought to take the whole soil-plant-atmosphere into account, and as such, have been suggested as the most direct way to measure plant water stress (Shackel, 2011). There are several techniques for measuring plant water status as described by Fernández (2017), however, for the majority of strategies discussed, a degree of interpretation is required for a given species and cultivar (Collins and Loveys, 2010). In addition, despite being considered effective and accurate detectors of vine water stress, strategies involving plant water status have historically lacked commercial applicability (Jones, 2004), and, until only recently, had largely been confined to the research domain. Presently, only a handful of Australian vineyards utilise plant water status sensors to determine irrigation schedules and typically these are vineyards > 100 ha (AWRI, 2019). Irrigation scheduling based on evaporative demand involves the quantitative determination of vine water consumption, typically, crop evapotranspiration ($ET_c$) to dictate how much water needs to be replaced in a subsequent irrigation cycle. One of the strengths of ET-based irrigation scheduling is the ability to quantitatively determine how much water to apply based on the Penman-Monteith energy balance model (Allen et al., 1998). However, this methodology has limitations depending on the method and data used to calculate reference evapotranspiration ($ET_0$), in addition to obtaining and using accurate crop coefficients (Gautam et al., 2021). Although each of the aforementioned strategies has been successfully used to carry out irrigation scheduling, the efficacy of each of these strategies is dependent on the thresholds used, with the choice of threshold potentially being influenced by factors such as production goals, cultivar traits and environmental conditions.

Considering that the effectiveness of commonly used decision metrics for irrigation scheduling can be impacted by a range of environmental, production, physiological and operator-driven factors, it is difficult to compare strategies based on existing research, which has motivated the present work. To the best of our knowledge, the aforementioned irrigation scheduling strategies have not been directly compared against one another in a single study in grapevine that also assesses WUE as a primary objective. We therefore conducted such a study on Cabernet Sauvignon and Shiraz grapevines in the Coonawarra viticultural region of South Australia between 2018-2022. As part of the study, we assessed a variety of continuous soil moisture and plant water status sensors that are commercially available and utilised these sensors to determine irrigation schedules targeted at increasing leaf and crop WUEs. Furthermore, we utilised high resolution remote sensing to build a spatial and temporal predictive model of vine water status and WUE, which can be utilised to implement precision irrigation in vineyards down to the single vine level.

In a recent review of climate change and viticultural adaptation strategies, Santos et al. (2020) highlight the value in utilising new technologies including drones and automatic plant-based irrigation systems to determine the most appropriate irrigation practices in the future; this foresight was provided two years after the commencement of this study and underscores its relevance.

# 3 Project Aims

The following aims and deliverables were defined for each of the four seasons, S1-S4, from 2018 to 2022:

**Table 1: Project outputs and activities, 2018-2022**

| Season | Outputs | Activities |
|---|---|---|
| **S1** - 2018/19 | A. Vineyard blocks identified and set up for irrigation trial.<br>B. Proximal plant sensors developed and deployed.<br>C. Identification, purchase, and operation of the UAS-based remote sensing platform.<br>D. Remote, proximal and direct field data collection.<br>E. Winemaking, juice/wine chemical composition analysis. | Identify trial sites and set up experiment.<br>Deploy plant and soil moisture sensors.<br>Purchase and tested/used remote sensing equipment.<br>Collect seasonal soil moisture and vine performance data.<br>Conduct juice and wine chemical analysis. |
| **S2** - 2019/20 | A. Validation of plant sensor data against a different level of irrigation.<br>B. Data of vine performance against conventionally-scheduled irrigation.<br>C. Economic (cost-benefit) analysis of sensor-driven irrigation vs conventional irrigation.<br>D. Present findings of study through articles, presentation, and conferences. | Plant sensor data collected and validated vs direct plant measures.<br>Collect seasonal soil moisture and vine performance data.<br>Economic model development begun for Cabernet Sauvignon.<br>Write and publish two papers on irrigation scheduling. |
| **S3** - 2020/21 | A. Validation of data on vine performance, yield, water use efficiency, grape quality and wine quality, and comparison of sensor-driven irrigation vs conventionally scheduled irrigation<br>B. Validation of industry irrigation practices benchmarks.<br>C. Wireless connectivity of sensors to Cloud based data platforms. | Collect and analyse grape and wine data.<br>Conduct survey of Limestone Coast wine industry of irrigation practices.<br>Implement wireless (4G) connectivity to the Cloud. |
| **S4** - 2021/22 | A. Assessment of the impact of sensor-driven vs conventionally scheduled irrigation on vine performance, yield, water use efficiency, grape quality and wine quality of SHI<br>B. Economic (cost-benefit) analysis of sensor-driven irrigation vs conventional irrigation.<br>C. Present findings of study through articles, presentation, and conferences. | Grape and wine data collection and analysis.<br>Analyse financials of Shiraz and Cabernet under different irrigation regimes.<br>Data dissemination through industry workshops and conferences. |

# 4 Materials and methods

## 4.1 Design of irrigation trials

In 2017/18, the field trial was conducted at Wynns Coonawarra Estate's Alex88-East vineyard for Cabernet Sauvignon (CAS) on Schwarzmann rootstock. A conventional (non-intervention) irrigation treatment was compared against evapotranspiration (ET)-based, plant water status (PWS)-based and soil water status (SWS)-based treatments. In the 2018/19 season, the irrigation trials were expanded from the existing 2017/18 trials with a clear aim to: i) increase statistical power by replication, ii) understand the influence of soil type on water status and iii) understand the influence of genotype/phenotype on water status. The trial was expanded from AX88-East to AX88-West and Katnook Estate Homestead Block (Shiraz/Teleki 5C). At Katnook, an additional Shiraz block, Prodigy, was monitored for benchmarking purposes, as this is the highest quality Shiraz (SHI) vineyard at the estate; no irrigation treatments were applied in this block. In the 2019/20 and 2020/21 seasons, irrigation trials were repeated at all three locations. However, based on experience from the 2018/19 season, data collection was restricted to two replications (blocks), which was found suitable for available resources. In the fourth and final season, 2021/22, due to budgetary constraints and already having three years of data from the Cabernet block, the trial was conducted only at Katnook (Shiraz) with additional treatments as mentioned bellow.

### 4.1.1 Location




*Figure 1: The four vineyards in Coonawarra, SA used for this study*

The irrigation trials were established at three vineyards: Cabernet Sauvignon/Schwarmann at TWE/Wynns-Alex88-east (Terra rossa soil), TWE/Wynns-Alex88-west (Rendzina soil), and Accolade/Katnook Estate Shiraz/Teleki 5C (Homestead Block) (Terra rossa soil). The Prodigy Shiraz vineyard at Katnook (Terra rossa soil) was observed for benchmarking purpose without any irrigation trial.

Alex88-East (AX88E) and Alex88-West (AX88W) both have CAS planted in 1988 with a total area of 17.3 ha. The east side of the vineyard consistently produces higher quality grape/juice in comparison, predominantly due to the soil type. The soil type in the AX88E is the red porous Terra rossa soil with an underlying bed of limestone rock. Moving towards the west, the soil gradually transforms into a much heavier and darker clay type called Rendzina. The water holding capacity and regulation of water through these two

soil types result in the different water status of the plant for the same level of irrigation and subsequently, the final quality of the wine. The setup in AX88E and AX88W helped assess the soil and vine water status of the CAS blocks with quite different soil types while keeping the rootstock and scion genotypes and viticulture practices consistent.

The Katnook vineyard is a younger SHI (on Teleki 5C rootstock) planted in 2013 on porous Terra rossa soil. The Prodigy vineyard is an older SHI block, which consistently produces high-quality wine. Vines regulate water differently with the age of the plant, thus resulting in different water status in Katnook and Prodigy for the same irrigation practice. The setup in Katnook and Prodigy will help to understand how the younger SHI at different irrigation treatment compares to the older high-quality SHI. By understanding the age effect, the quality of the younger vines could be improved by co-replicating the water status of the older vines. Moreover, comparing Katnook with Alex88-east may unravel the differences in water status between the SHI and CAS under similar treatment, terroir and irrigation practices. We expect to understand the isohydric vs anisohydric behaviour of the plant to cope with the water stress and thus better manage plant water use efficiency without compromising the yield and quality of the wine.

### 4.1.2 Experimental design

All the irrigation trials (Alex88-east, Alex88-west and Katnook) are set up similarly, whereas the Prodigy does not contain any irrigation trials. The experimental design – Randomised Complete Block - is shown in Figure 2.

**2018-2021 seasons (CAS, SHI)**

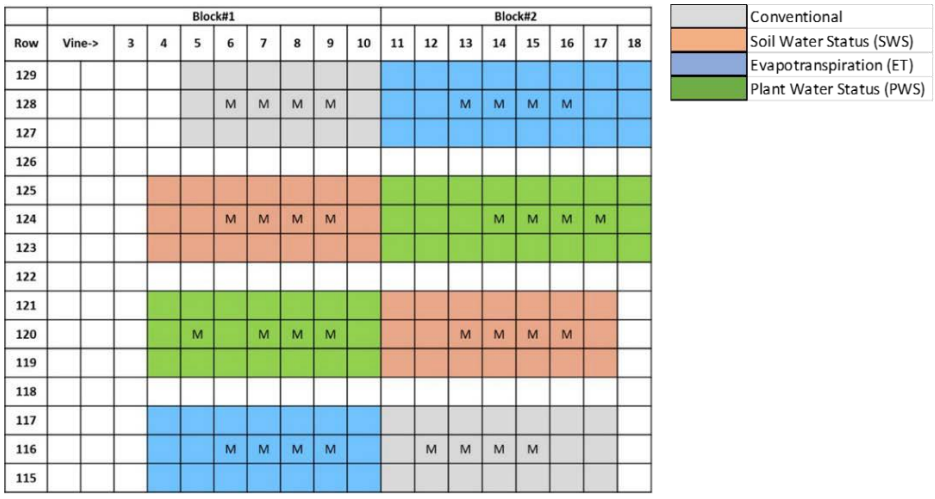



*Figure 2: Experimental designs at Alex88-east, Alex88-west and Katnook.*

**2021/22 season (SHI)**

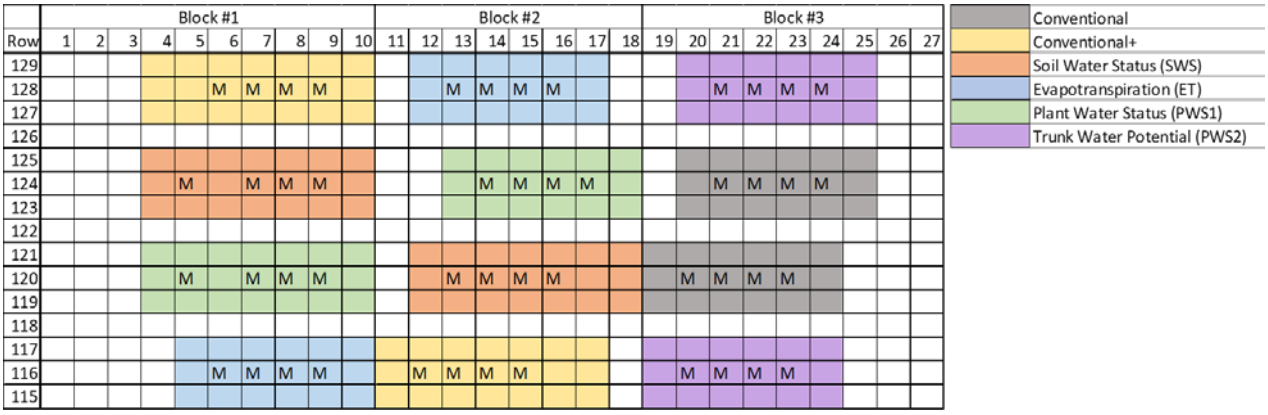



*Figure 3: Experimental designs at Alex88-east, Alex88-west and Katnook.*

The experimental design consisted of two blocks with four different treatment types (Conventional, ET, SWS and PWS). The conventional treatment is where the growers apply as much water as they normally would; as such it was a non-intervention treatment. In the other treatments, SWS, PWS and ET, we scheduled irrigation based on quantitative (sensor-based) evidence of soil moisture, plant water status and evapotranspiration, respectively. Each irrigation treatment in each block was separated by 1-2 buffer vine rows between them. A single treatment consisted of three rows where only the vines from the middle row were measured (marked M in Figure 2). Thus, each set of measurement vines had buffers between rows and also within the row to ensure no overlap between the irrigation treatments. Except for CONV, all data-driven irrigation treatments used thresholds before each irrigation cycle to decide whether irrigation should be applied**.**

In the 2020/21 growing season, the conventional or grower-driven treatment (CONV) received double the amount of irrigation relative to the previous season (CONV+), which represented an extra treatment. Other treatments SWS, PWS and ET were applied based on the measurement value of soil moisture, canopy conductance and crop evapotranspiration ($ET_c$), respectively.

In the 2021/22 season, in addition to the irrigation treatments applied in the previous season, two treatments (non-altered original grower-driven (CONV) and trunk water potential-based (PWS2)) were also assessed.

## 4.2 Scientific equipment and sensors

### 4.2.1 Direct, proximal and continuous sensors

This category of sensors includes the sensors located on the ground including continuous measurement sensors such as weather station, infrared towers (plant-based sensors, PWS1) and soil moisture sensors (Figure 3).

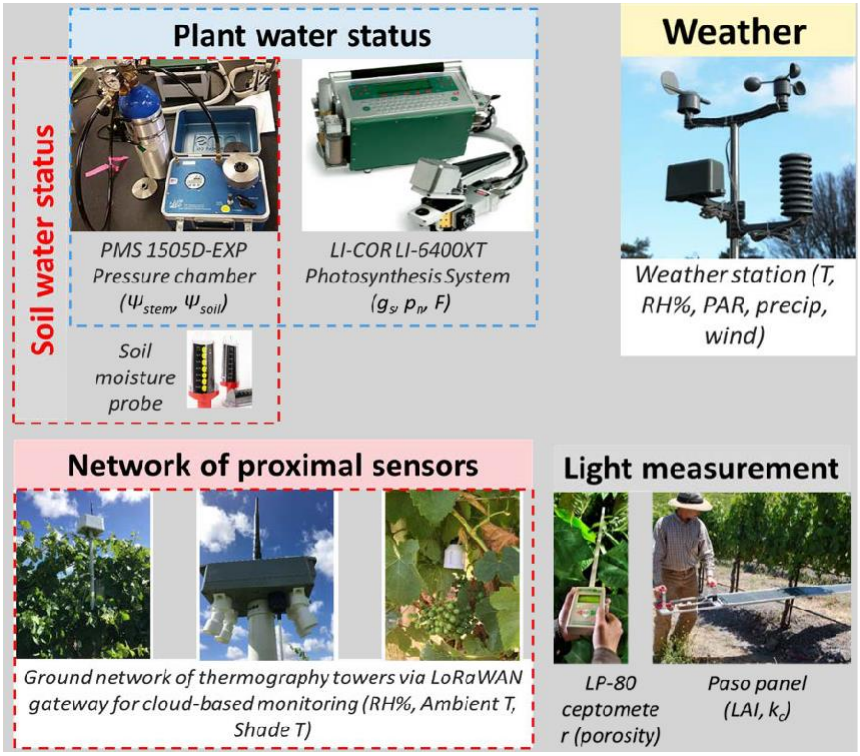



*Figure 4: Direct, proximal and continuous sensors used in this study of grapevine irrigation*

#### *4.2.1.1 Direct and proximal sensors*

Multiple direct/proximal sensors were employed for this experiment and included sensors that required manual operation.

##### 4.2.1.1.1 Pressure chamber

A pressure chamber (Figure 3) is used to measure the pre-dawn leaf water potential and mid-day stem water potential. The pre-dawn measurement is an indication of the total water that is accessible to the plant's root system. This information is reflected in the pre-dawn measurement of the water potential. One measurement per plant was made using the pressure chamber between 0230-0500 h.

The midday stem water potential shows the water status of the plant when the plant is transpiring at full potential. For this, a mature leaf per sentinel vine was selected from the shoulder of the vine. The selection criteria for the leaves was neither too young, nor too mature, from within 1/3-2/3 shoot length, without obvious disease/discolouration and from a full sunlit shoot. The selected leaf was bagged in the aluminium bag at least 30 minutes before the measurement. The bagging enabled equilibrium of the leaf water potential to the overall water potential of the shoot. The measurement was carried out between 1100–1400 h.

##### 4.2.1.1.2 Portable photosynthesis system

An infrared gas analyser (IRGA; Figure 3) was used to measure leaf gas exchange of sentinel vines: stomatal conductance, rate of transpiration and net photosynthesis rate, among others. These measurements give an indication of the plants' physiological performance in response to the given amount of soil water availability and environmental conditions. This measurement was carried out on fully sunlit leaves from the same shoot as the bagged leaf (for stem water potential) using a LI-COR 6400XT infrared gas analyser, between 1100–1400 h.

##### 4.2.1.1.3 Ceptometer

An Accu-PAR LP-80 ceptometer (Figure 3) was used to measure the canopy light interception. The light interception measurements included the canopy porosity (T) and the leaf area index (LAI). Canopy porosity

gives an indication of the amount of light penetrating the canopy reaching the fruit, which is also a good predictor of anthocyanin in the berries. The LAI is a measure of the number of leaves per square metre of the area. These measurements were also made at solar noon (1230-1400 h).

#### 4.2.1.1.4 Crop coefficient measurement

A Paso-panel (Figure 3) was custom-built to measure the crop coefficient ($K_c$) of the canopy. $K_c$ is a measure of the canopy size to the vineyard macrostructure such as fractional cover. This crop coefficient, together with reference evapotranspiration ($ET_0$), is used to estimate crop evapotranspiration ($ET_c$), which is one of the irrigation strategies (treatments) evaluated in this study. Using an empirical relationship, $K_c$ is estimated indirectly based on the sunlight intercepted by the Paso-panel (a flexible solar panel) when in the full sun vs when under the canopy (partially shaded). These measurements were also made at solar noon (1230-1400 h).

### *4.2.1.2 Continuous sensors*

The continuous sensors employed in this trial include Transp-IR thermography sensors (Athena Irrigation Technologies, Adelaide, SA), soil moisture sensors (Teros-12, METER, Pullman, WA, USA), BOM weather station, and microtensiometers (FloraPulse, USA). These instruments measured data continuously without the need for operators, with data accessed remotely through various Cloud-based interfaces.

#### 4.2.1.2.1 Thermography towers

Proximal infrared (IR/thermal) 'Transp-IR' (Gen 1) sensors were obtained from Athena Irrigation Technologies (Adelaide, SA) for continuous measurement of vine water status. Four sensors per vineyard were tested and deployed in the three trial sites in early January 2020. The sensor platform consists of sensor nodes (Figure 4.a) that are mounted over a wooden post (Figure 4.b) and a temperature-humidity sensor for VPD measurement (Figure 4.c). The sensor nodes collect continuous canopy temperature as well as VPD data and transmit the data using 4G mobile network to an Amazon Web Services (AWS) Cloud platform. Each sensor node acquires canopy temperature from two vines per node on both sides of the canopy, as well as in-canopy temperature and humidity for the estimation of ambient VPD. The sensor data are collected every 10 min and a daily value of vine water index (VWI), a thermal water stress indicator, was provided as a measure of vine water status/stress. The data visualisation and download occurred through a web-based interface (dashboard).



*Figure 5: 'Transp-IR' continuous water status sensors (Athena IR-Tech, Adelaide, SA).*

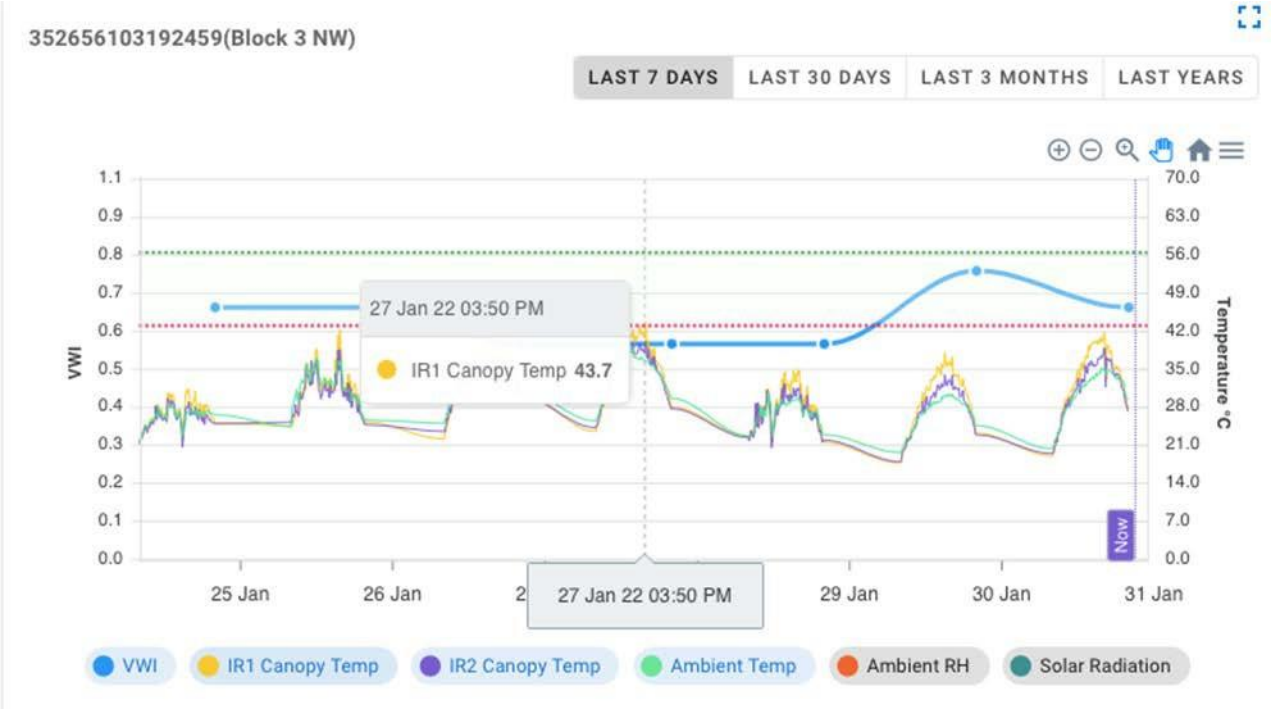



*Figure 5: Dashboard providing data visualisation of Transp-IR sensor data. The Vine Water Index (VWI) is shown graphically as a coloured scale bar on the top of the dashboard. Individual sensor data is shown below the scale bar along with canopy temperature, ambient temperature, relative humidity, and solar radiation.*

Continuous measurements of canopy temperature and VPD were used to derive an index of water stress, Vine Water Index (VWI). The VWI was mapped onto traditional metrics including $g_s$ and $\Psi_{stem}$ for validation. This mapping allowed the determination of thresholds of VWI based on known or established $g_s$ or $\Psi_{stem}$ thresholds to maximise WUE, yield or grape quality. In doing so, growers can target specific objectives of individual blocks through VWI thresholds (optimum ranges).

Optimised VWI thresholds to maintain 80-85% of the maximum photosynthetic rates ($A_N$) were derived from the non-linear relationships between $g_s$ and $A_N$ for each cultivar. The VWI values were related to $g_s$ through correlation analysis using data measured over the growing season under a range of vine water status.

#### 4.2.1.2.2 Soil moisture sensors

In addition to the surrogate soil moisture, the pre-dawn leaf water potential measurement or matric potential, actual soil volumetric water content was measured using a network of soil moisture sensors. These sensors (TEROS-12, Meter Group, Pullman, WA, USA) were installed 30 cm below the ground and measured three parameters: soil salinity, soil temperature and volumetric water content (%). One soil moisture sensor was installed per vineyard in each SWS treatment. The soil moisture was logged hourly onto an online dashboard (Green Brain, MEA, Adelaide, SA).

#### 4.2.1.2.3 Weather station

Daily meteorological data were acquired from the Bureau of Meteorology local weather station (Coonawarra Station ID: 94817) that was in proximity to the field (approximately 1 km south of the CAS block and 5 km north of the SHI block). The meteorological data included the daily minimum and maximum temperatures, minimum and maximum humidity, total solar radiation and precipitation. These data, together with the $K_c$ were used to compute $ET_c$.

#### 4.2.1.2.4 Microtensiometers

Microtensiometers (Figure 6) were embedded into the trunk of SHI and CAS grapevines as described by Pagay et al., (2021). The data of trunk water potential were obtained every 20 min, wirelessly transmitted to a Cloud-based server (Amazon Web Services, USA) and visually displayed on a user interface (FloraPulse, Davis, CA, USA).



*Figure 6: Novel direct plant microtensiometers (FloraPulse) used during 2020/21 season for measuring trunk water potential*

### 4.2.2 Remote sensing equipment

#### *4.2.2.1 The unmanned aerial vehicle*

A DJI Matrice 600 Pro hexacopter was used as the sensor carrier for this research. This UAV offered a flight time of about 16-20 min and a payload capacity of about 6 kg, easily accommodating the sensor payload, which included a thermal, a multispectral and an RGB camera (see Figure 7).

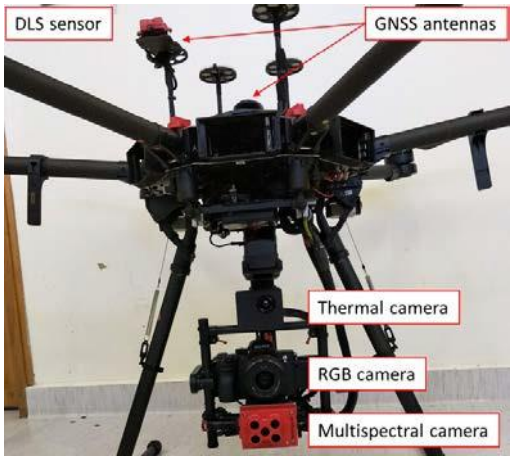



*Figure 7: The UAV platform and the sensors for the remote sensing of vine water status.*

The flight planning and data capturing strategy were determined before the field campaign. The flights took place at a height of 30 m in a regular mapping ('lawnmower') flight pattern. The camera was programmed to capture images once every second (maximum frame rate). The speed of the flight (3 m/s) was set to match with the image capture rate such that at least 80% forward overlap between subsequent images was achieved. The separation of the subsequent flight strips was set such that over 70% side overlap was achieved. With 80% forward and 70% side overlap, the images were expected to produce high resolution maps via mosaicking (photogrammetry). Furthermore, consideration was provided to the total flight time (14 min battery life) balancing out with the flight altitude. For higher altitudes, the UAV could fly faster without compromise in the image overlap and complete the mission in a shorter time. The selected parameter was a compromise between the desired overlap, the maximum operating rate of the camera, the life of the battery and the size of the site. The flight planning and operation were performed in the DJI Ground Station Pro software application (Fig. 8).



*Figure 8: DJI GS Pro software to plan the UAV flight and capturing of the remote data.*

The use of independent cameras (thermal, multispectral and RGB) requires spatial overlay between the output products (e.g. maps) such that correct plants are observed in each map. For this, we used two-

step processing to acquire maps with correct geographic location and with correctly overlaid layers. The first step is to use a GNSS antenna onboard the UAV that can provide a spatial reference to each image of at least one camera. The GNSS antenna of the multispectral camera was capable of geotagging the multispectral images. As a result, the products from the multispectral images were in a correct geographic location. The images were acquired in WGS84 coordinate frame and the post-processed products were derived in MGA54 projected coordinate frame. The second step set in the field was to have permanent control points on the field. For this, we hammered about 15 wooden pegs (sized 35 x 5 x 5 cm) on each of the test sites, and manufactured ground targets (sized 30 cm diameter). The ground targets were placed at the peg location, for each of our field campaigns. This way, the targets are captured by all the cameras and hence are used as tie-points to align and overlay the maps from the cameras.

#### *4.2.2.2 RGB camera*

A full-frame RGB camera (Sony α7RIII) was used to capture the high-resolution natural colour images from the UAV. The camera had a wide field of view of 65.3° x 46.4°, a focal length of 28 mm and the CCD chip had 7952 x 5304 pixels. Given the camera parameters, the proposed flying height resulted in a single image coverage of 38.5 x 25.7 m with a spatial resolution of 0.5 cm (at 30 m altitude). This level of spatial resolution was adequate to capture single leaves at high resolution, and for our application, which requires measurement at a single vine canopy level.

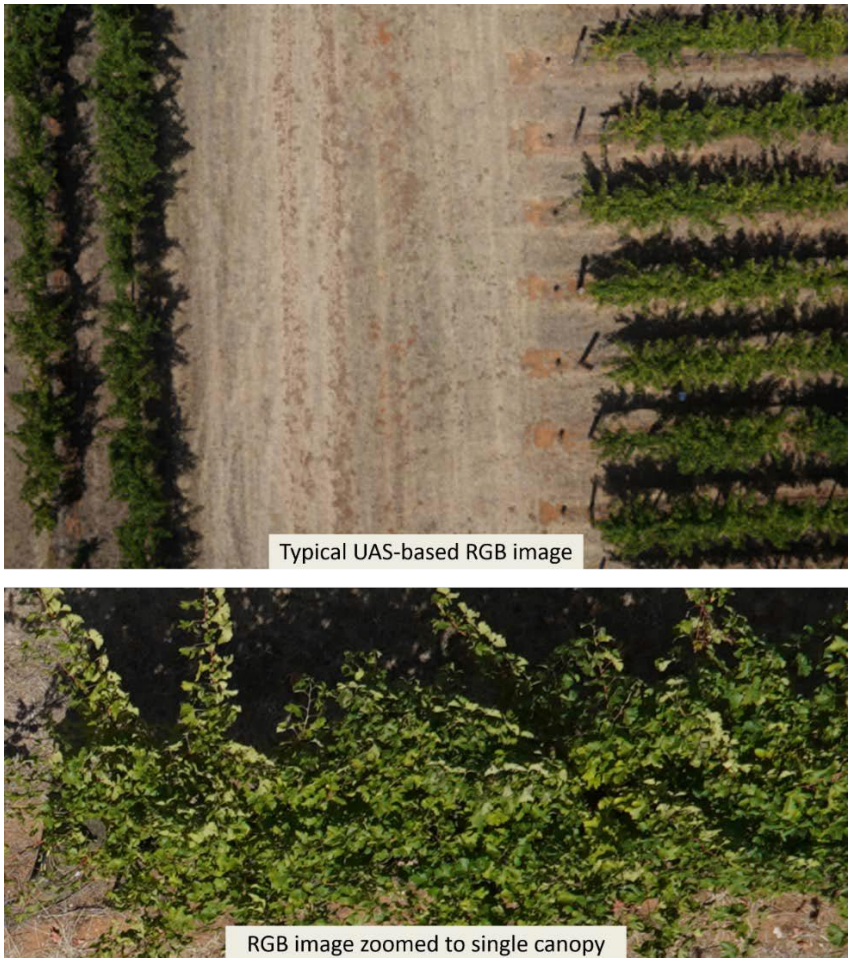



*Figure 9: Typical single RGB image captured from a UAV. Note that leaf-level spatial resolution is achievable.*

#### 4.2.2.3 Multispectral camera

A five-band multispectral camera (MicaSense RedEdge-M) was used to co-capture the multispectral images. The five discrete bands captured five independent images at blue (475 nm), green (560 nm), red (670 nm), red edge (720 nm) and near infrared (840 nm) region of the electromagnetic spectrum. The camera had a field of view of 47.9° x 36.9°, focal length of 5.4 mm and each discrete CCD chip had 1280 x 960 pixels. The resulting image for the proposed flying height had coverage of 26.7 x 20 m with a spatial resolution of 2.1 cm (at 30 m altitude).

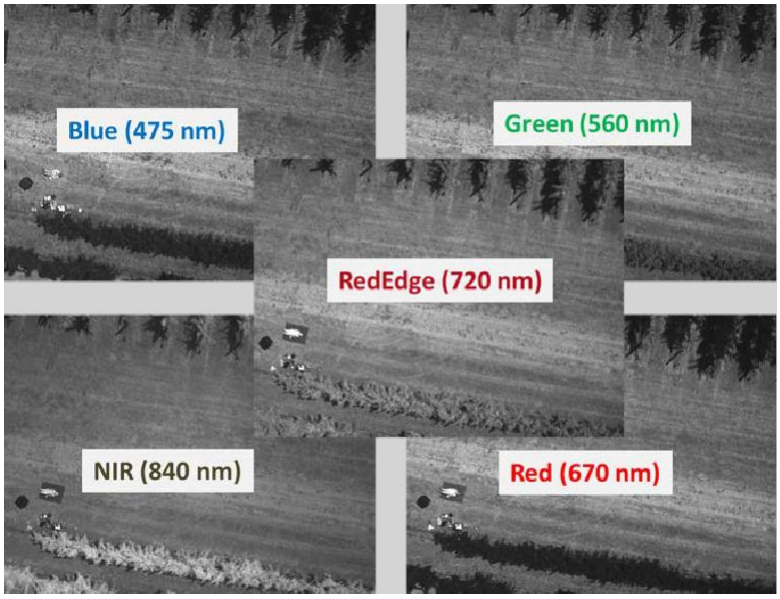



*Figure 10: A typical single multispectral image. Note that the camera captures a discrete image for each discrete band.*

#### 4.2.2.4 Thermal camera

Thermal images were captured using a FLIR Tau2 640 core with TeAx acquisition board. The sensor captured, at 7.5 – 14 µm, the latent heat coming to the sensor from the scene. The camera had a field of view of 45.4° x 37°, a focal length of 13 mm and contained 640 x 520 microbolometers arranged as pixels. The resulting thermal image for the proposed flying height had coverage of 25.1 x 20.1 m with a spatial resolution of 3.9 cm. The achievable resolution is sufficient for our application to measure a single canopy. At 3.9 cm resolution, a single canopy will still have several hundred pixels allowing accurate measurement of the pure canopy temperature.

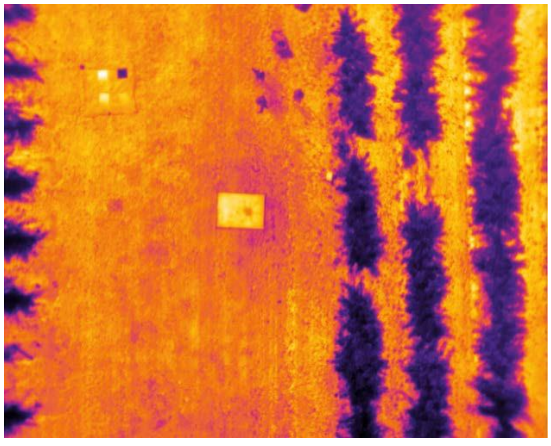


*Figure 11: Typical single thermal image. Note the thermal image requires image-stretching techniques for visualisation purpose. The raw thermal image appears completely dark to human eyes.*

### 4.2.3 Thresholds for irrigation scheduling

The four irrigation strategies used measurements of different factors to drive the irrigation. The strategies resulted in different total irrigation volumes (per season) as well as different times or schedules of irrigation each week. The decision to irrigate was based on historical (CONV, CONV+), measured (SWS, PWS) or calculated (ET) information. A set of thresholds based on quantitative measurement values was set for each of the non-control treatments. For each irrigation cycle, the measurements are compared against the predetermined threshold. Treatments were irrigated only if the quantitative measurements dropped below the predetermined threshold (see below for details).

#### *4.2.3.1 Conventional*

The CONV irrigation treatment is the 'control' group for this study, which was irrigated by the growers without intervention by the trial researchers. The irrigation amount and timing incorporated a combination of historical irrigation schedules, weather conditions, visual inspection of the vines and occasional soil moisture measurements. In the 2020/21 growing season, due to the high levels of water stress observed in the CONV vines during the previous season (2019/20), the amount of irrigation was doubled for the CONV irrigation treatment (CONV+) to ensure the vines were well-watered. In the 2021/22 season, both CONV and CONV+ treatments were compared with other sensor-driven treatments.

#### *4.2.3.2 Plant water status*

The PWS treatment received irrigation based on the measurement of plant water status, specifically the VWI value derived from the Transp-IR towers. These VWI values corresponded to canopy conductance ($g_c$) values of between 120-140 mmol $H_2O/m^2/s$. This threshold range was established from a preliminary study at the trial site during the 2017/18 season targeted at achieving 80-85% of maximum photosynthesis of each cultivar.

#### *4.2.3.3 Crop evapotranspiration*

The crop evapotranspiration method aimed to replace the water loss from the vineyard via the evaporation and transpiration. Based on the measurement of the plant crop coefficient ($K_c$) and meteorological data ($ET_0$), the $ET_c$ was computed weekly. This computation was the basis of the irrigation decision for each irrigation cycle. Following deficit irrigation strategies in literature and experience from the region and specific vineyard where 40-50% $ET_c$ was used for the CONV treatment, we maintained the deficit irrigation for the ET treatment at 15% $ET_c$ from fruit set to véraison and 25% $ET_c$ from véraison to harvest.

#### *4.2.3.4 Soil water status*

The SWS treatment aimed to maintain the soil volumetric water content throughout the season. This threshold was determined from the capacitance probe historical data. The threshold was set at 30% below the historical volumetric water content of the vineyards, which was around 33% VWC. The resulting volumetric water content threshold to trigger the irrigation in the SWS treatment was 21% in both vineyards, CAS and SHI.

## 4.3 Data collection time points

We aimed to acquire direct, proximal and remote sensing field data at key phenological stages of vine development. The purpose of the data was two-fold: a) to decide on the irrigation of the particular treatments, and b) to monitor the performance of the vine as a result of the different irrigation practices. Table 2 shows the data collection time points corresponding to different phenological stages in each season for CAS and SHI.

*Table 2: Data collection time points at different phenological stages in each season.*

| Phenological stage of growth | 2018/19 | 2019/20 | 2020/21 | 2021/22 |
|---|---|---|---|---|
| Winter rainfall May-August, mm | 334.2 | 272.6 | 272.5 | 256.6 |
| | Cabernet Sauvignon | | | |
| EL stage<br>Budburst (BB) – 4<br>Flowering (F)– 19<br>Fruit set (FS)– 27<br>Pea sized (P)– 31<br>Véraison (V)– 35<br>Preharvest (PH)– 37<br>Harvest (H)– 38 | BB – 2nd Oct 2018<br>F – 20th Nov 2018<br>FS– 12th Dec 2018<br>P– 16th Jan 2019<br>V – 12th Feb 2019<br>PH – 7th Mar 2019<br>H – 11th Apr 2019 | BB – 24th Sept 2019<br>F – 18th Nov 2019<br>FS – 17th Dec 2019<br>P – 13th Jan 2020<br>V – 5th Feb 2020<br>PH – 10th Mar 2020<br>H – 8th Apr 2020 | BB – 21st Sept 2020<br>F – 20th Nov 2020<br>FS – 7th Dec 2020<br>P – 4th Jan 2021<br>V – 9th Feb 2021<br>PH – 18th Mar 2021<br>H – 14th Apr 2021 | |
| | Shiraz | | | |
| | BB – 30th Sept 2018<br>F – 5th Dec 2018<br>FS – 12th Dec 2018<br>P – 27th Dec 2019<br>V – 5th Feb 2019<br>PH – 7th Mar 2019<br>H – 21st Mar 2019 | BB – 30th Sept 2019<br>F – 7th Dec 2019<br>FS – 19th Dec 2019<br>P – 30th Dec 2020<br>V – 10th Feb 2020<br>PH – 9th Mar 2020<br>H – 17th Apr 2020 | BB – 17th Sept 2020<br>F – 20th Nov 2020<br>FS – 7th Dec 2020<br>P – 14th Dec 2021<br>V – 2nd Feb 2021<br>PH– 1st Mar 2021<br>H – 31st Mar 2021 | F- 30th Nov 2021<br>P- 30th Jan 2022<br>V- 22nd Feb 2022<br>PH- 18th Mar 2022<br>H- 06th Apr 2022 |

## 4.4 Methodology and processing

### 4.4.1 Ground data methodology and processing

All the ground data were sorted by date, treatment, block and vine number. A pre-established empirical equation was used for the computation of crop coefficient. Data were statistically analysed by two-way ANOVA using GraphPad Prism 8 Prism software.

### 4.4.2 Harvest, yield components and pruning

At harvest, yield parameters such as weight of fifty berries, number of clusters per vine, total bunch weight and cordon length were measured on eight vines per treatment. Vines were pruned later in the season and pruning weight was measured in each vine.

### 4.4.3 Winemaking

After harvesting, clusters were randomly selected from eight different vines per treatment and they were mixed for winemaking. Twelve small-scale ferments (one 5 L ferment per treatment per vineyard) were prepared according to the following procedure developed by the University of Adelaide. Fruits were crushed using a mechanical crusher de-stemmer and 20 mL of a 2% $SO_2$ solution was added. Diammonium phosphate was added at 100 ppm to each must before inoculating with the yeast (Lalvin EC-1118 *Saccharomyces cerevisiae bayanus*, Lallemand, Denmark) at 300 mg/L. All ferments were incubated in a temperature-controlled room at 22 °C and skins were hand-plunged twice a day. After two weeks, juice was extracted

using a basket press and wines were racked after a week. Malolactic fermentation was initiated by inoculating the wine with lactic acid bacteria (strain). Wines were bottled after adding sulfur dioxide (30 ppm) and they were stored at 15 $^{o}$C until chemical composition analyses was performed.

### 4.4.4 Berry, juice and wine chemical analyses

All fruit chemical analyses were done on a per vine basis. The following chemical parameters were determined as described below.

#### *4.4.4.1 pH/titratable acidity (TA) and total soluble solids (TSS)*

TSS was measured using a refractometer. pH and TA were simultaneously assessed using an autotitrator (Mettler Toledo T50).

#### *4.4.4.2 Colour/hue analysis*

To identify colour and hue of grape juice and wine, absorbance at 420 and 520 nm wavelengths was measured against a blank using a UV/Vis spectrophotometer. A glucose solution (20%) with 1 g tartaric acid was used as a blank for grape juice, whereas 10% ethanol was used for wine. Colour density and hue/tint were calculated using the following formulae:

$$\text{Colour density} = A_{520} + A_{420}$$

$$\text{Hue/Tint} = A_{420}/A_{520}$$

#### *4.4.4.3 Total anthocyanin*

Anthocyanin content was determined by measuring the differential absorbance at 520 nm between wines at pH 1.0 and pH 4.5. Ten-fold diluted samples were prepared using pH 1.0 and pH 4.5 buffers and absorbance at 420 and 520 nm was measured following 1 hr of dark incubation. Total anthocyanin concentration was calculated as malvidin chloride 3, 5-diglucoside (equivalents) using the following formula.

$$\text{Total anthocyanins (mg/L)} = (A^{520}{}_{\text{pH 1.0}} - A^{520}{}_{\text{pH 4.5}}) \text{ X } 255.75$$

#### *4.4.4.4 Total phenolics*

Two microlitres of the sample (or 20 µL of the 10:1 diluted sample), 1.58 mL of distilled water and 100 µL of Folin & Ciocalteu's phenol reagent were added to a glass cuvette and after 1 min incubation at room temperature, 300 µL of sodium carbonate solution was added. The solution was incubated at 40 $^{0}$C for 30 min under dark and absorbance was measured at 765 nm against a blank. Total phenolics were then quantified using a Gallic acid standard curve and expressed in mg/L of gallic acid equivalents (GAE).

### 4.4.5 Remote sensing data methodology and processing

#### *4.4.5.1 Mosaicking*

Three cameras (multispectral, thermal and RGB) were used to co-acquire aerial imagery of the vineyards at four phenological stages (Flowering (EL-19), Pea-size (EL-31), Véraison (EL-35), and Pre-harvest (EL-37)). Initially, the photogrammetric software, Agisoft Metashape, was used to mosaic the series of images to create a map.

The RGB images were mosaicked using a standard workflow of image alignment followed by camera calibration, dense point cloud generation, 3D model generation, and orthomosaic generation. The output from the RGB images includes orthomosaic and report for each orthomosaic. Since the bands presented in the RGB are a subset of the multispectral camera, the multispectral products were sufficient and hence the RGB products were not used in further processing.

The Multispectral images were mosaicked using the workflow recommended by the Agisoft Metashape. The workflow includes: a) creating multi-spectral images, b) image alignment, c) camera calibration, d) dense point cloud, e) classification of point cloud, f) DEM generation, g) DSM generation and h)

orthomosaic generation. The multispectral camera generated most of the basic products for this project. The output from a multispectral camera included 12 sets of the following products: a) georeferenced orthomosaic, b) digital elevation model, c) digital surface model, d) 3D point cloud, e) processing report.

The thermal camera was new to the processing chain, requiring a unique workflow. Firstly, the thermal camera in *.TMZ format was converted to raw image files. Using a batch processing script the *.TMZ files captured by the camera were converted to raw *.TIFF files along with the metadata encoded in a *.CSV file. The image files were then processed in Agisoft Metashape to generate thermal maps. The thermal images contained value of temperature data encoded in 14-bit format. As the variation in temperature between the scenes was not minimal, thermal images appeared completely dark when viewed in raw. This resulted in minimum, at best, match points between the consecutive images, failing image alignment. As a solution, raster transformation was applied before processing the images in Agisoft Metashape and reverted before exporting products out of Metashape. The processing workflow of the thermal images in Agisoft Metashape included: a) raster transformation, b) image alignment, c) camera calibration, d) dense point cloud generation, e) 3D model generation, f) orthomosaic generation, g) reset of raster transformation, h) exporting of products. The products from the thermal images included the orthomosaic and processing report.

The orthomosaic, DEM and DSM from the multispectral camera and the thermal orthomosaic were processed further within the scope of this project. Whereas, the processing of the RGB orthomosaic and multispectral 3D point cloud were considered of low priority.

#### *4.4.5.2 Georeferencing*

The multispectral camera had a functional GPS antenna encoding a navigation-grade position to each of the images. This information is exploited to georeference the multispectral images within the Agisoft Metashape via direct georeferencing, whereby, all the products from the multispectral camera were in projected MGA 54 projected coordinate frame.

The thermal orthomosaics were not georeferenced to any coordinate frame, due to the lack of functional GPS antenna. In this process of georeferencing, the thermal orthomosaics were georeferenced on top of the multispectral orthomosaic. For this, the GCPs spread across the scene were used as the common tie-points between two orthomosaics. Using a polynomial fit, the thermal orthomosaics were fitted to the multispectral orthomosaics in ArcGIS software.

#### *4.4.5.3 Atmospheric radiometric correction*

The thermal and multispectral images were captured at various time points throughout the season. As each time point was environmentally different, we required a calibration to account for changing environmental conditions between different days and times of the day. This calibration corrects for environmental factors such as high/low solar illumination and VPD, and highlights the plants' spectral/thermal signal. For this, four shaded standard calibration panels were used in the field for each of the flight. The calibration panels were sized (45 x 45 cm) such that they are visible and had sufficient pixels (over 50) representing a single panel. The calibration panels were manufactured using black enamel paint and white $BaSO_4$ following a prescribed mixing ratio, coating thickness and number of coats. The panels were expected to have a uniform reflectance profile throughout the season. The manufactured panels were four shade of grey: a white (90% white and 10% black), light grey (70% white and 30% black), dark grey (30% white and 70% black) and black (10% white and 90% black) (see Figure 5). For spectral calibration, the panel reference spectra were measured, at the start and the end of the season, on the ground using an ASD Handheld2 spectroradiometer. On each flight, the multispectral camera captured a few snaps of the panels. Using the reference spectral profile (measured on the ground), the calibration was applied to the raw spectral profile (acquired during flight).

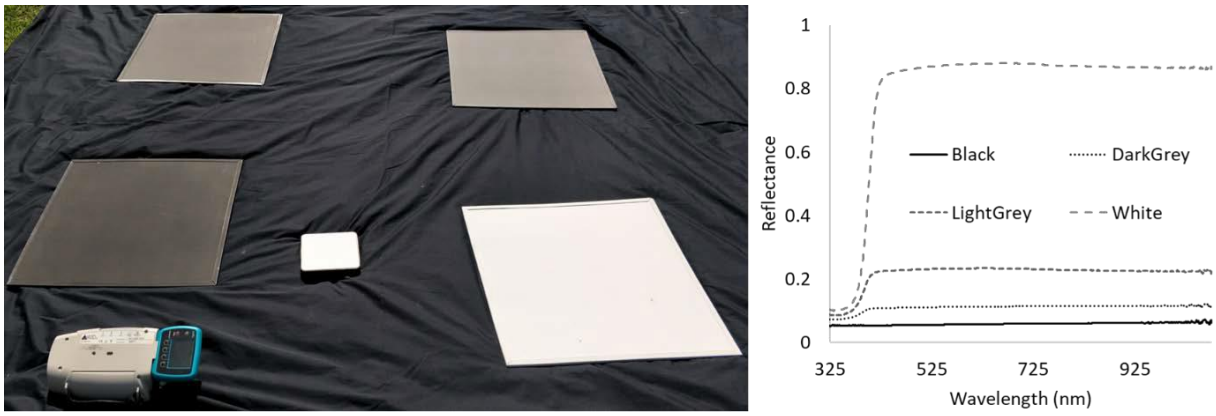



*Figure 6: The four calibration panels: White (90% white, 10% black), Light Grey (70% white, 30% black), Dark Grey (30% white, 70% black), Black (10% white, 90% black) along with the Spectralon panels (calibrated and non-calibrated), and the ASD handheld2 spectroradiometer used to acquire the spectral calibration data. The reflectance profile of the four calibration panels is displayed in the right pane.*

The shaded panel also develops a unique temperature when placed under the sun. This was exploited to calibrate the thermal camera using the same calibration panels prepared for the multispectral. The panels were placed in the field, under full sun, at least 45 minutes before the flight. By about 45 minutes, each panel reached a unique and stable temperature. For a typical day, the observed difference between the white and black panel was in the order of 30° C. During the flight, the thermal camera captured several images of the panels whenever the panels were in the field of view. Concurrently, on the ground, the panel temperature was measured continuously using a high accuracy Fluke IR temperature gun. Using the known panel temperature (measured on the ground), the calibration was applied to the raw thermal data (acquire during flight).

#### *4.4.5.4 Single canopy data extraction*

Following the radiometric/atmospheric calibration of the georeferenced orthomosaics, single canopy level data were extracted. For this, a global mask was applied to the orthomosaics. The mask incorporated the normalised difference vegetation index (NDVI) and the canopy height thresholds to remove any non-canopy pixels from the orthomosaic (see Figure ).

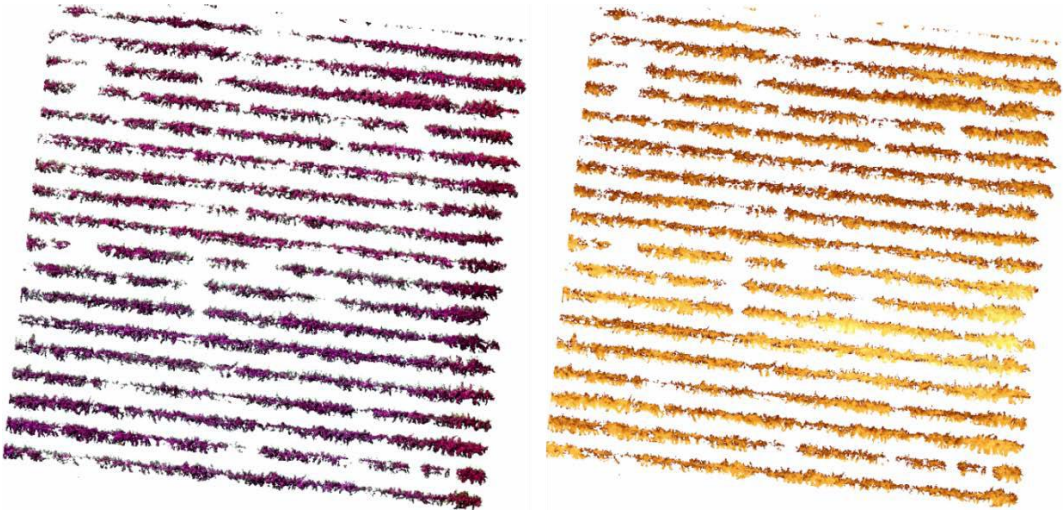


*Figure 13: The masked multispectral (left pane) and thermal (right pane) orthomosaics from Alex88-east at EL-35. Note the masking is performed using the NDVI threshold (0.4) and the canopy height threshold (1 m).*

From the masked multispectral and thermal orthomosaic, single canopy (vine-level) data were extracted by using the ArcGIS/QGIS Zonal Statistics tool. For zonal statistics to be applied, the vines within the scene were

digitised using a grid (in Q-GIS) where one polygon represented the vine space (row x vine spacing) for a single canopy (see Figure ).

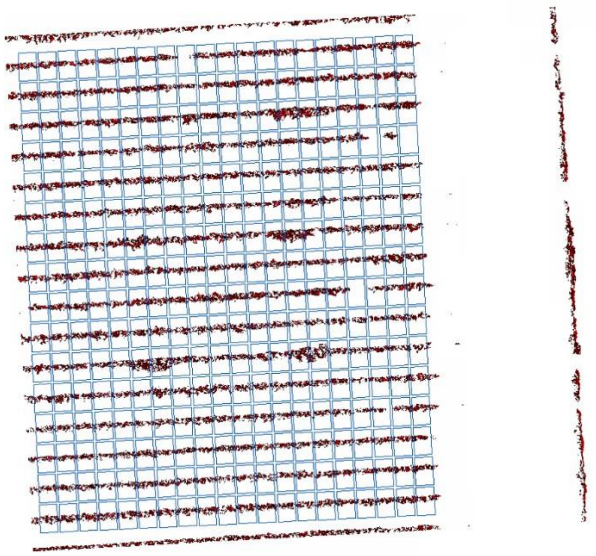


*Figure 14: The digitised canopy space for the Katnook Homestead block at EL-31. Note each of the rectangular polygons represents the vine space for a single canopy. The gap between two polygons is used as inter-canopy 20 cm buffer.*

#### *4.4.5.5 Identification of key indices*

Numerous structural, spectral, thermal and composite indices were computed from the remote sensing data. These indices were, at a later stage, used for spatial prediction of grapevine ecophysiology including stomatal conductance, net photosynthesis, predawn and stem water potentials, crop coefficient and LAI.

##### 4.4.5.5.1 Structural indices

From the single vine data, the following structural properties of each canopy were extracted and structural indices computed (see Table ):

*Table 3: Structural properties and indices computed using remote sensing*

| SN | Name | Description | Formula |
|---|---|---|---|
| 1 | p_height | Mean height of the canopy | n/a |
| 2 | area | The top surface area of the canopy | n/a |
| 3 | width | Width of the canopy | n/a |
| | P_fraction | Fractional cover of the canopy within the vine space | area/(rowSpacing*vineSpacing) |

##### 4.4.5.5.2 Spectral indices

Various spectral indices were computed using the five bands of the multispectral images (see Table 4).

*Table 4: The spectral indices computed using the MicaSense RedEdge-M. Note b = Blue, g = Green, r = Red, nir = near-infrared, re = RedEdge.*

| SN | Name | Description | Formula |
|---|---|---|---|
| 1 | CAR | Chlorophyll absorption ratio | ((re-b)*r+r+(g-((re-b)*r)*g))/np.sqrt(((re-b)*r)**2) |
| 2 | CAR1 | Chlorophyll absorption ration#1 | CAR*re/r |
| 3 | GI | Greenness index | g/r |

| | | | |
|---|---|---|---|
| 4 | GNDVI | Green normalised difference vegetation index | (nir-g)/(nir+g) |
| 5 | NDVI | Normalised difference vegetation index | (nir-r)/(nir+r) |
| 6 | MCARI | Modified chlorophyll absorption in reflectance | ((re-r)-0.2*(re-g))*(re/r) |
| 7 | MCARI1 | Modified chlorophyll absorption in reflectance#1 | 1.2*(2.5*(nir-r)-1.3*(nir-g)) |
| 8 | MCARI2 | Modified chlorophyll absorption in reflectance#2 | MCARI1/np.sqrt((2*nir+1)**2-6*(nir-5*r)-0.5) |
| 9 | MSAVI | Modified soil adjusted vegetation index | (1/2)*(2*nir+1-np.sqrt((2*nir+1)**2-8*(nir-r))) |
| 10 | OSAVI | Optimised soil adjusted vegetation index | (1+0.16)*(nir-r)/(nir+r+0.16) |
| 11 | SRI | Simple ratio index | nir/g |
| 12 | MSR | Modified simple ratio | ((nir/r)-1)/(np.sqrt((nir/r)+1)) |
| 13 | MTVI | Modified triangular vegetation index | 1.2*(1.2*(nir-g)-2.5*(r-g)) |
| 14 | PCD | Plant canopy density | nir/r |
| 15 | PRI | Photo-chemical reflective index | (g-b)/(g+b) |
| 16 | RDVI | Renormalised difference vegetation index | (nir-r)/np.sqrt(nir+r) |
| 17 | TCARI | Transformed chlorophyll absorption reflectance index | 3*((re-r)-0.2*(re-g)*(re/r)) |
| 18 | TCARI/OSAVI | | TCARI/OSAVI |
| 19 | VDVI | Visible-band difference vegetation index | (2*g - r - b)/(2*g + r + b) |
| 20 | ENDVI#1 | Enhanced normalised difference vegetation index#1 | ((nir+g)-2*b)/(nir+g+2*b) |
| 21 | ENDVI#2 | Enhanced normalised difference vegetation index#2 | ((nir+g)-2*r)/(nir+g+2*r) |
| 22 | ENDVI#3 | Enhanced normalised difference vegetation index#3 | ((nir+g)-r-b)/(nir+g+r+b) |

#### 4.4.5.5.3 Thermal indices

Various thermal indices were computed using the five bands of the multispectral images (see Table ).

*Table 5: The indices computed using the thermal data.*

| SN | Name | Description | Formula |
|---|---|---|---|
| 1 | Tc | Mean temperature of the canopy | n/a |
| 2 | Tc/Ta | Canopy to atmospheric temperature ratio | Tc/Ta |

| | | | |
|---|---|---|---|
| 3 | Tc-Ta | Canopy to the atmosphere temperature difference | Tc-Ta |
| 4 | CWSI | Crop water stress index | (Tc-Twet)/(Tdry-Twet) |
| 5 | ig | Crop water stress index | (Tdry-Tc)/(Tc-Twet) |
| 6 | i3 | Crop water stress index | (Tc-Twet)/(Tdry-Tc) |

#### 4.4.5.5.4 Composite indices

Various thermal indices were computed using the five bands of the multispectral images (see Table 6).

*Table 6: The composite indices computed using the thermal, spectral, and structural indices.*

| SN | Name | Description | Formula |
|---|---|---|---|
| 1 | cum_ndvi | Cumulative NDVI for entire canopy | NDVI*area |
| 2 | TVDI | Temperature vegetation dryness index | Tc/NDVI |
| 3 | TVDI#1 | Temperature vegetation dryness index#1 | (Tc-Ta)/NDVI |
| 4 | TVDI#2 | Temperature vegetation dryness index#2 | CWSI/NDVI |
| 5 | TVDI#3 | Temperature vegetation dryness index#3 | ig/NDVI |
| 6 | TVDI#4 | Temperature vegetation dryness index#4 | i3/NDVI |

### 4.4.6 Financial Analysis

The following economic parameters were calculated for the last 3 seasons (2018-2021): Economic Productivity (EP), Economic Water Productivity (EWP), unit production cost, total operational cost, income, cash flow, Net Present Value (NPV), Internal Rate of Return (IRR), Pay-back Period (PB) and total margin.

$$EEEE = \frac{GGGGGGGGGG\ \ mmmmGGmmmmmm\ \ (\$)}{TTGGTTmmTT\ \ yymmyyTTyy\ \ ()}$$

$$EEEEEE = \frac{GGGGGGGGGG\ \ mmmmGGmmmmmm\ \ (\$)}{TTGGTTmmTT\ \ mmGGGGmmmmmmTTmmGGmm\ \ wwmmTTyyGG\ \ (\text{Ⅲ})}$$

$$BBEE = \frac{TTGGTTmmTT\ \ GGooyyGGmmTTmmGGmmmmTT\ \ ccGGGGTTGG\ \ (\$)}{TTGGTTmmTT\ \ yymmyyTTyy\ \ ()}$$

Discounted cash flow analysis (DCFA) was undertaken in order to investigate each irrigation strategy based on estimated future farm returns to calculated the net present value (NPV):

$$NNEENN = -kk + \sum_{TT=11}^{mm} \frac{CCCC_{m\ \ m}}{(11+mm)^{mm}}$$

See the attached paper in the Appendix for details on these financial parameters as well as model assumptions.

### 4.4.7 Vineyard Irrigation Survey

A survey was conducted to understand the irrigation practices of grapevine growers in the Limestone Coast viticultural regions. This survey was launched on 14 June 2021 and closed on 23 August 2021. Growers were asked about their current operation, irrigation practices, use of data to inform irrigation scheduling and awareness of water status sensors and their value.

# 5 Results and discussion

## 5.1 Seasonal irrigation

Table 7 shows the total irrigation, in ML/ha, supplied to all irrigation treatments across the three vineyards.

*Table 7: Total irrigation (ML/ha) supplied across the three vineyards during each season.*

| | AX88-E | | | AX88-W | | | Katnook | | | |
|---|---|---|---|---|---|---|---|---|---|---|
| **Season** | S1 | S2 | S3 | S1 | S2 | S3 | S1 | S2 | S3 | S4 |
| **CONV** | 0.6 | 0.55 | 0.55 | 0.45 | 0.46 | 0.35 | - | 0.936 | 1.2 | 0.72 |
| **CONV+** | - | - | 1.01 | - | - | 0.7 | - | - | 2.39 | 1.43 |
| **ET** | 0.3 | 0.4 | 0.21 | 0.14 | 0.34 | 0.21 | - | 0.672 | 0.5 | 0.57 |
| **PWS1** | 0.3 | 0.44 | 0.37 | 0.14 | 0.31 | 0.25 | - | 0.672 | 0.54 | 0.42 |
| **PWS2** | - | - | - | - | - | - | - | - | - | 0.62 |
| **SWS** | 0.6 | 0.34 | 0.34 | 0.45 | 0.37 | 0.25 | - | 0.552 | 0.53 | 0.59 |

As shown in Table 8, the evidence-based strategies reduced the amount of irrigation applied significantly relative to conventional treatment.

*Table 8: Irrigation supplied as a percentage of CONV treatment across the three vineyards during each season.*

| | AX88-E | | | AX88-W | | | Katnook | | | |
|---|---|---|---|---|---|---|---|---|---|---|
| **Season** | **S1** | **S2** | **S3** | **S1** | **S2** | **S3** | **S1** | **S2** | **S3** | **S4** |
| **ET** | 50 | 73 | 38 | 31 | 74 | 60 | - | 72 | 42 | 79 |
| **PWS1** | 50 | 80 | 67 | 31 | 67 | 71 | - | 72 | 45 | 58 |
| **PWS2** | - | - | - | - | - | - | - | - | - | 86 |
| **SWS** | - | 62 | 62 | 100 | 80 | 71 | - | 59 | 44 | 82 |

## 5.2 Soil moisture and vine performance measured via proximal sensing

### 5.2.1 Seasonal soil moisture

Soil moisture content significantly varied across three different vineyards and between vines irrigated according to different sensor-driven schedules.

***2018/19 season***

In both Alex88-East and Alex88-West, no statistically significant differences were observed in $\Psi_{pd}$ between irrigation treatments at the pre-véraison stage. However, during post-véraison stage, $\Psi_{pd}$ was significantly lower in both ET and PWS vines relative to CONV (Figure 19). In Alex88-east, the percentage of volumetric water content (%VWC) of ET vines was slightly higher that CONV vines throughout the season, whereas PWS vines exhibited lower VWC relative to CONV. In contrast, both ET and PWS vines exhibited lower VWC compared to CONV vines. The SHI vines in Prodigy vineyard had consistently higher soil moisture levels compared to the treatment block (Fig 19e).

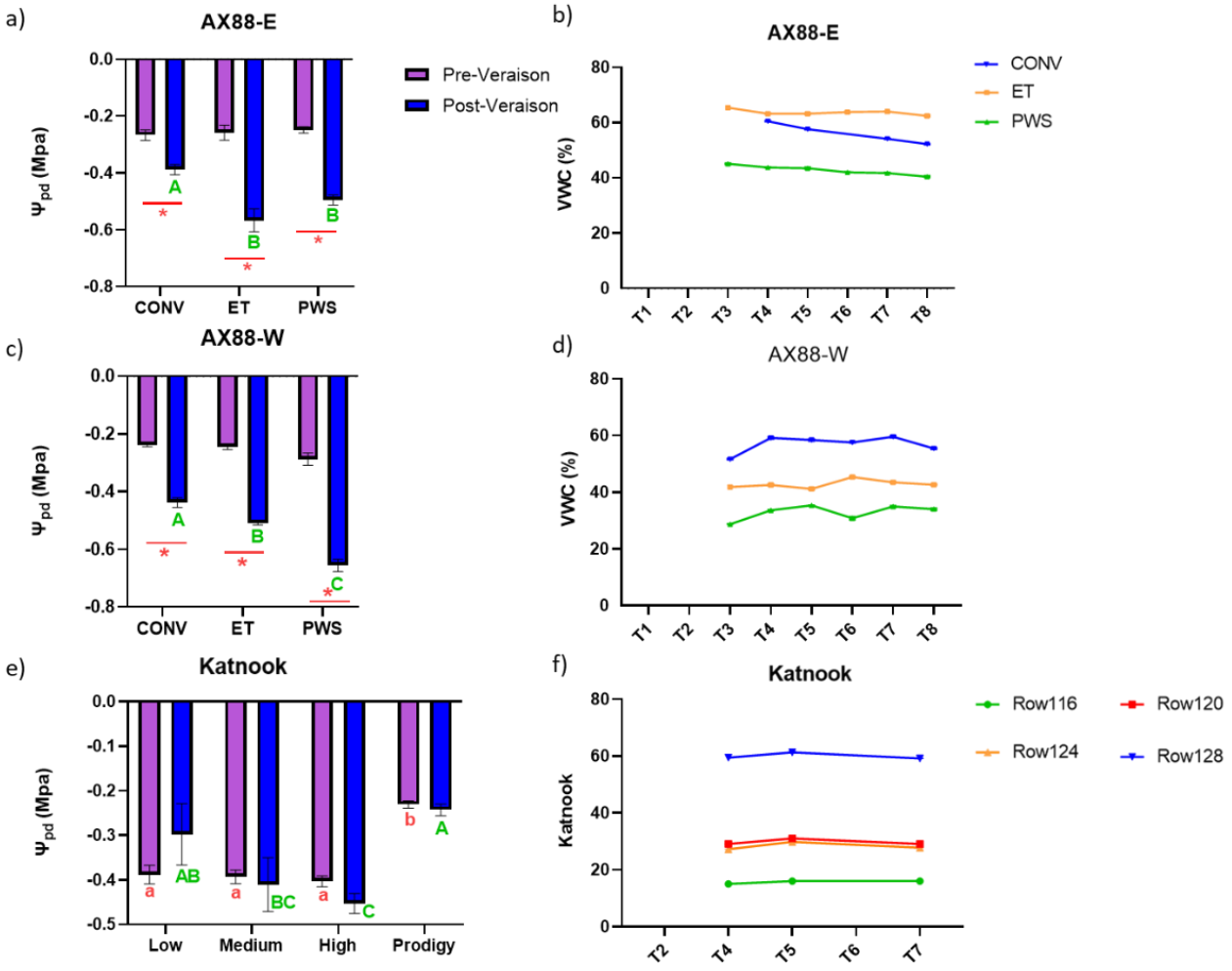



*Figure 19: Variations in pre-dawn water potential ($\Psi_{pd}$) (a, c, e) and percentage of volumetric water content (%VWC) (b, d, f) in CAS and SHI in response to different irrigation treatments. Values are means ± SEM of four biological replicates. Statistical analysis was conducted using two-way ANOVA. Asterisks indicate statistically significant differences (P<0.05) between pre- and post-véraison stages. Lowercase letters indicate statistically significant differences (P<0.05) between irrigation treatments at pre-véraison stage. Uppercase letters indicate statistically significant differences (P<0.05) between irrigation treatments at post-véraison stage.*

### *2019/20 season*

Similar to the previous season, no statistically significant differences were observed in $\Psi_{pd}$ between irrigation treatments in both Alex88-east and Katnook vines before véraison. After véraison, $\Psi_{pd}$ was significantly higher in ET, PWS and SWS vines in Alex88-east relative to CONV vines. However, any irrigation treatment in Katnook, did not cause any differences in $\Psi_{pd}$ after véraison. Even though, PWS and SWS vines in Alex88-west exhibited similar $\Psi_{pd}$ to CONV vines before and after véraison, their $\Psi_{pd}$ was significantly lower throughout the season relative to ET vines (Figure 20). The soil moisture levels in the Prodigy block were similar to the treatment block.

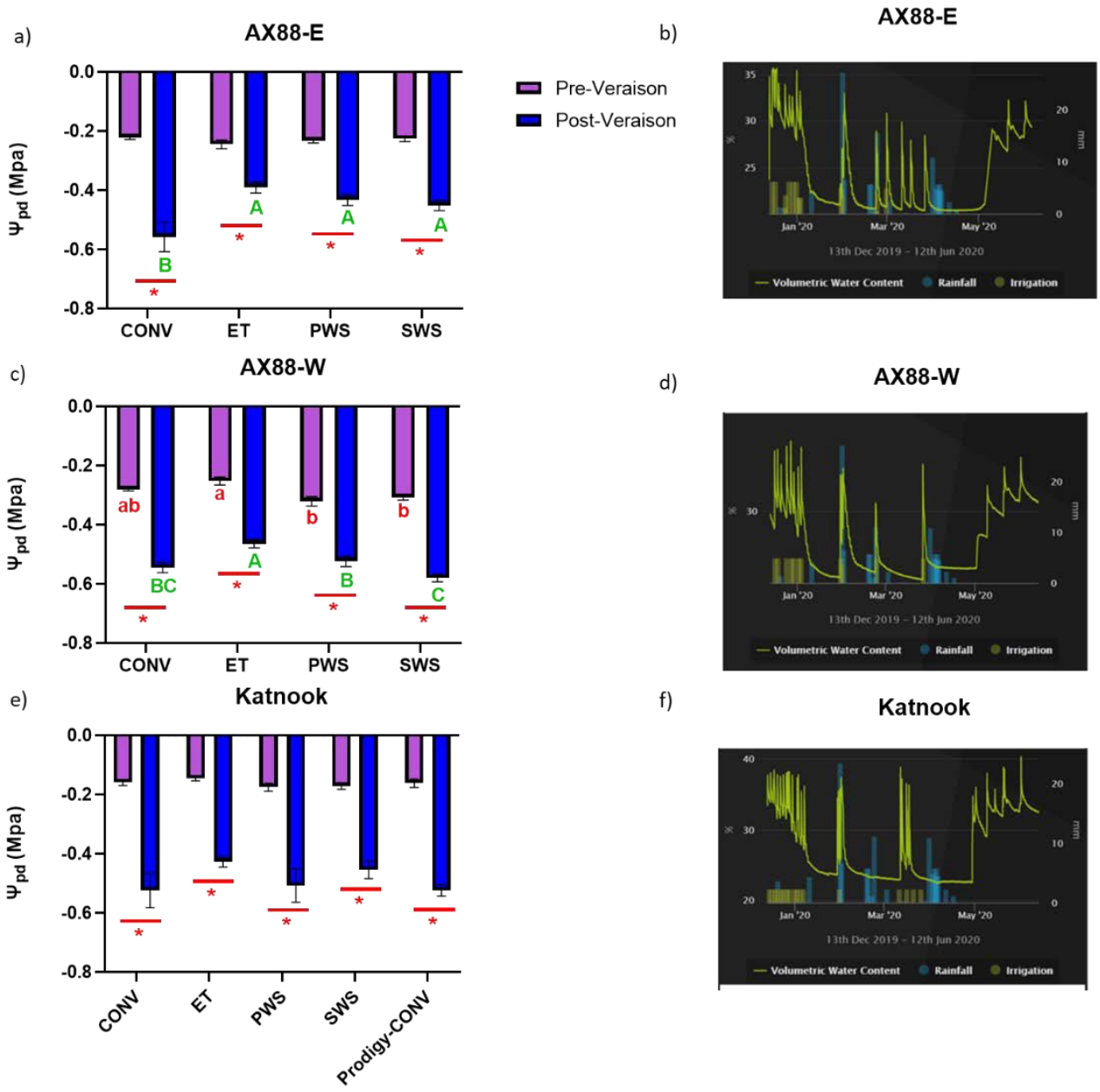



*Figure 20: Variations in predawn water potential ($\Psi_{pd}$) (a, c, e) and percentage of volumetric water content (%VWC) (b, d, f) in CAS and SHI in response to different irrigation treatments. Values are means ± SEM of eight biological replicates. Statistical analysis was conducted using two-way ANOVA. Asterisks indicate statistically significant differences (P<0.05) between pre- and post-véraison stages. Lowercase letters indicate statistically significant differences (P<0.05) between irrigation treatments at pre-véraison stage. Uppercase letters indicate statistically significant differences (P<0.05) between irrigation treatments at post-véraison stage.*

### *2020/21 season*

In Alex88-east, $\Psi_{pd}$ was similar in ET and SWS vines relative to CONV vines before the véraison, whereas PWS vines showed significantly lower $\Psi_{pd}$. The post-véraison $\Psi_{pd}$ in PWS and SWS was similar to CONV, but ET vines displayed significantly lower $\Psi_{pd}$ compared to CONV. In Alex88-west, PWS and SWS vines had significantly lower pre-véraison $\Psi_{pd}$ values relative to CONV, but after véraison, $\Psi_{pd}$ was significantly lower in ET and SWS treatments compared to CONV. In SHI in Katnook, pre-véraison $\Psi_{pd}$ did not change in response to different irrigation treatments, however, $\Psi_{pd}$ in ET, PWS and SWS vines after véraison were markedly lower relative to CONV (Figure 21).

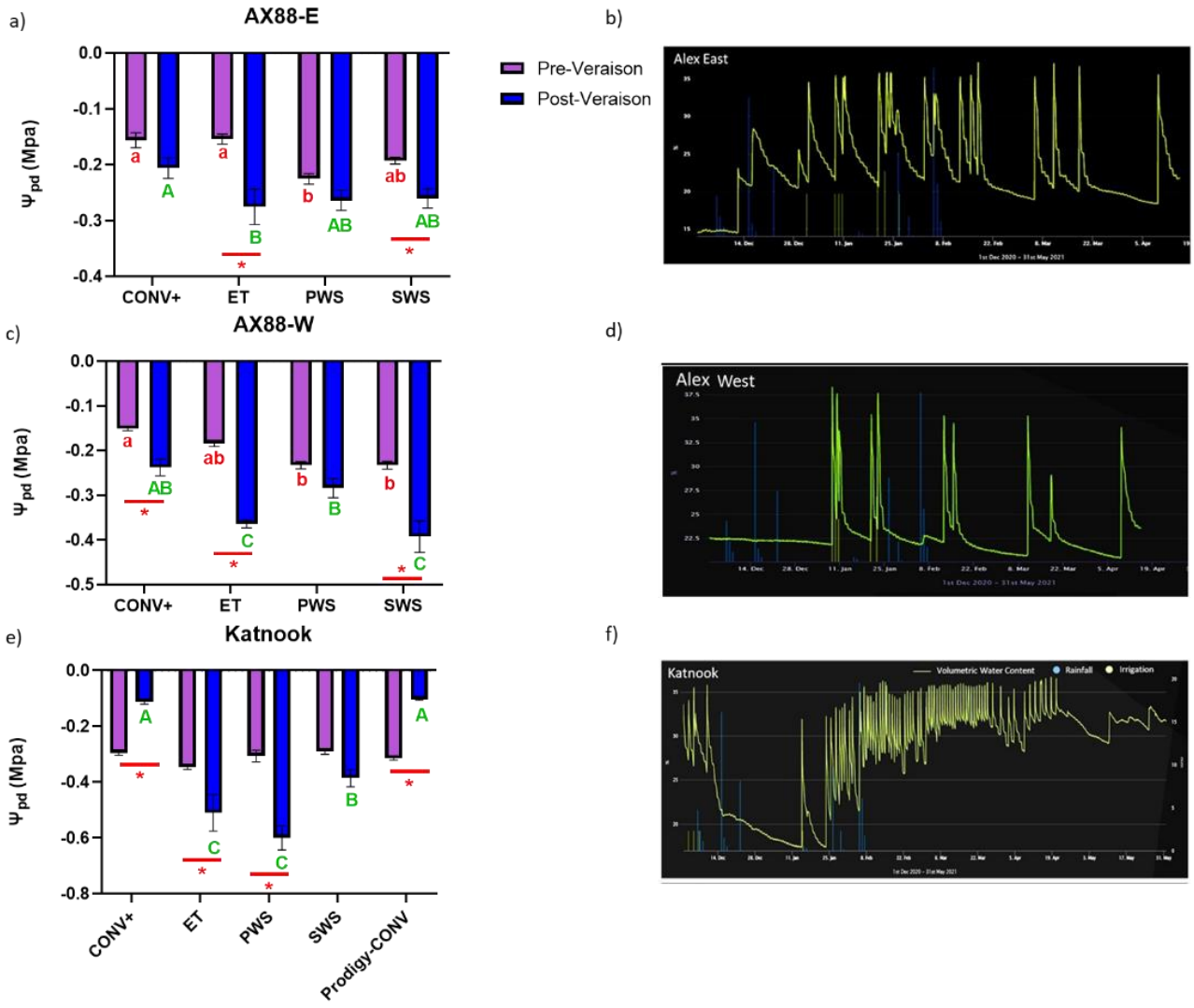



*Figure 21: Variations in predawn water potential ($\Psi_{pd}$) (a, c, e) and percentage of volumetric water content (%VWC) (b, d, f) in CAS and SHI in response to different irrigation treatments. Values are means ± SEM of eight biological replicates. Statistical analysis was conducted using two-way ANOVA. Asterisks indicate statistically significant differences (P<0.05) between pre- and post-véraison stages. Lowercase letters indicate statistically significant differences (P<0.05) between irrigation treatments at pre- véraison stage. Uppercase letters indicate statistically significant differences (P<0.05) between irrigation treatments at post- véraison stage.*

### *2021/22 season*

Unlike previous seasons, different irrigation treatments caused significant variations in $\Psi_{pd}$ in SHI. For instance, before and after véraison, $\Psi_{pd}$ was significantly lower in ET, PWS1, PWS2 and SWS vines relative to CONV, CONV+ and Prodigy vines (Figure 22). The Prodigy block had consistently higher soil moisture levels compared to the treatment block.

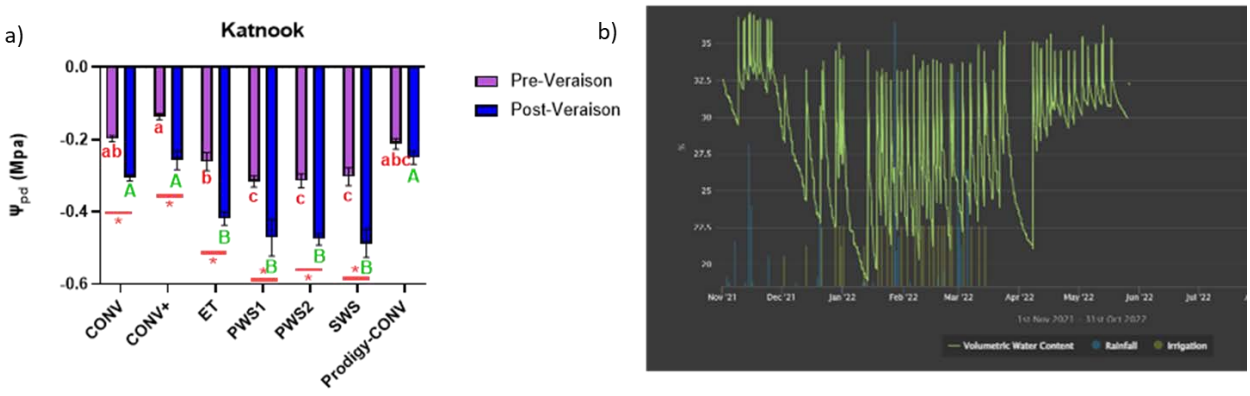



*Figure 22: Variations in predawn water potential ($\Psi_{pd}$) (a, c, e) and percentage of volumetric water content (%VWC) (b, d, f) in SHI in response to different irrigation treatments. Values are means ± SEM of eight biological replicates. Statistical analysis was conducted using two-way ANOVA. Asterisks indicate statistically significant differences (P<0.05) between pre- and post-véraison stages. Lowercase letters indicate statistically significant differences (P<0.05) between irrigation treatments at pre-véraison stage. Uppercase letters indicate statistically significant differences (P<0.05) between irrigation treatments at post-véraison stage.*

### 5.2.2 Seasonal light interception and vine vigour (Leaf area index and porosity)

In Alex88-East and Alex88-West, no statistically significant differences in LAI and porosity were observed between irrigation treatments both at pre- and post-véraison stages across three seasons (2018/19, 2019/20 and 2020/21). Even though it was consistently observed across three seasons that the LAI and porosity in SHI at Katnook were similar between irrigation treatments both before and after véraison (except in 2020/21 season), Prodigy vines always produced relatively smaller canopy sizes and higher porosity levels (Figure 23, 24, 25 and 26). The high porosity in Prodigy may have been a contributing factor to the high grape composition and quality in that block.

*2018/19 season*

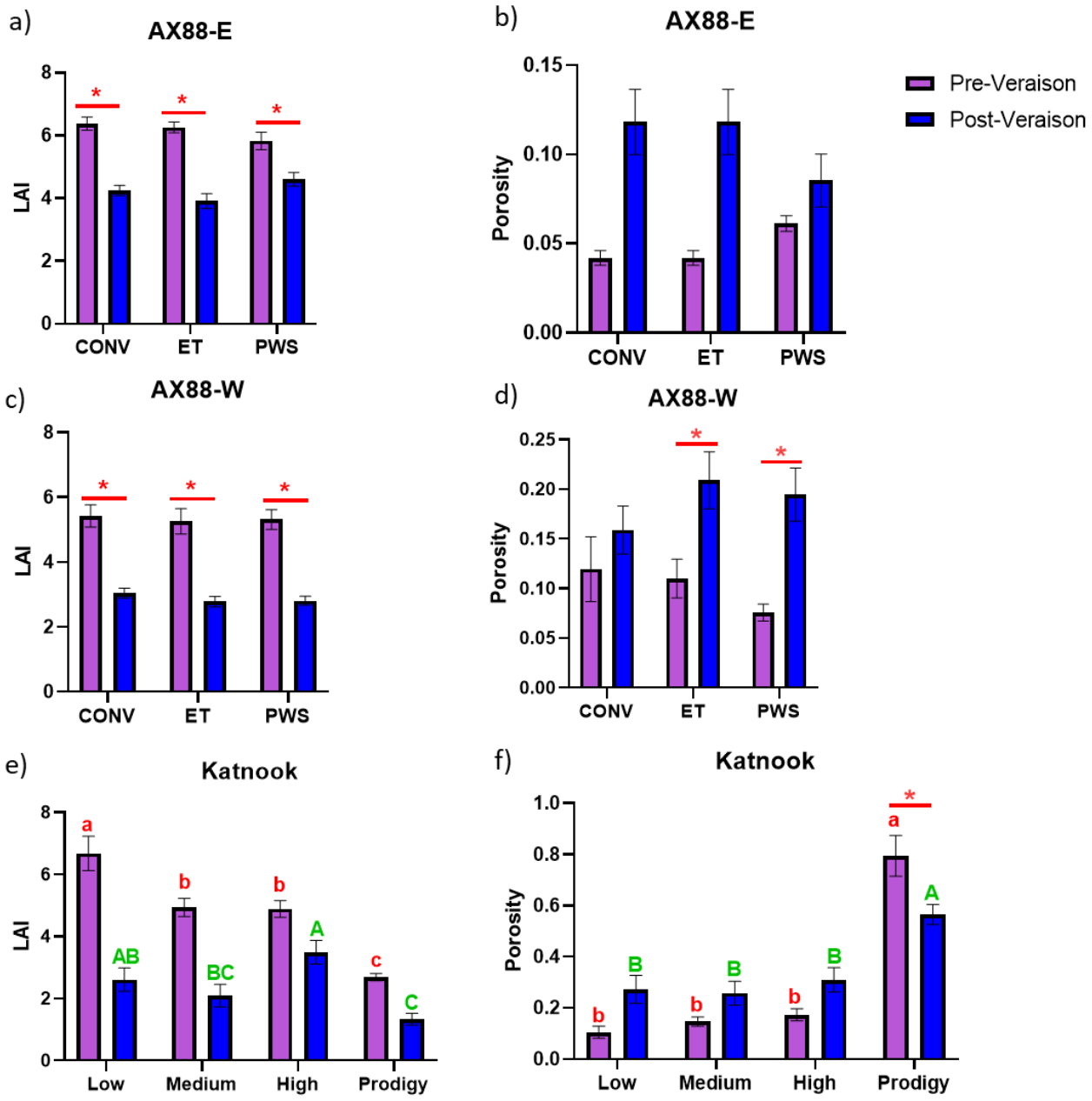



*Figure 23: Changes in Leaf Area Index (LAI) (a, c, e) and porosity (b, d, f) in CAS and SHI in response to different irrigation treatments. Values are means ± SEM of eight biological replicates. Statistical analysis was conducted using two-way ANOVA. Asterisks indicate statistically significant differences (P<0.05) between pre- and post-véraison stages. Lowercase letters indicate statistically significant differences (P<0.05) between irrigation treatments at pre-véraison stage. Uppercase letters indicate statistically significant differences (P<0.05) between irrigation treatments at post-véraison stage.*

### *2019/20 season*

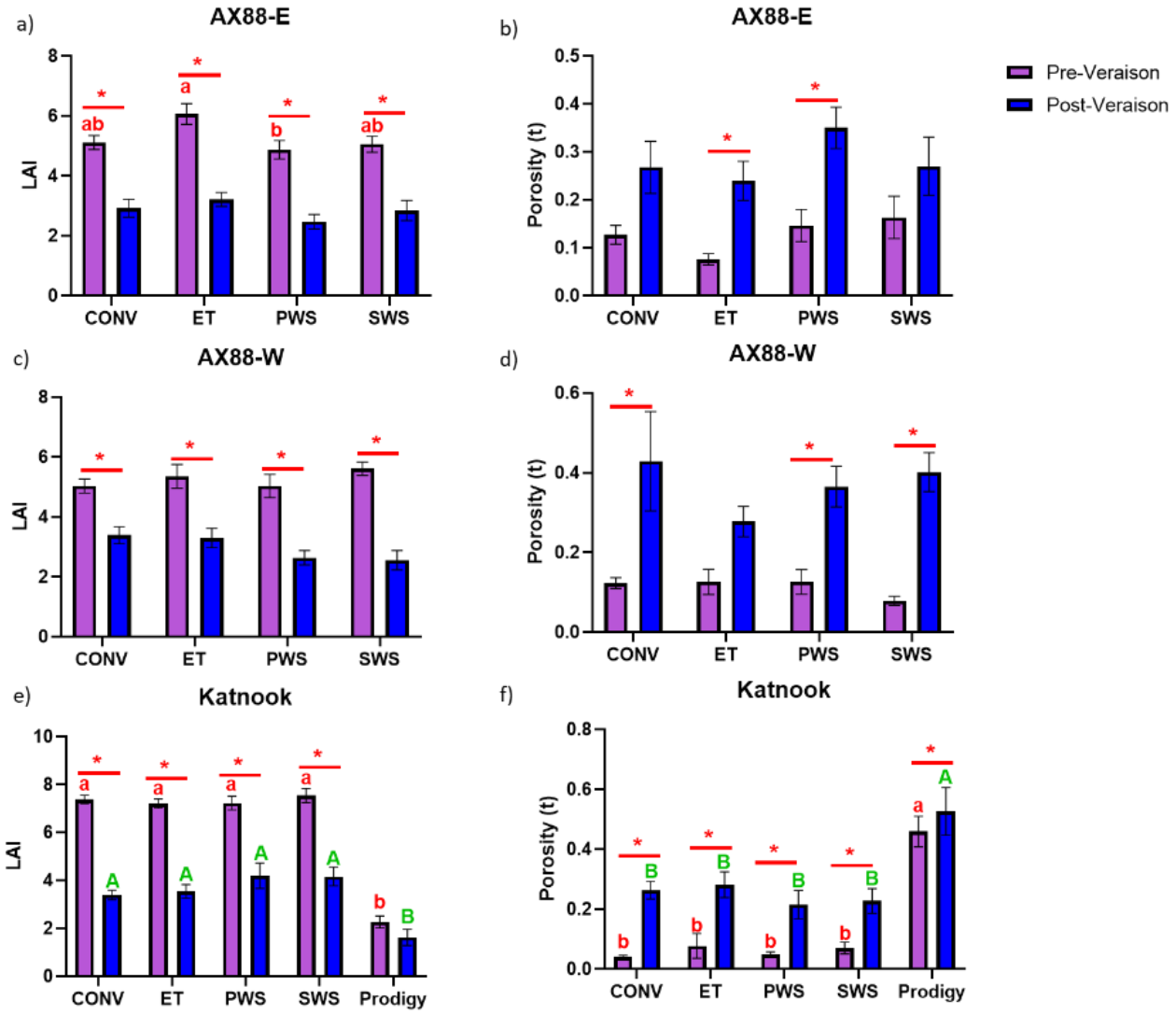



*Figure 24: Changes in Leaf Area Index (LAI) (a, c, e) and porosity (b, d, f) in CAS and SHI in response to different irrigation treatments. Values are means ± SEM of eight biological replicates. Statistical analysis was conducted using two-way ANOVA. Asterisks indicate statistically significant differences (P<0.05) between pre- and post-véraison stages. Lowercase letters indicate statistically significant differences (P<0.05) between irrigation treatments at pre-véraison stage. Uppercase letters indicate statistically significant differences (P<0.05) between irrigation treatments at post-véraison stage.*

### *2020/21 season*

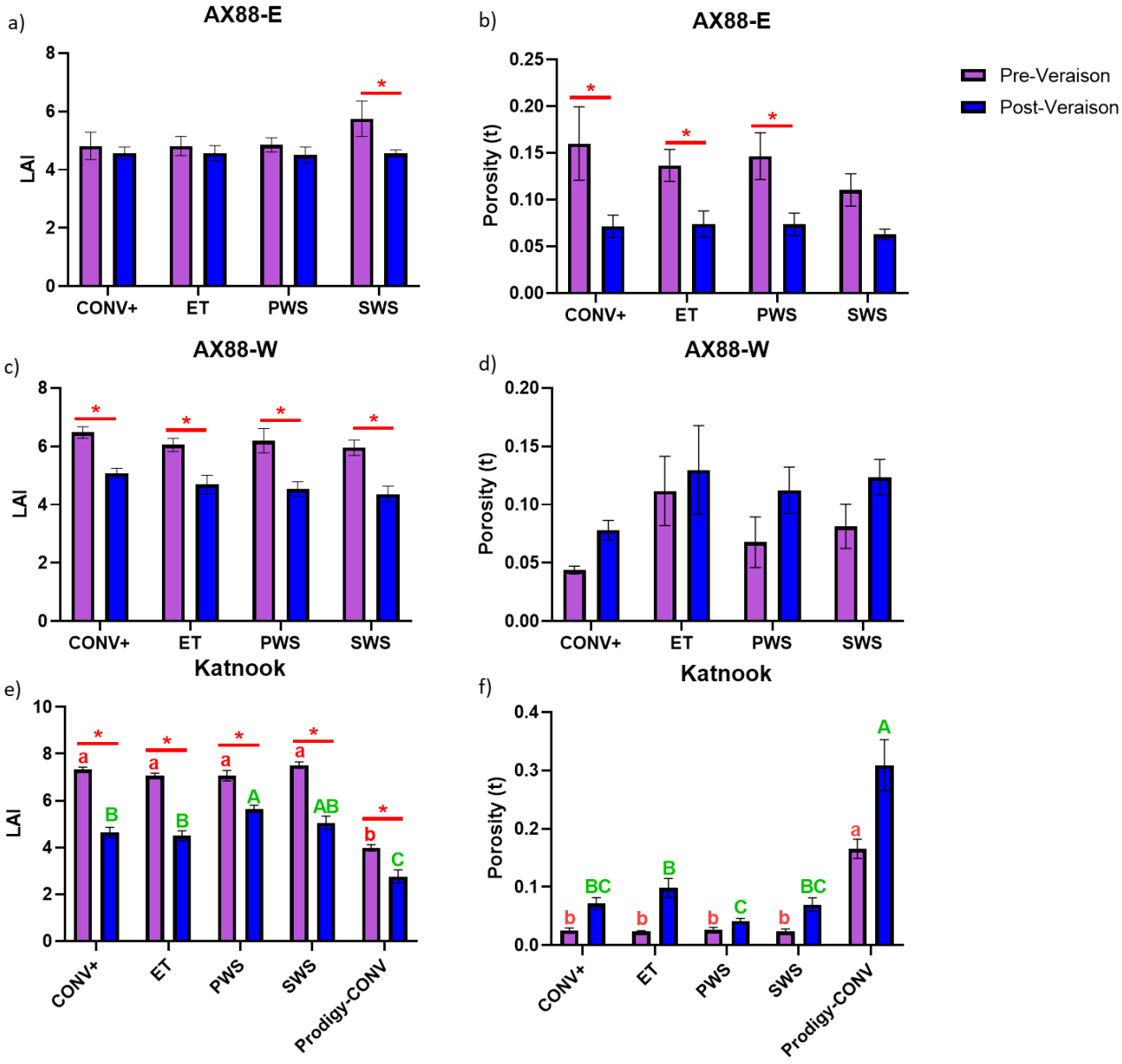



*Figure 25: Changes in Leaf Area Index (LAI) (a, c, e) and porosity (b, d, f) in CAS and SHI in response to different irrigation treatments. Values are means ± SEM of eight biological replicates. Statistical analysis was conducted using two-way ANOVA. Asterisks indicate statistically significant differences (P<0.05) between pre- and post-véraison stages. Lowercase letters indicate statistically significant differences (P<0.05) between irrigation treatments at pre-véraison stage. Uppercase letters indicate statistically significant differences (P<0.05) between irrigation treatments at post-véraison stage.*

### *2021/22 season*

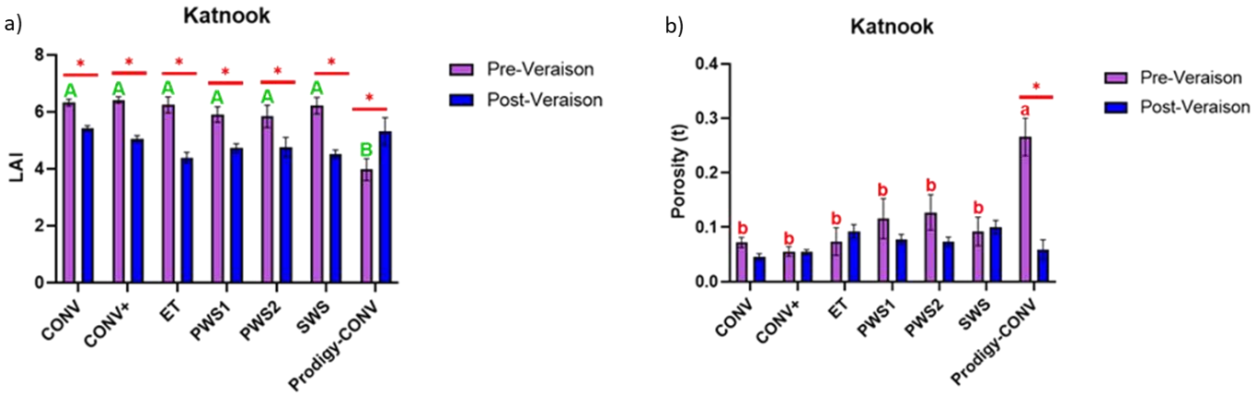



*Figure 26: Changes in Leaf Area Index (LAI) (a, c, e) and porosity (b, d, f) in SHI in response to different irrigation treatments. Values are means ± SEM of eight biological replicates. Statistical analysis was conducted using two-way ANOVA. Asterisks indicate statistically significant differences (P<0.05) between pre- and post-véraison stages. Lowercase letters indicate statistically significant differences (P<0.05) between irrigation treatments at pre-véraison stage. Uppercase letters indicate statistically significant differences (P<0.05) between irrigation treatments at post-véraison stage.*

### 5.2.3 Seasonal evapotranspiration ($ET_0$) and crop coefficient ($K_c$)

Variation in rainfall, evapotranspiration and crop coefficient during each season are shown in Figures 27-30.

***2018/19 season***

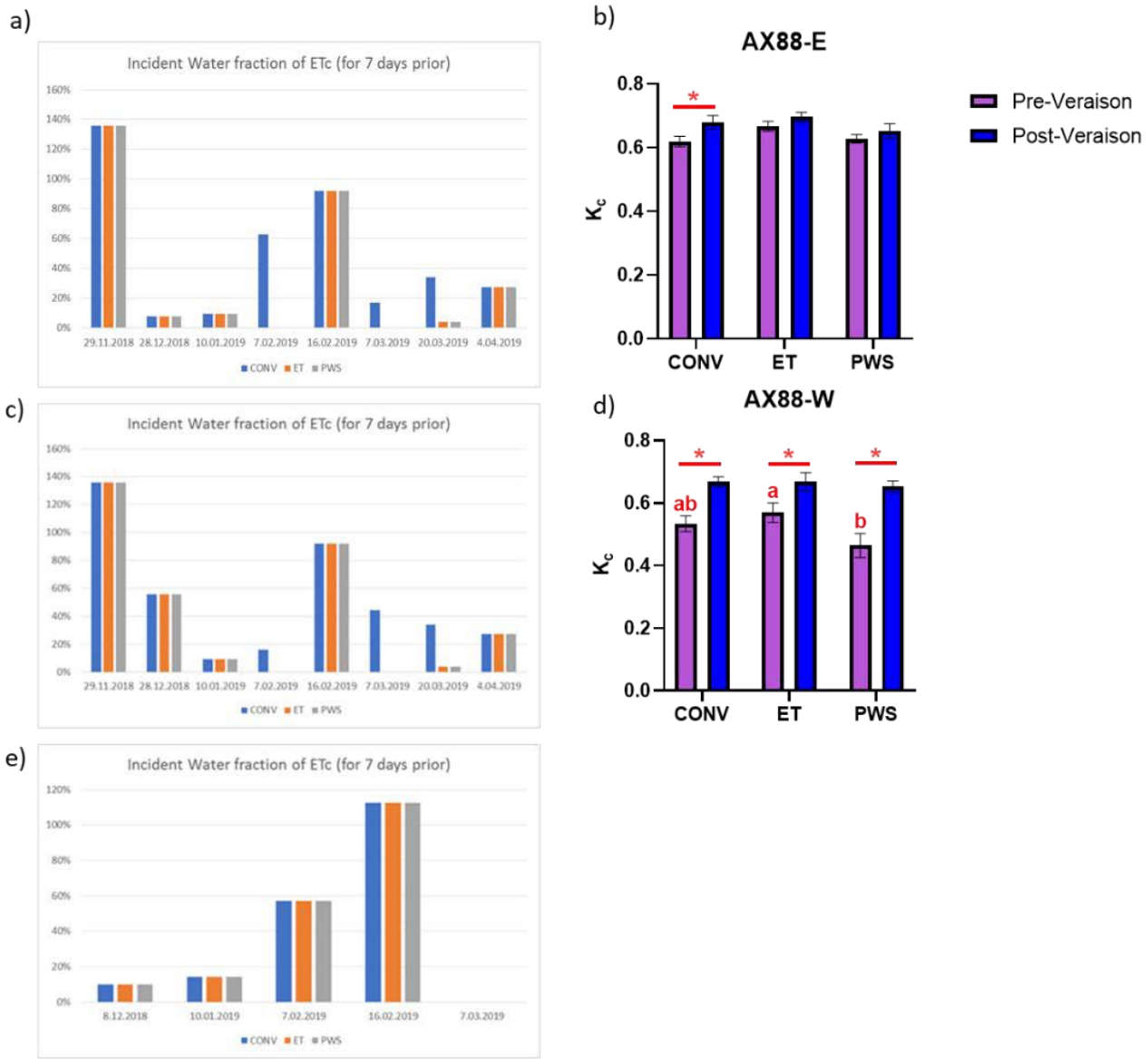



*Figure 27: Seasonal Crop Evapotranspiration (ETc) (a, c, e) and crop factor (Kc) (b, d) in CAS (a-d) and SHI (e) in response to different irrigation treatments. Values are means ± SEM of eight biological replicates. Statistical analysis was conducted using two-way ANOVA. Asterisks indicate statistically significant differences (P<0.05) between pre- and post-véraison stages. Lowercase letters indicate statistically significant differences (P<0.05) between irrigation treatments at pre-véraison stage.*

## *2019/20 season*

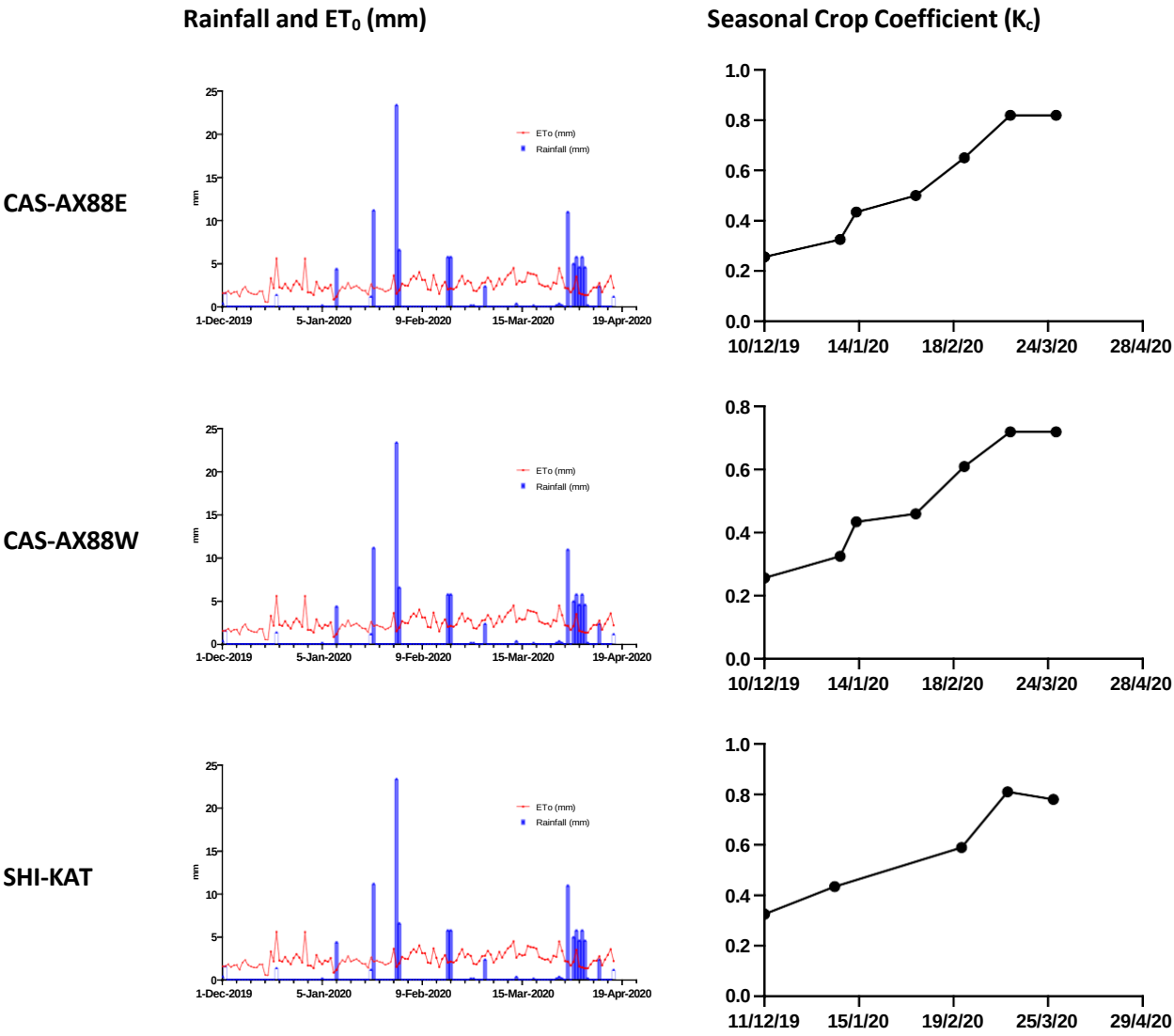



*Figure 28: Seasonal Crop Evapotranspiration (ETc) (a, c, e) and crop factor (Kc) (b, d) in CAS and SHI in response to different irrigation treatments.*

### *2020/21 season*

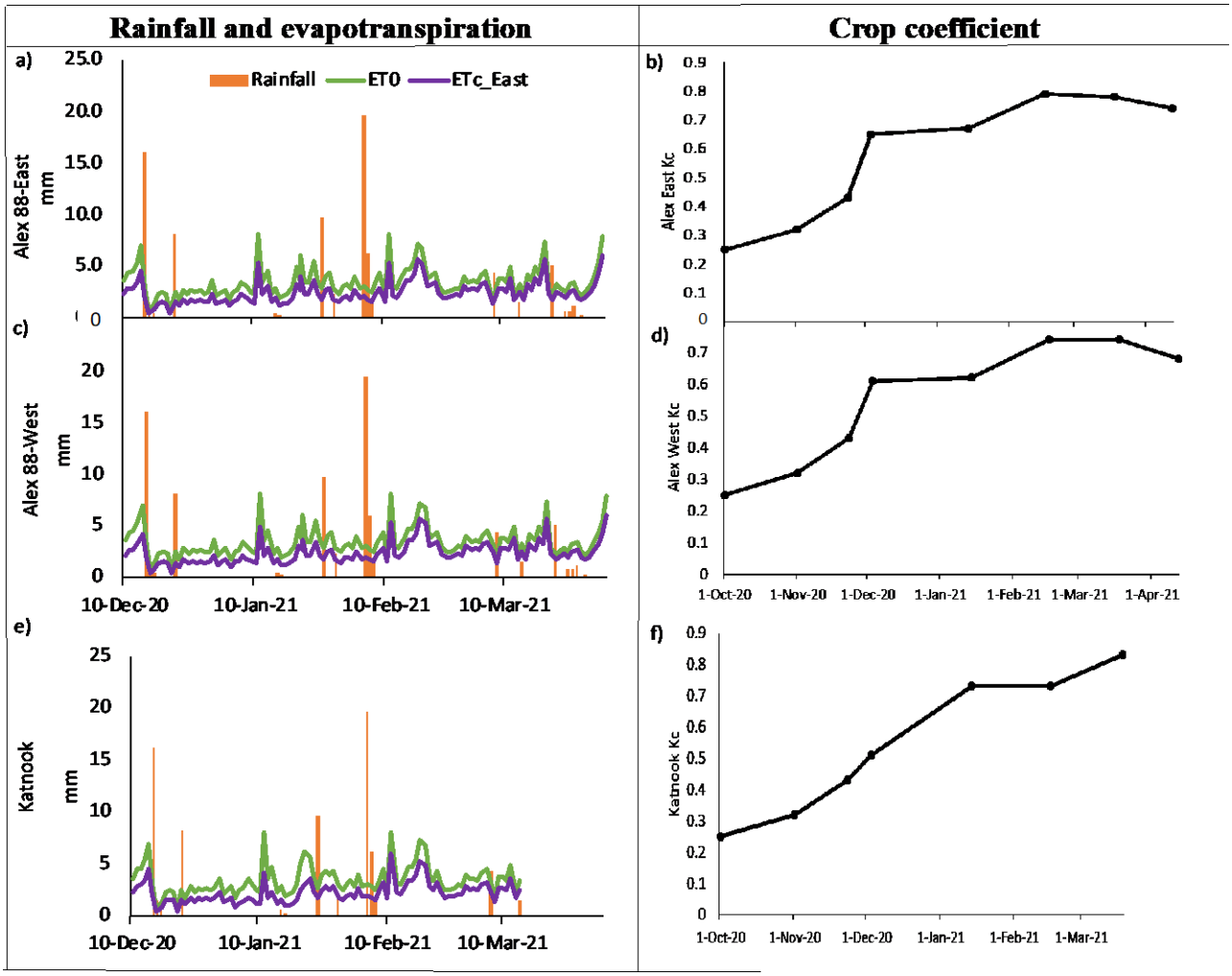



*Figure 29: Seasonal Crop Evapotranspiration (ETc) (a, c, e) and crop factor (Kc) (b, d) in CAS and SHI in response to different irrigation treatments.*

### *2021/22 season*

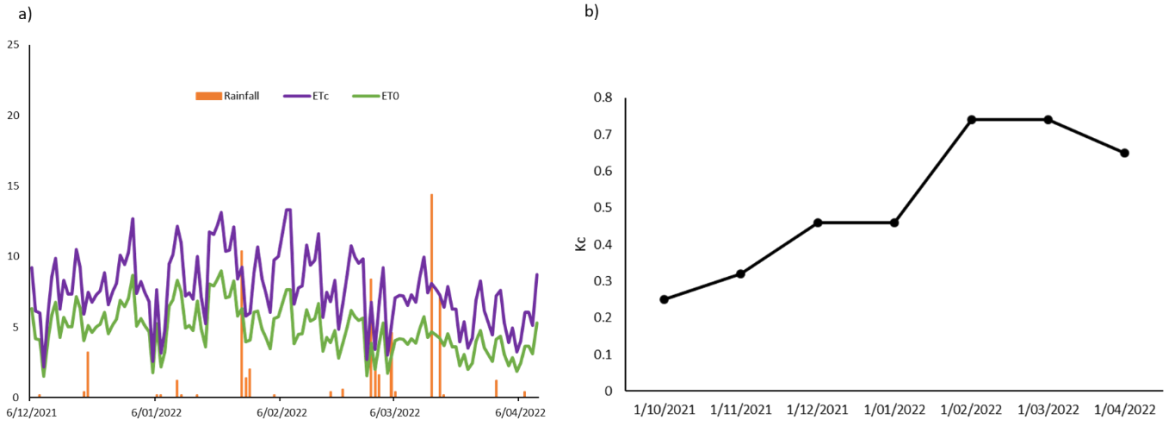



*Figure 30: Seasonal Crop Evapotranspiration (ETc) (a, c, e) and crop factor (Kc) (b, d) in SHI in response to different irrigation treatments.*

### 5.2.4 Seasonal plant water status and stomatal conductance

In both Alex88-East and Alex88-west, plant water status did not significantly change at the pre-vérasion stage, across three seasons from 2018 to 2021, except in 2020/21 season where PWS and SWS vines showed significantly lower $\Psi_{stem}$ relative to ET vines. However, after véraison, ET and PWS vines exhibited significantly lower $\Psi_{stem}$ relative to CONV in the 2018/19 season. Similar reduction of $\Psi_{stem}$ was also observed in ET, PWS and SWS vines in the 2020/21 season in Alex88-east. In the same season, in Alex88-west, $\Psi_{stem}$ in ET and SWS was also significantly lower relative to CONV. In the 2019/20 season, no statistically significant differences in $\Psi_{stem}$ were detected between irrigation treatments post-véraison in SHI. In the 2020/21 season, $\Psi_{stem}$ was similar between CONV, PWS and SWS, whereas ET vines displayed significantly lower $\Psi_{stem}$ relative to the Prodigy vines. Interestingly, in the 2021/22 season, pre-véraison $\Psi_{stem}$ did not change in response to sensor-driven irrigation treatments relative to CONV. However, post-véraison $\Psi_{stem}$ was significantly higher in CONV+ and lower in PWS1, PWS2 and SWS compared to CONV.

In the 2018/19 growing season, PWS-based irrigation scheduling did not change pre-véraison stomatal conductance ($g_s$) in Alex88-East, however, it was significantly increased in response to ET treatment. After véraison, $g_s$ was markedly declined in both ET and PWS vines relative to CONV. Pre-véraison $g_s$ remained unchanged in all the treated vines in Alex88-east and Alex88-west across the rest of the seasons. However, after véraison, statistically significant variations were observed in $g_s$ in response to different irrigation treatments. In both 2019/20 and 2020/21 seasons, post-véraison $g_s$ remained unchanged in response to different irrigation scheduling in Katnook. However, the Prodigy vines displayed significantly lower $g_s$ relative to SHI in Katnook in the 2019/20 growing season. In the 2021/22 season, CONV+ and Prodigy vines exhibited significantly higher pre-véraison $g_s$ relative to other treatments. Among all the irrigation treatments, only PWS1 caused significant reduction in $g_s$ relative to CONV (Figure 31, 32, 33 and 34).

### *2018/19 season*

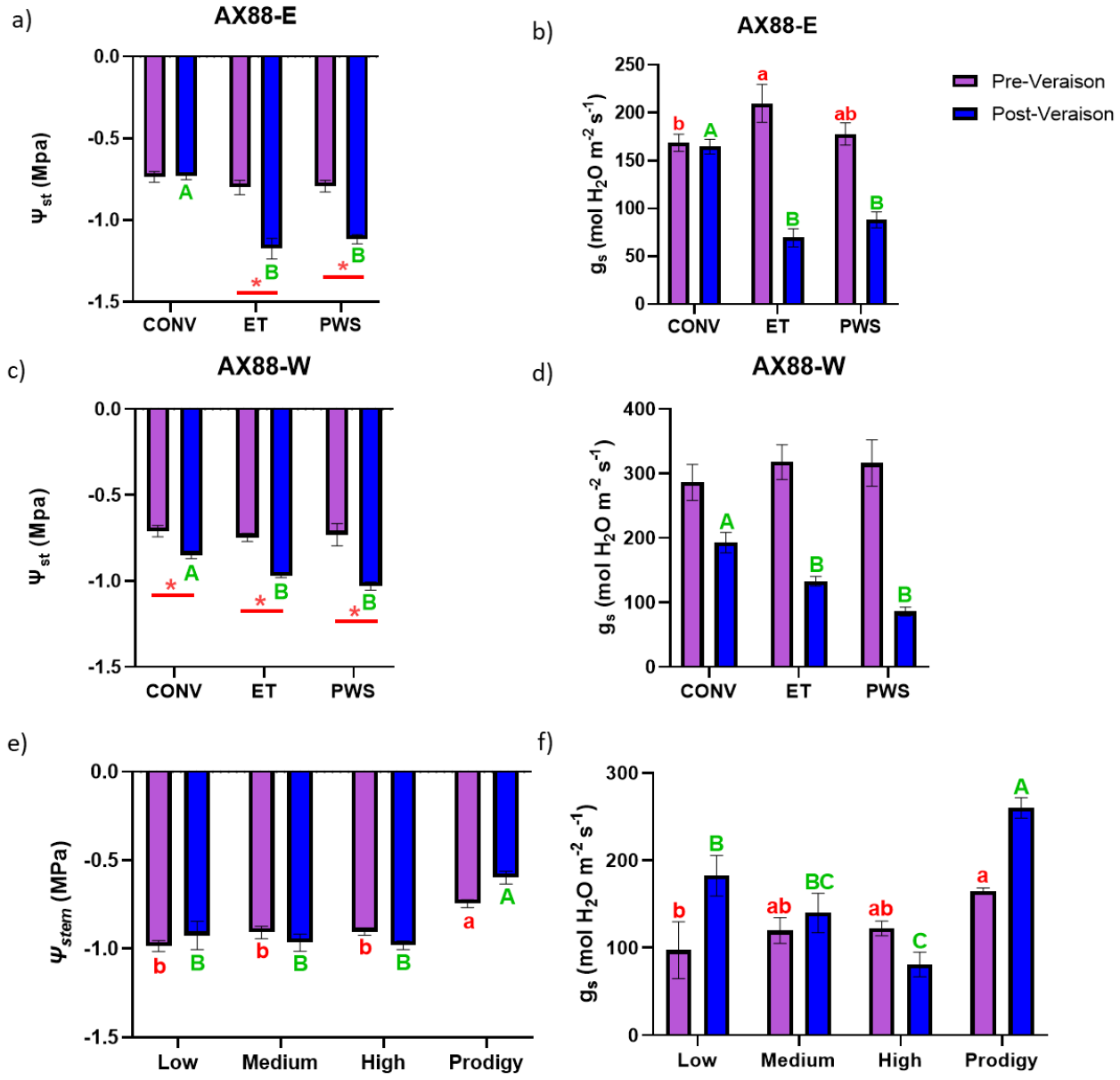



*Figure 31: Changes in Mid-day stem water potential ($\Psi_{stem}$) (a, c, e) and stomatal conductance ($g_s$) (b, d, f) in CAS and SHI in response to different irrigation treatments. Values are means ± SEM of four biological replicates. Statistical analysis was conducted using two-way ANOVA. Asterisks indicate statistically significant differences (P<0.05) between pre- and post-véraison stages. Lowercase letters indicate statistically significant differences (P<0.05) between irrigation treatments at pre-véraison stage. Uppercase letters indicate statistically significant differences (P<0.05) between irrigation treatments at post-véraison stage.*

### *2019/20 season*

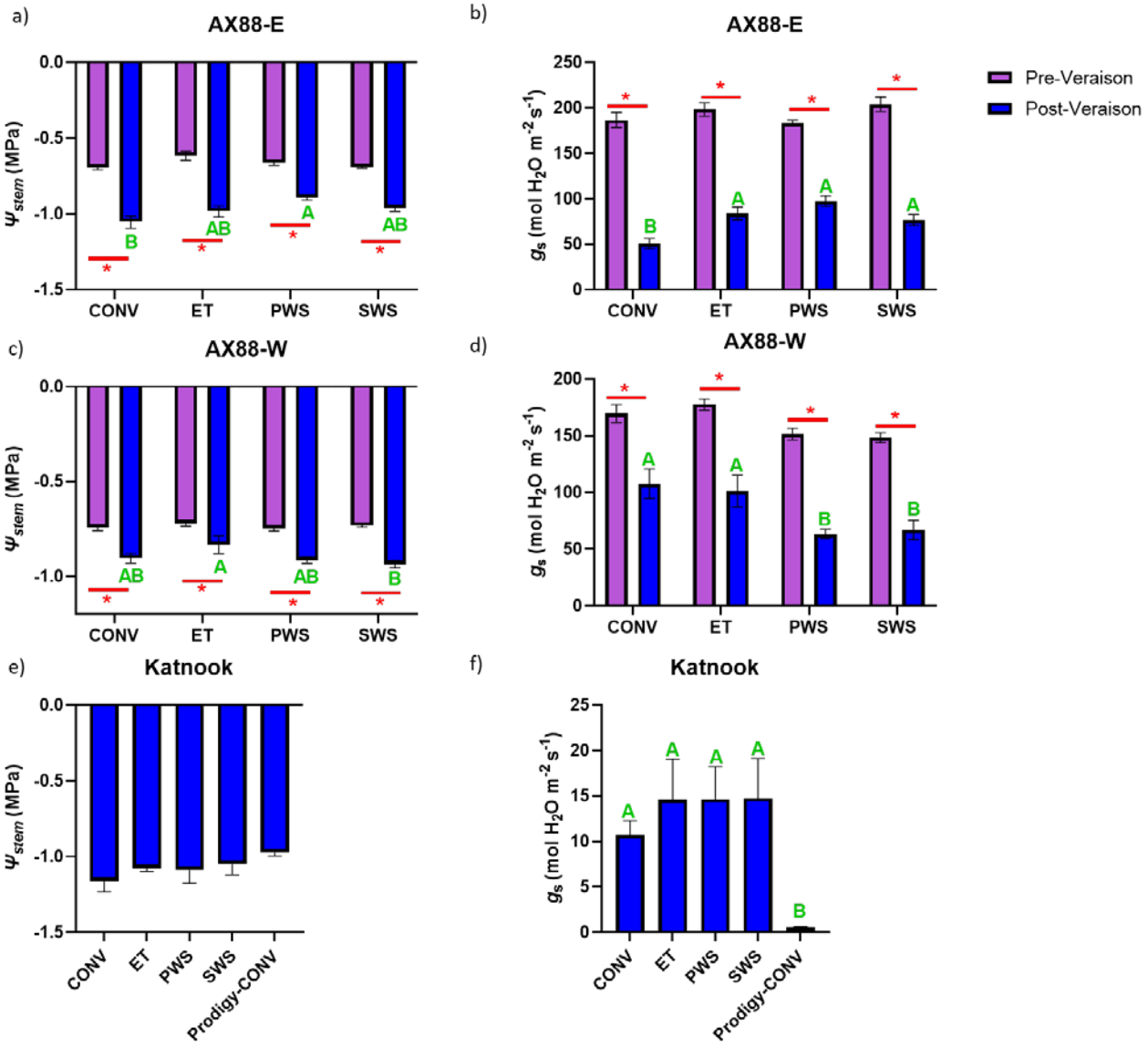



*Figure 32: Changes in Mid-day stem water potential ($\Psi_{stem}$) (a, c, e) and stomatal conductance ($g_s$) (b, d, f) in CAS and SHI in response to different irrigation treatments. Values are means ± SEM of eight biological replicates. Statistical analysis was conducted using two-way ANOVA. Asterisks indicate statistically significant differences (P<0.05) between pre- and post-véraison stages. Lowercase letters indicate statistically significant differences (P<0.05) between irrigation treatments at pre-véraison stage. Uppercase letters indicate statistically significant differences (P<0.05) between irrigation treatments at post-véraison stage.*

### *2020/21 season*

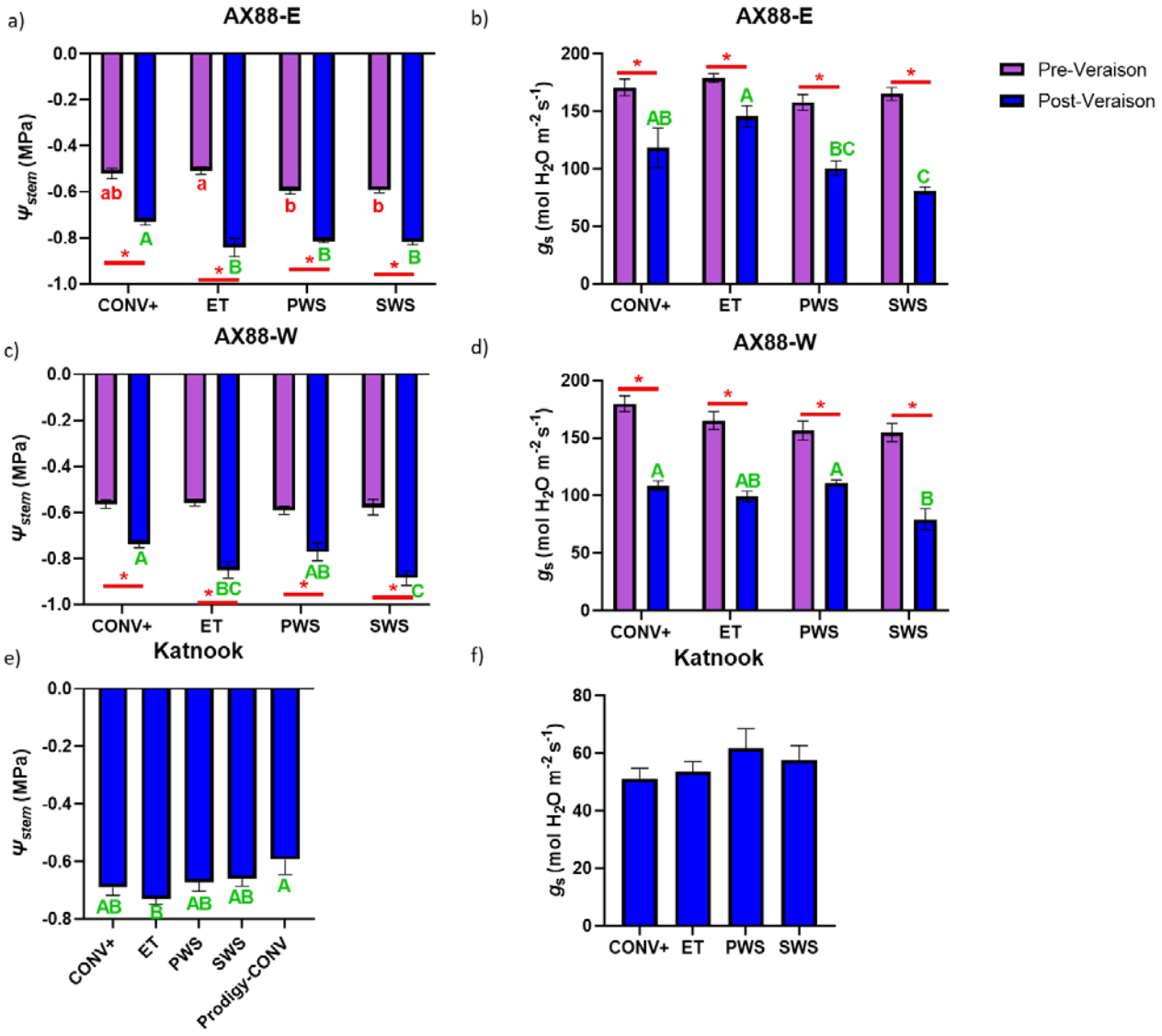



*Figure 33: Changes in Mid-day stem water potential ($\Psi_{stem}$) (a, c, e) and stomatal conductance ($g_s$) (b, d, f) in CAS and SHI in response to different irrigation treatments. Values are means ± SEM of eight biological replicates. Statistical analysis was conducted using two-way ANOVA. Asterisks indicate statistically significant differences (P<0.05) between pre- and post-véraison stages. Lowercase letters indicate statistically significant differences (P<0.05) between irrigation treatments at pre-véraison stage. Uppercase letters indicate statistically significant differences (P<0.05) between irrigation treatments at post-véraison stage.*

***2021/22 season***

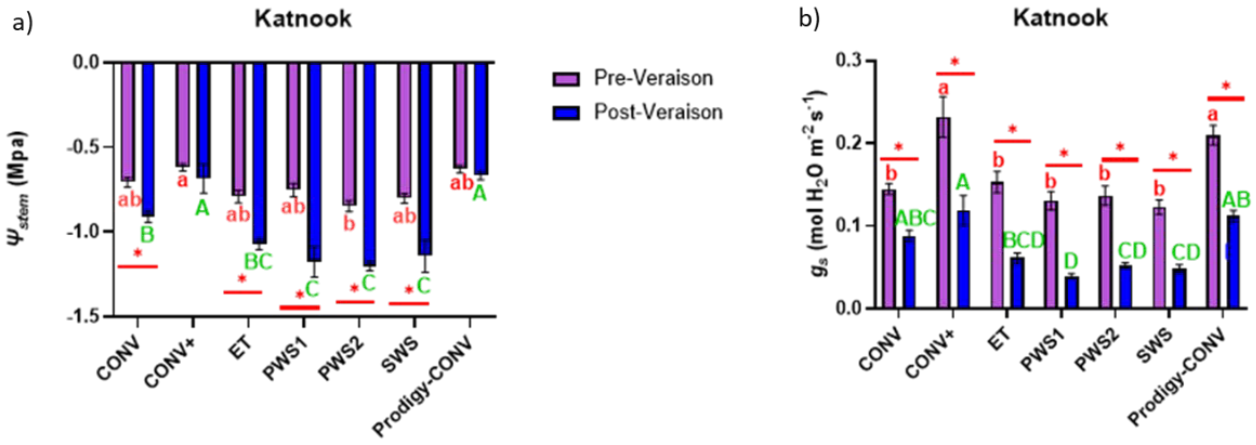



*Figure 34: Variations in mid-day stem water potential ($\Psi_{stem}$) and stomatal conductance ($g_s$) in response to different irrigation treatments. Values are the means ± SEM of eight biological replicates. Asterisk represents the statistically significant differences (p<0.05) between pre- and post-véraison stages. The lowercase letters on the graph represents the statistically significant differences between irrigation treatments at pre-véraison stage. The uppercase letters represent the statistically significant differences between irrigation treatments at post-véraison stage.*

### 5.2.5 Seasonal net photosynthesis and intrinsic water use efficiency

In both Alex88-East and Alex88-West, pre-véraison $A_N$ did not change in response to different irrigation treatments across four seasons. However, sensor-drive irrigation scheduling considerably changed post-véraison $A_N$ over different season. For instance, in the 2018/19 season, CAS vine in the Alex88-east, significantly reduced post-véraison $A_N$ in response to both ET and PWS treatments. However, in the Alex88-west, significantly lower post-véraison $A_N$ was observed only with PWs vines. In the 2019/20 season, post-véraison $A_N$ was significantly higher in Alex88-east ET, PWS and SWS vines relative to CONV vines. However, among Alex88-west vines, statistically significant differences were observed only between PWS, SWS and CONV. Intriguingly, in the 2020/21 season, only SWS vines in both Alex88-east and Alex88-west vineyards exhibited significantly lower $A_N$ relative to other irrigation treatments.

In 2019/20 and 2020/21 seasons, no statistically significant differences were observed in post-véraison $A_N$ between different irrigation treatments of SHI vines. However, in the 2019/20 season, Prodigy vines displayed significantly lower post-véraison $A_N$ relative to all the other treated SHI vines in the Katnook vineyard. In contrast, in the 2021/22 growing season, ET, PWS1, PWS2 and SWS vines exhibited significantly lower post-véraison $A_N$ relative to both CONV and CONV+. However, their pre-véraison $A_N$ did not change dramatically in response to different irrigation scheduling.

Pre-véraison $WUE_i$ remained unchanged in CAS across all seasons in both Alex88-east and Alex88-west. In the 2018/19 season, post-véraison $WUE_i$ also did not change in the Alex88-east vineyard. However, in both 2018/19 and 2019/20 seasons, Alex88-west, post-véraison $WUE_i$ was significantly higher in PWS vines relative to CONV vines. In contrast, in 2019/20 season, Alex88-east PWS vines displayed dramatic reduction of $WUE_i$ relative to CONV.

In both 2019/20 and 2020/21 seasons, different irrigation scheduling strategies did not affect post-véraison $WUE_i$ in SHI vines in Katnook. However, in the 2019/20 season, all SHI vines displayed significantly higher $WUE_i$ relative to Prodigy vines. Interestingly, during 2021/22 season, both PWS1 and PWS2 treatments significantly up-regulated post-véraison $WUE_i$ relative to all the other irrigation treatments (Figure 35, 36, 37 and 38).

### *2018/19 season*

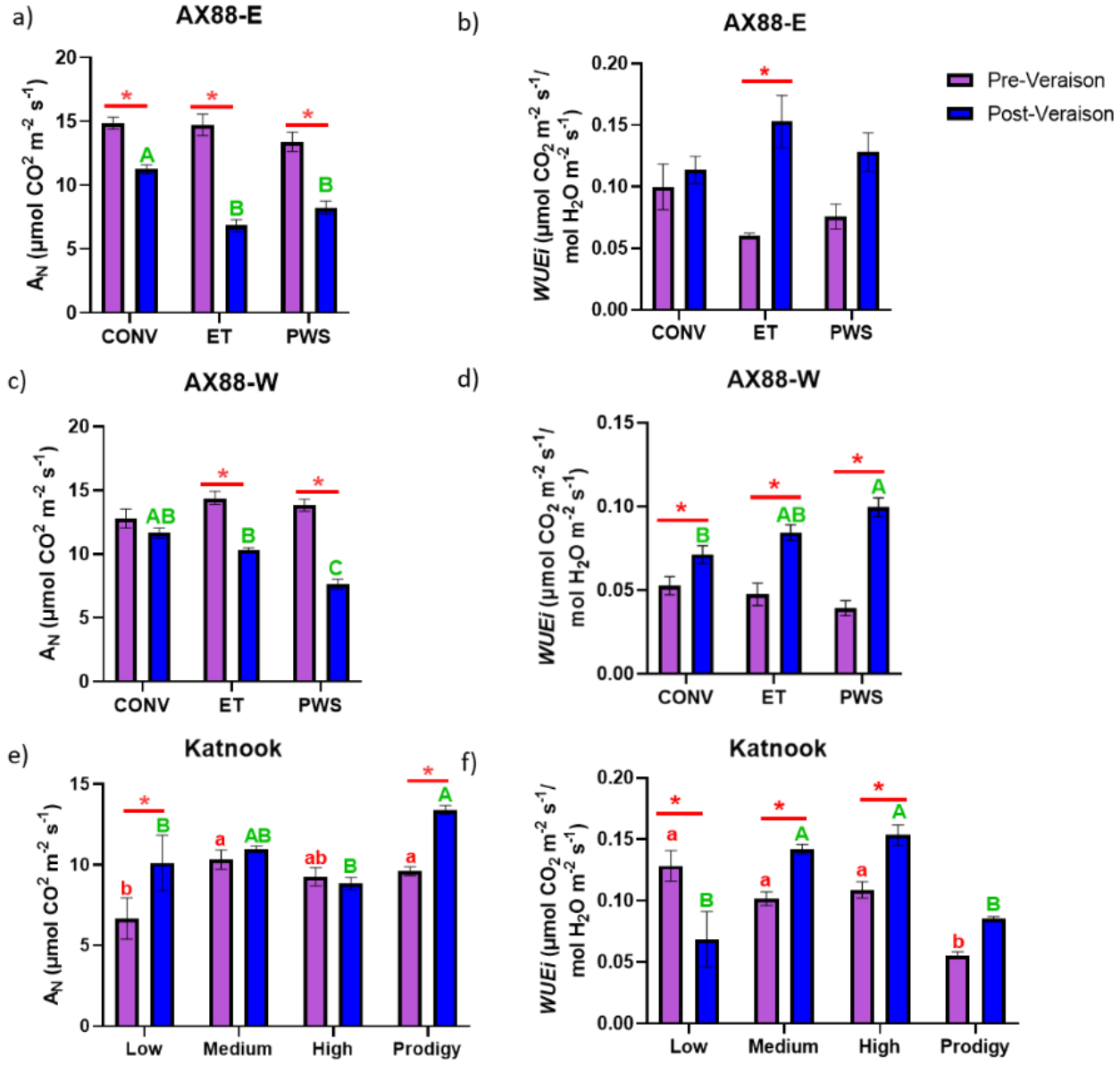



*Figure 35: Variations in net carbon assimilation ($A_N$) (a, c, e) and intrinsic water use efficiency ($WUE_i$) (b, d, f) in CAS and SHI in response to different irrigation treatments. Values are means ± SEM of four biological replicates. Statistical analysis was conducted using two-way ANOVA. Asterisks indicate statistically significant differences (P<0.05) between pre- and post-véraison stages. Lowercase letters indicate statistically significant differences (P<0.05) between irrigation treatments at pre-véraison stage. Uppercase letters indicate statistically significant differences (P<0.05) between irrigation treatments at post-véraison stage.*

### *2019/20 season*

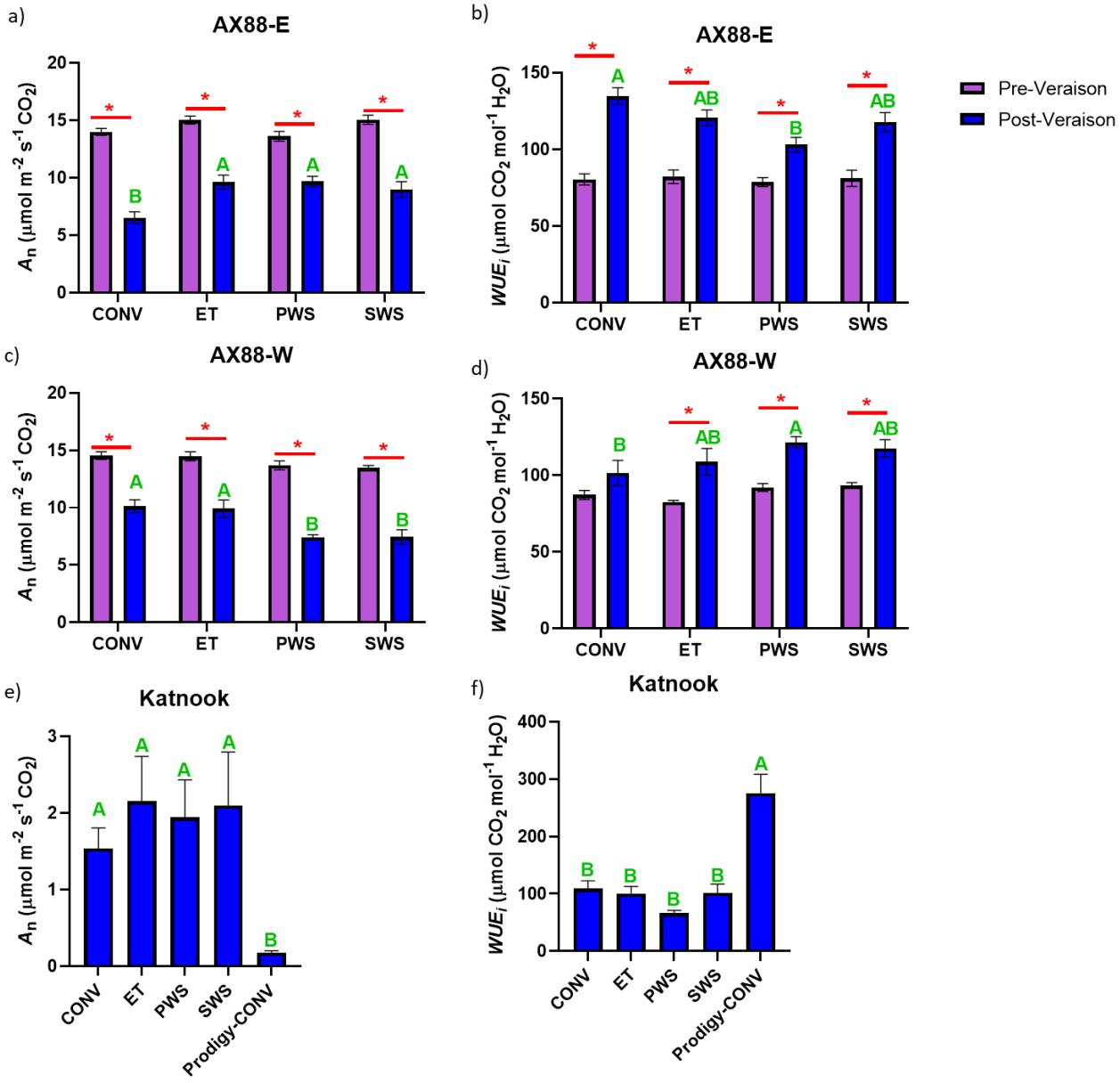



*Figure 36: Variations in net carbon assimilation ($A_N$) (a, c, e) and intrinsic water use efficiency ($WUE_i$) (b, d, f) in CAS and SHI in response to different irrigation treatments. Values are means ± SEM of four biological replicates. Statistical analysis was conducted using two-way ANOVA. Asterisks indicate statistically significant differences (P<0.05) between pre- and post-véraison stages. Lowercase letters indicate statistically significant differences (P<0.05) between irrigation treatments at pre-véraison stage. Uppercase letters indicate statistically significant differences (P<0.05) between irrigation treatments at post-véraison stage.*

## *2020/21 season*

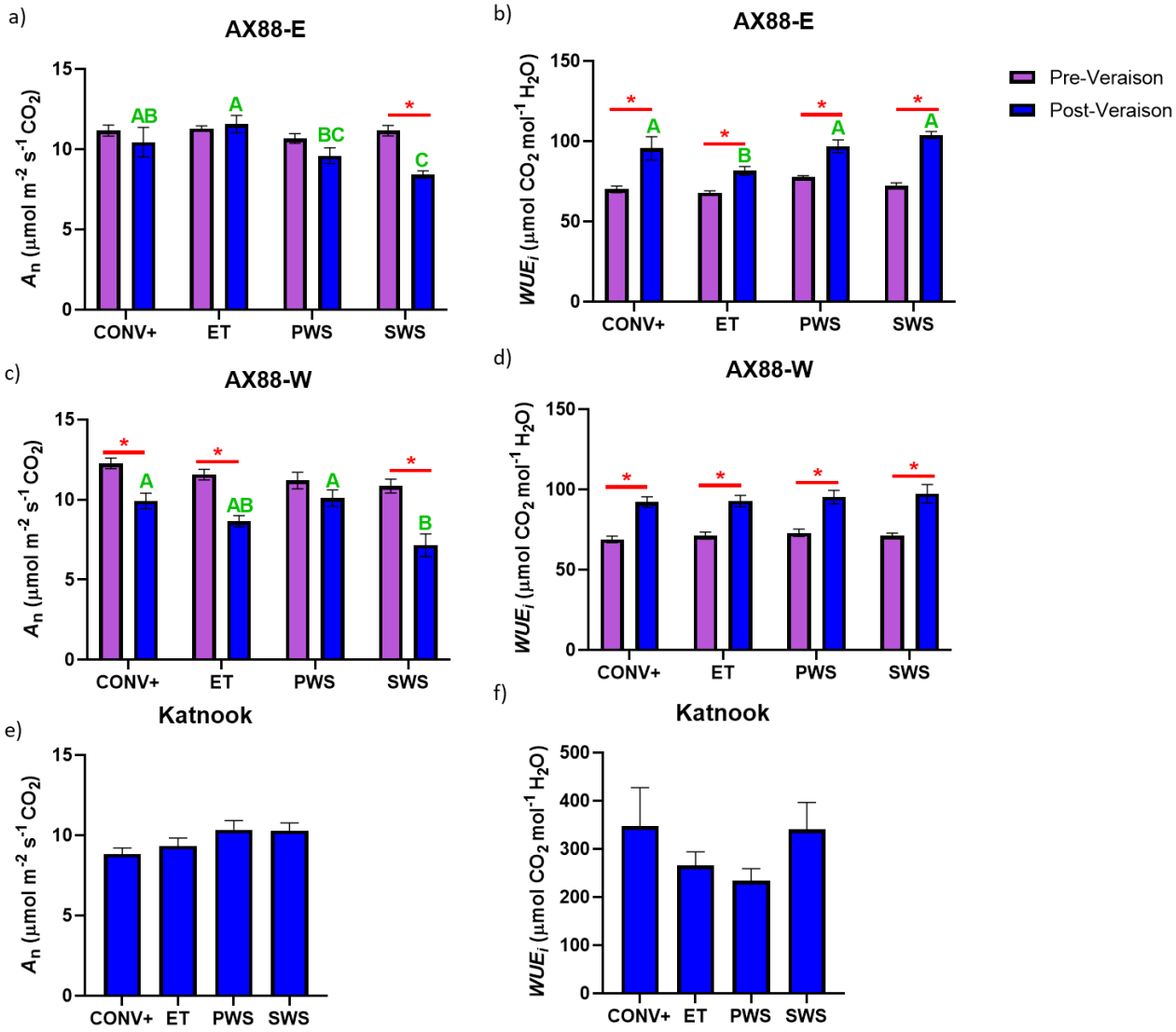



*Figure 37: Variations in net carbon assimilation ($A_N$) (a, c, e) and intrinsic water use efficiency ($WUE_i$) (b, d, f) in CAS and SHI in response to different irrigation treatments. Values are means ± SEM of four biological replicates. Statistical analysis was conducted using two-way ANOVA. Asterisks indicate statistically significant differences (P<0.05) between pre- and post-véraison stages. Lowercase letters indicate statistically significant differences (P<0.05) between irrigation treatments at pre-véraison stage. Uppercase letters indicate statistically significant differences (P<0.05) between irrigation treatments at post-véraison stage.*

### *2021/22 season*

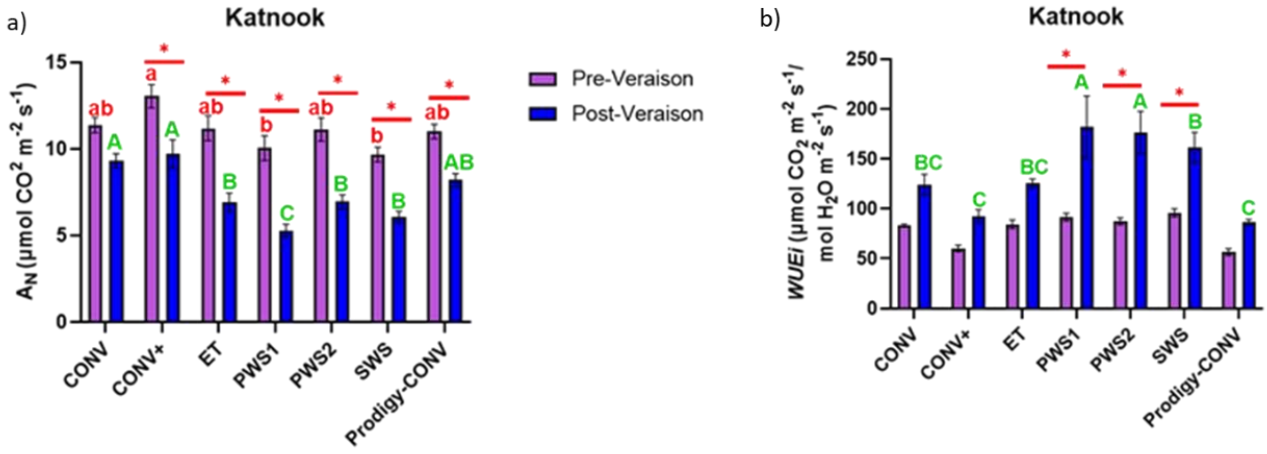



*Figure 38: The photosynthetic rate ($A_N$; a) and intrinsic water use efficiency ($WUE_i$, b) of SHI under different irrigation treatments. Values are the means ± SEM of eight biological replicates. Asterisk represents the statistically significant differences ($p<0.05$) between pre- and post-véraison stages. The uppercase letters represent the statistically significant differences between irrigation treatments at post-véraison stage.*

## 5.3 Continuous sensor-based data

**Soil moisture**

Volumetric water content of the soil, rainfall and irrigation applied during the 2019/20 and 2020/21 seasons are shown in the figure below.

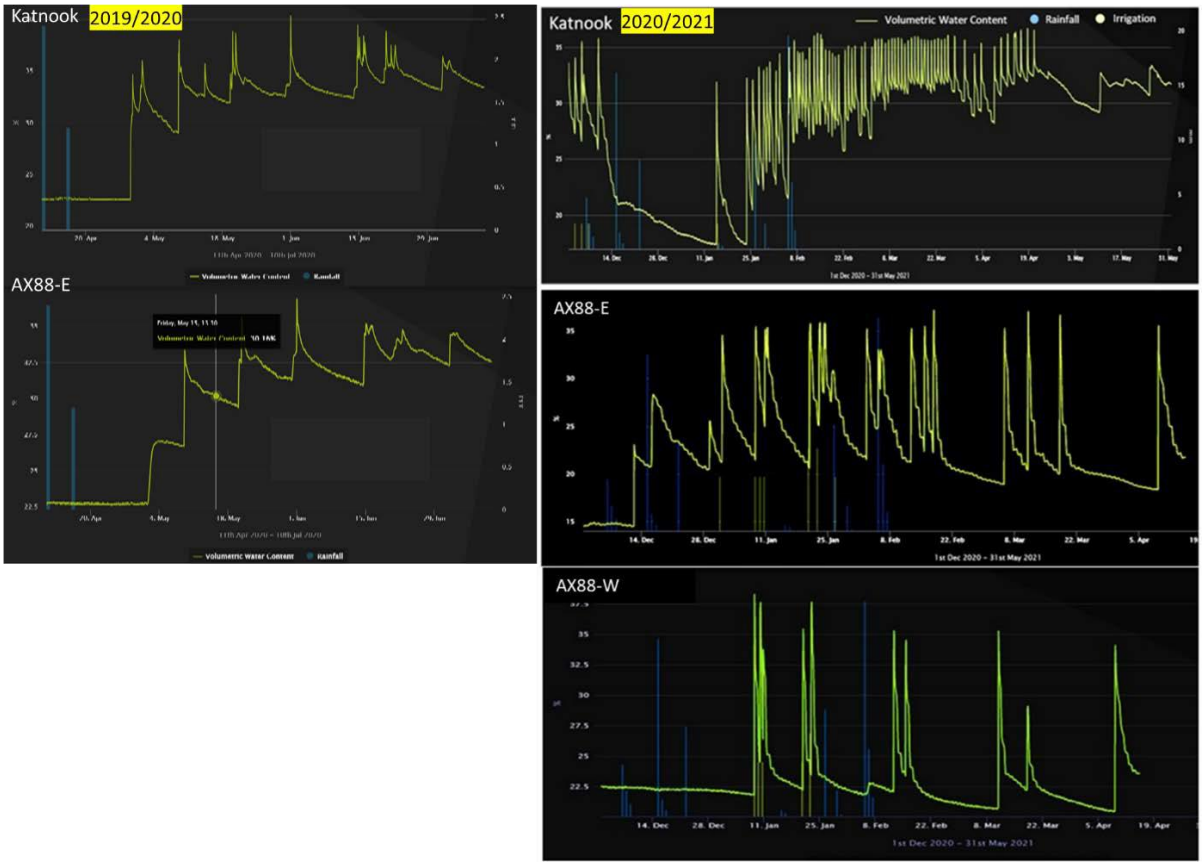



*Figure 39: Sample soil moisture data from Katnook, Alex88E and Alex88W during 2019/20 and 2020/21 seasons on the Green Brain dashboard*

Soil moisture levels in both vineyards were maintained between 22% (pre-irrigation) and 35% (post-irrigation), where the lower end of the range represented an approx. 30% reduction in historical seasonal soil moisture of the AX88 block. Due to the similarity in soil type between the CAS and SHI blocks, the same threshold of 22% VWC was applied to both as the minimum VWC to trigger an irrigation, done on a weekly basis. In AX88 (CAS), approx. four hours per week of irrigation was applied during the peak summer period starting in late-December through to harvest around early- to mid-April. This time equated to approx 21 L/vine/week or ~5 mm/week. In SHI, during the same peak period, three weekly irrigations of 3 h each were applied for a total of 9 h of irrigation. This translated to a water application of 7.2 mm/week or ~35 L/vine/week. The SHI irrigation season would typically commence earlier than the CAS season owing to differences in phenology, production targets (yield vs quality), and vine size and age.

**Vine Water Index (VWI)**

Transp-IR thermal sensors were used to continuously measure canopy temperature, and ambient temperature and relative humidity to calculate a daily index of plant water stress termed 'Vine Water Index' (VWI). This index utilises several time points of the day to determine the relevant values for the VWI number that vary based on environmental conditions (e.g. hot vs cool day), cultivar isohydricity and soil moisture. A snapshot of the Transp-IR dashboard is shown in the figure below.

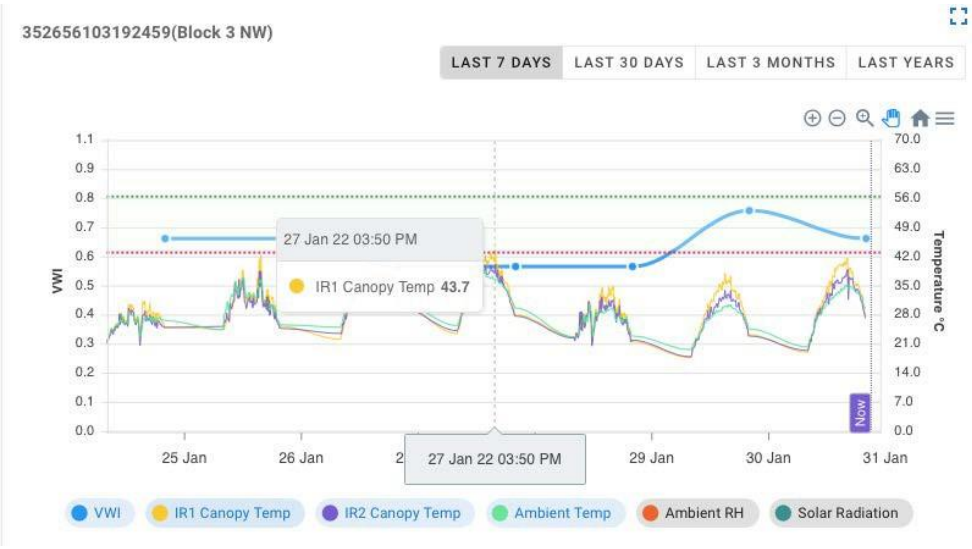



*Figure 39: Transp-IR dashboard during the 2020/21 season in Shiraz grapevines showing the daily VWI value, and 10-min data of canopy temperatures, ambient temperature and relative humidity. The dashboard also provides an option to visualise incident solar radiation.*

A key benefit of using the Transp-IR solution is the provision of an 'optimum' VWI range, indicated on the dashboard as a horizontal green band. This region of VWI values corresponds to a stomatal conductance ($g_s$) value that in turn corresponds to 80-85% of the maximum net photosynthesis ($P_n$) of the leaves thereby achieving high water use efficiencies. The optimum range and VWI values vary per crop species and cultivar. This strategy was used to schedule irrigation in the PWS or PWS1 treatment.

**Trunk Water Potential ($\Psi_{trunk}$)**

Microtensiometers were used to continuously measure trunk water potential in CAS and SHI during the 2020/21, shown in the figure below (sub-figure (c)).

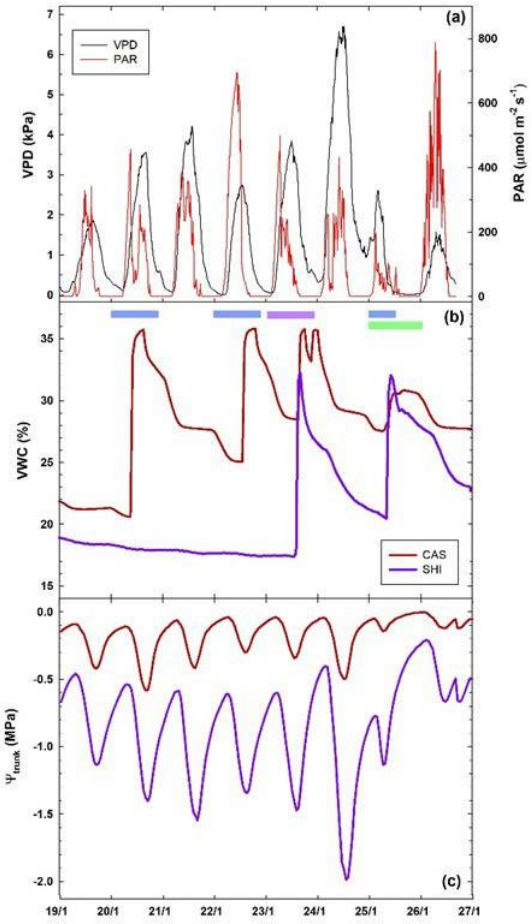



*Figure 40: Trunk water potential of CAS and SHI during the 2020/21 season (c) in response to VPD (a) and volumetric water content (b)*

Due to the nature of their continuous measurements of plant (trunk) water potential, microtensiometers can be used to effectively measure both soil moisture – through the highest $\Psi_{trunk}$ value at pre-dawn – as well as vine water status at maximum transpiration rate – the lowest value of $\Psi_{trunk}$ on a diurnal basis. As seen above and reported in detail in Pagay (2022), $\Psi_{trunk}$ corresponded to both soil moisture availability (VWC) as well as environmental demand (VPD). Higher VPD days and/or low soil moisture tended to decrease $\Psi_{trunk}$ and vice-versa. It should be noted that using $\Psi_{trunk}$ for irrigation scheduling needs new thresholds to be developed, rather than using the values reported in the literature for stem or leaf water potentials.

## 5.4 Remotely-sensed canopy performance

High resolution remote sensing using unmanned aerial vehicles (UAVs) allowed for the capture of sub-vine level spectral reflectance data over the growing season. These datasets were used in conjunction with ground-based physiological measurements, to model the same physiological measurements across space and time. We predicted select physiological parameters at key phenological stages; maps were generated for the pre-harvest period as an example of what predictions are possible with these models.

### 5.4.1 Correlation analysis

Initial steps in the modelling involved assessing which of the spectral bands were highly correlated with the ground-based physiological data. Select spectral bands (horizontal axis of matrix below) and physiological indicators (left vertical column) for CAS indicate a high degree of correlation between canopy leaf area as observed from the UAV and soil and vine water status, and canopy conductance. The thermal wavelengths were also significantly correlated with the same parameters, as might be expected.

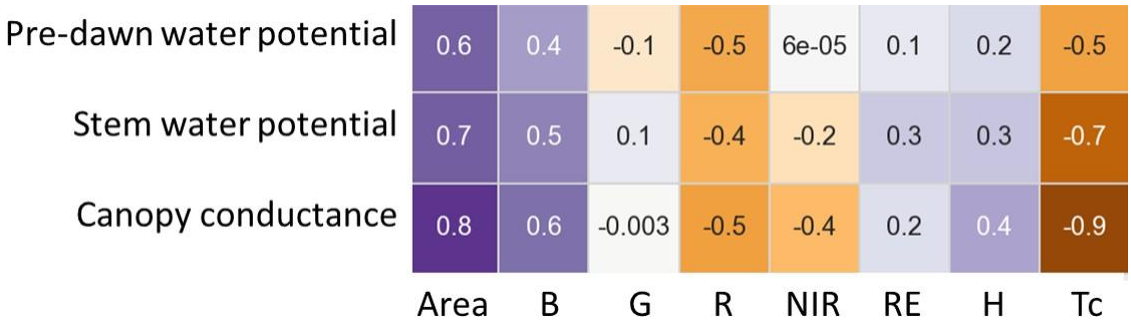
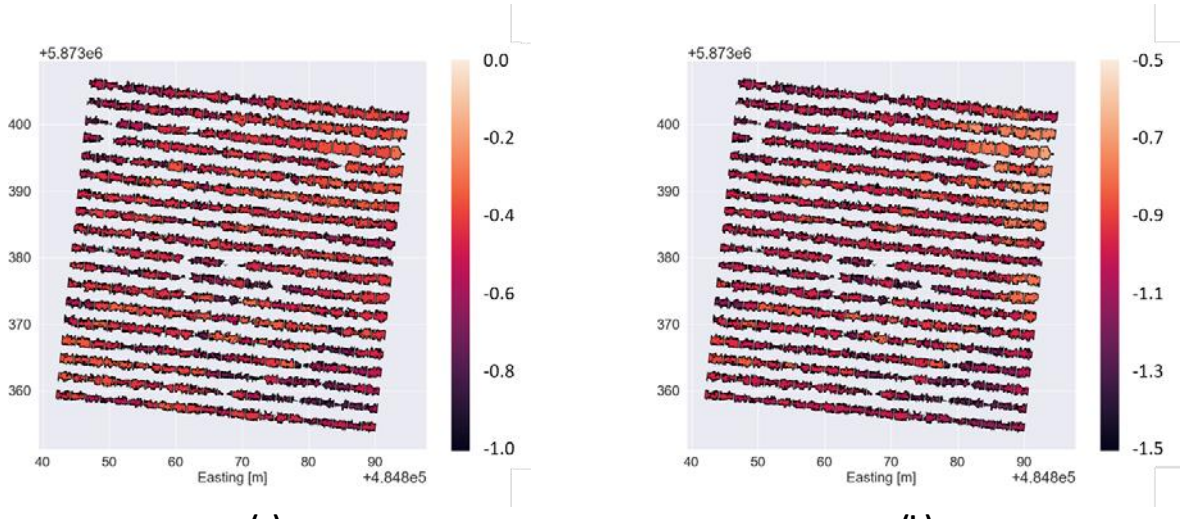



*Figure 7: Correlation analysis of soil and vine water status metrics with UAV-derived thermal, structural and spectral responses of CAS grapevines.*

### 5.4.2 High resolution prediction of soil and vine water status

**Cabernet Sauvignon**




**(a)** **(b)**

*Figure 42: Spatial and temporal prediction of pre-dawn leaf water potential, an indicator of soil moisture (a), and stem water potential at midday (b). Single vine level data are presented for the entire mapping area of the AX88E (CAS) vineyard beyond the sentinel vines at EL-37 (pre-harvest).*

Using a model developed through statistical and machine learning methods with high resolution multispectral and thermal imagery from a low-altitude UAV, we were able to obtain predictions of soil and vine water status

at the single vine level (Fig. 42). This method is an alternative to spatial interpolation methods such as kriging that are based on sparse spatial data. The variations in soil moisture across the AX88E block (Fig 42a) were captured with low MAE (Table 9), particularly with the random forest model, which is an ensemble of models based on decision trees. From the map, it was obvious that the south end of the block had lower soil moisture availability, which translated into higher vine water stress (Fig. 42b). This knowledge can help growers implement precision irrigation whereby that (more stressed) section of the block is zoned via a valve, and irrigated at a higher level or rate.

*Table 9: Accuracy of various linear and non-linear statistical models and machine learning models for the prediction of various CAS vine components at EL-37 (pre-harvest). RMSE = root mean square error; $R^2$ = correlation coefficient; MAE = mean absolute error. Models: Linear, GLM = Generalised Linear Model, RF = Random Forest.*

| | **Pre-dawn leaf water potential ($\Psi_{pd}$, MPa)** | | | **Midday stem water potential ($\Psi_s$, MPa)** | | |
|---|---|---|---|---|---|---|
| Model | RMSE | $R^2$ | MAE | RMSE | $R^2$ | MAE |
| Linear | 0.150 | 0.371 | 0.127 | 0.265 | 0.293 | 0.181 |
| GLM | 0.138 | 0.505 | 0.102 | 0.130 | 0.726 | 0.108 |
| RF | 0.096 | 0.068 | 0.068 | 0.117 | 0.087 | 0.087 |

**Shiraz**

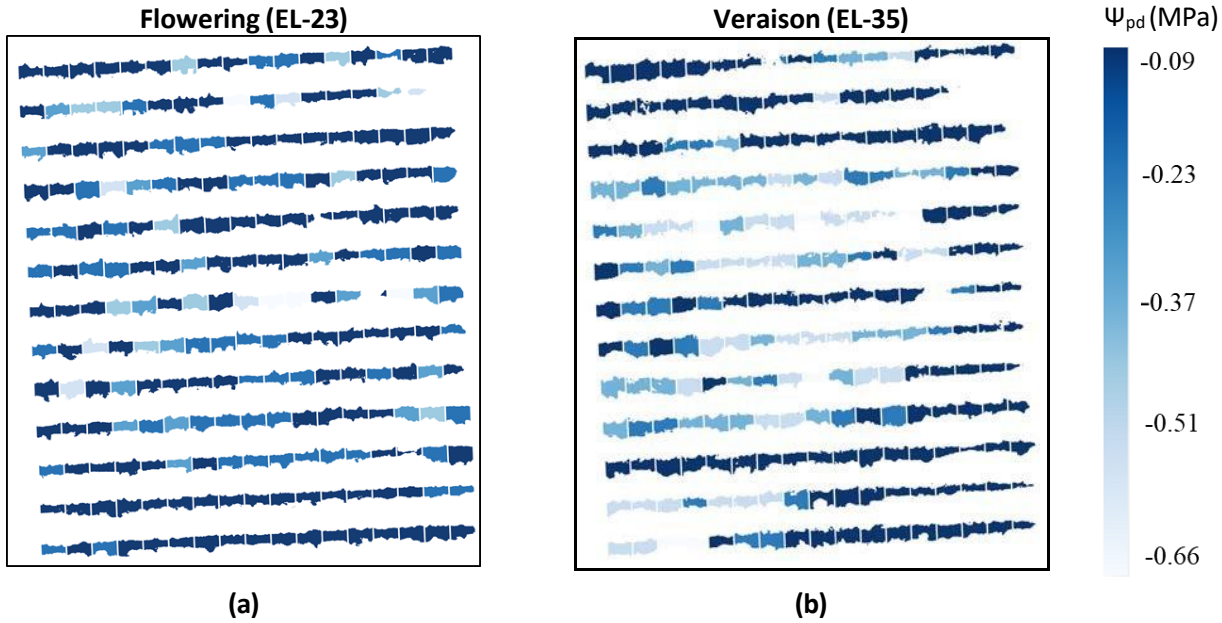



*Figure 43: Spatial and temporal prediction of pre-dawn leaf water potential, an indicator of soil moisture. Single vine level data are presented for the entire mapping area of the KAT (SHI) vineyard beyond the sentinel vines at EL-23 (flowering) and EL-35 (véraison).*

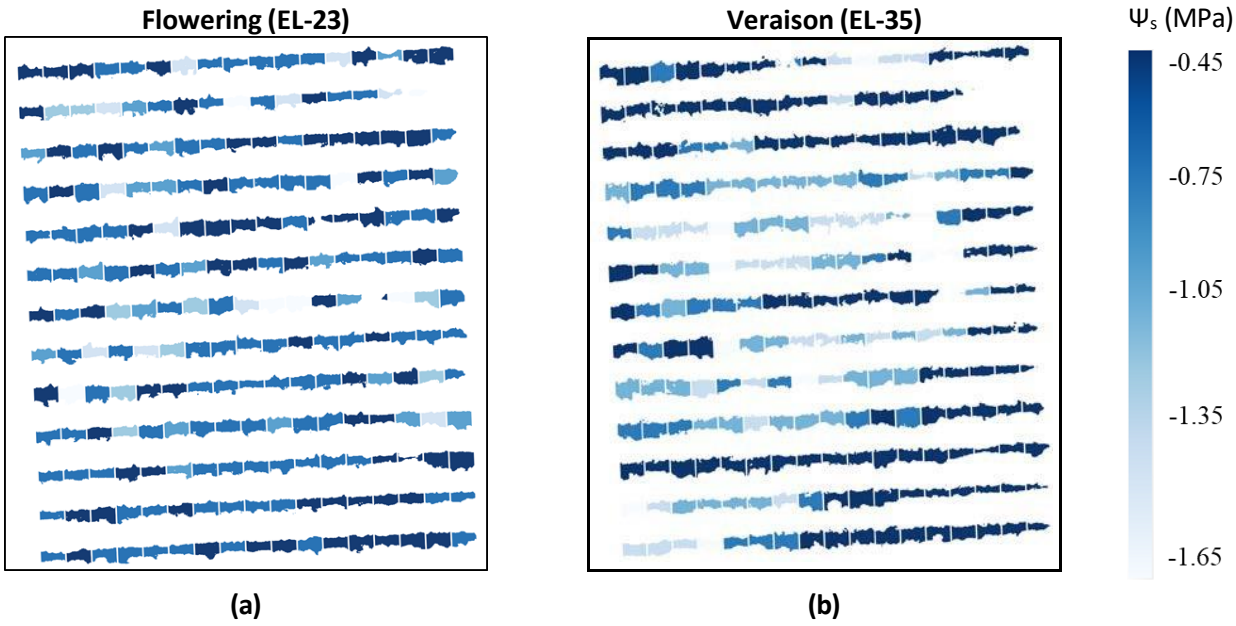



*Figure 44: Spatial and temporal prediction of midday stem water potential. Single vine level data are presented for the entire mapping area of the KAT (SHI) vineyard beyond the sentinel vines at EL-23 (flowering) and EL-35 (véraison).*

In the Katnook Shiraz block, both pre-dawn leaf and midday stem water potentials were modelled to provide a spatial (single vine resolution) and temporal (two important phenological stages, flowering and véraison) prediction of soil and vine water status, respectively. Pre-dawn leaf water potentials ($\Psi_{pd}$), which reflect the available soil moisture to the vines, ranged from -0.1 to -0.4 MPa at flowering and -0.1 to -0.7 MPa by véraison (Fig. 43). The extent of spatial variation of soil moisture across the block was not significant, as indicated by the narrow range of $\Psi_{pd}$ values. By véraison, a significantly higher proportion of vines had access to less soil moisture, as expected, due to deficit irrigation and greater vine size that uses more water.

With regards to midday stem water potentials ($\Psi_s$), reflecting the vine's water status, values ranged from -0.5 to -1.3 MPa at flowering, and -0.5 to -1.7 MPa by véraison. There was clearly a central section of the block that

had lower vine water status (more water stress); this region would be a candidate for increased irrigation through zoning. The central section also had lower $\Psi_{pd}$ values at véraison, perhaps due to shallower soils and smaller rootzones.

### 5.4.3 High resolution prediction of vine crop coefficient

**Cabernet Sauvignon**

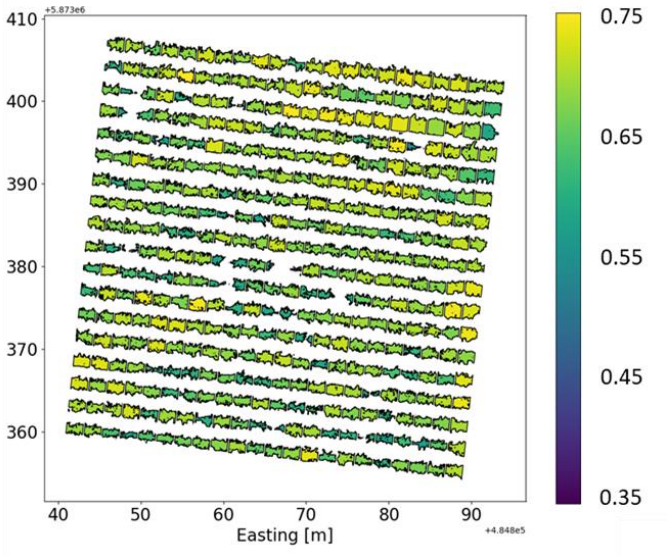



*Figure 44: Spatial prediction of crop coefficient ($K_c$) of AX88E (CAS) at pre-harvest. Single vine level data are presented for the entire mapping area of the vineyard beyond the sentinel vines.*

The crop coefficient ($K_c$) is an important variable for the calculation of crop evapotranspiration ($ET_c$) for determining irrigation schedules (i.e. timing and volume of irrigation applications). Here, we predicted the spatial variation in $K_c$ across the AX88E block on a per-vine basis such that precision irrigation could be implemented in the future (Fig. 44). The spatial pattern of $K_c$ appears to be highly variable across the mapped region, with values ranging from 0.4 through 0.75 at the EL-37 stage, which is a large variation in vine size (leaf area) and canopy light interception, both of which drive transpiration and vine water use and consequently determine irrigation rates. Such large variability in the $K_c$ suggests that there may be high underlying variation in the rooting depth of the vines (due to considerable spatial variations in the depth to the impermeable limestone layer) and/or high variations in vine health e.g. due to trunk diseases, which are common in the region.

*Table 10: Accuracy of various linear and non-linear statistical models and machine learning models for the prediction of CAS crop coefficient ($K_c$) at EL-37 (pre-harvest). RMSE = root mean square error; $R^2$ = correlation coefficient; MAE = mean absolute error. Models: Linear, GLM = Generalised Linear Model, GAM = Generalised Additive Model, CNN = Convolution Neural Network, RF = Random Forest.*

| | **Crop coefficient ($K_c$)** | | |
|---|---|---|---|
| Model | RMSE | $R^2$ | MAE |
| Linear | 0.091 | 0.295 | 0.076 |
| GLM | 0.074 | 0.528 | 0.061 |
| GAM | 0.069 | 0.594 | 0.055 |
| CNN | 0.072 | 0.619 | 0.060 |
| RF | 0.062 | 0.675 | 0.047 |

The various statistical and machine learning models employed compared quite similarly to one another; the best predictions were obtained with the RF model (lowest RMSE and MAE values, highest $R^2$). Considering the low values of MAE for all models tested, even the linear model did well in predicting $K_c$. This allows the use of simple tools and spreadsheets for future prediction of $K_c$.

A manuscript was published in the journal *Remote Sensing* based on this work on $K_c$ and is attached to this report.

**Shiraz**

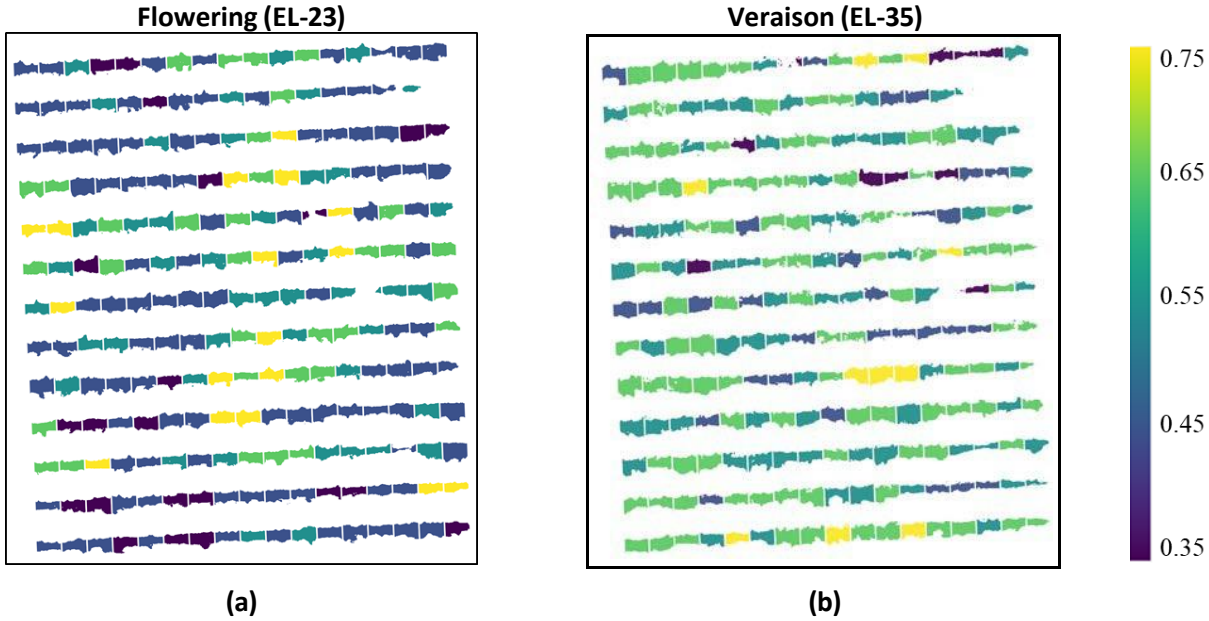
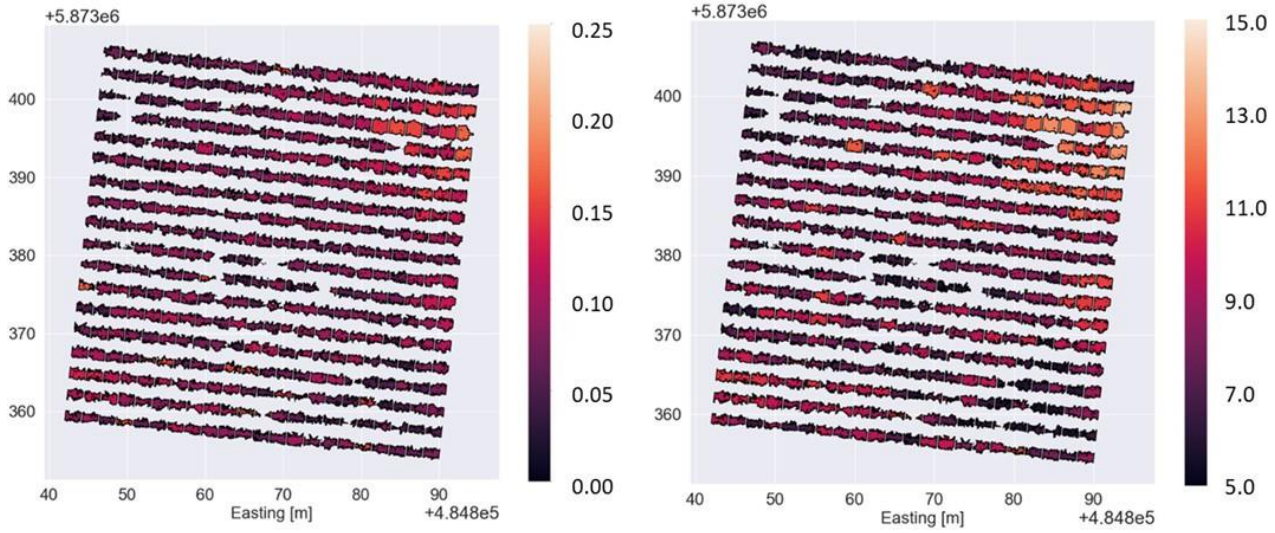



*Figure 45: Spatial and temporal prediction of crop coefficient ($K_c$) for KAT Shiraz grapevines at flowering (a) and véraison (b). Single vine level data are presented for the entire mapping area of the vineyard including and beyond the sentinel vines.*

Variations in $K_c$ across the Shiraz block during the early season (flowering, EL-23) ranged from 0.35 to 0.55 with a few vines exceeding 0.7. By véraison, most of the vines had $K_c$ values exceeding 0.6, with only a few vines around 0.75, suggesting that canopies were not overly large in terms of leaf area intercepting light. These single-vine values of $K_c$ allow for the delineation of irrigation zones (if adopting the ET strategy) although the uniformity in this block was relatively high, thereby not requiring zoning of irrigation, unlike the Alex88 CAS block which had much higher spatial variation of $K_c$.

### 5.4.4 High resolution prediction of canopy gas exchange

**Cabernet Sauvignon**




(a) (b)

*Figure 46: Spatial prediction of canopy conductance, $g_c$ (a) and net photosynthesis, $A_n$ (b) in AX88E (CAS) at pre-harvest. Values for $g_c$ are shown in mol $H_2O$ $m^{-2}$ $s^{-1}$; values for $A_n$ are shown in µmol $CO_2$ $m^{-2}$ $s^{-1}$. Single vine level data are presented for the entire mapping area of the vineyard beyond the sentinel vines.*

High resolution remote sensing using thermal and multispectral cameras allowed for the modelling of canopy gas exchange parameters, canopy conductance ($g_c$) and net photosynthesis ($A_n$). Spatial variations in $g_c$ indicate a range of 0.05 – 0.2 mol $H_2O$ $m^{-2}$ $s^{-1}$, which reflects the consistently high vine-to-vine variability in water status and physiological performance in this block. Net photosynthesis rates are also similarly variable; values range from 5 – 13 µmol $CO_2$ $m^{-2}$ $s^{-1}$. These values match the range of values obtained from our ground measurements with an infrared gas analyser.

*Table 11: Accuracy of various linear and non-linear statistical models and machine learning models for the prediction of CAS canopy gas exchange at EL-37 (pre-harvest). RMSE = root mean square error; $R^2$ = correlation coefficient; MAE = mean absolute error. Models: Linear, GLM = Generalised Linear Model, RF = Random Forest.*

| | **Canopy conductance ($g_c$)** | | | **Canopy net photosynthesis ($A_n$)** | | |
|---|---|---|---|---|---|---|
| Model | RMSE | $R^2$ | MAE | RMSE | $R^2$ | MAE |
| Linear | 0.059 | 0.149 | 0.047 | 1.497 | 0.371 | 1.272 |
| GLM | 0.055 | 0.265 | 0.042 | 1.379 | 0.505 | 1.015 |
| RF | 0.039 | 0.622 | 0.030 | 0.962 | 0.751 | 0.681 |

Comparing the performance of the various models, the Random Forest model again was superior to the other two evaluated in this study. Values of RMSE and MAE were the lowest for both parameters, $g_c$ and $A_n$.

Further work on this dataset would include predictions of spatial and temporal patterns of leaf and crop water use efficiencies, as well as extending these predictions to other neighbouring vineyards with the same cultivar based on limited ground-based measurements in those blocks to fine-tune the models developed here.

**Shiraz**

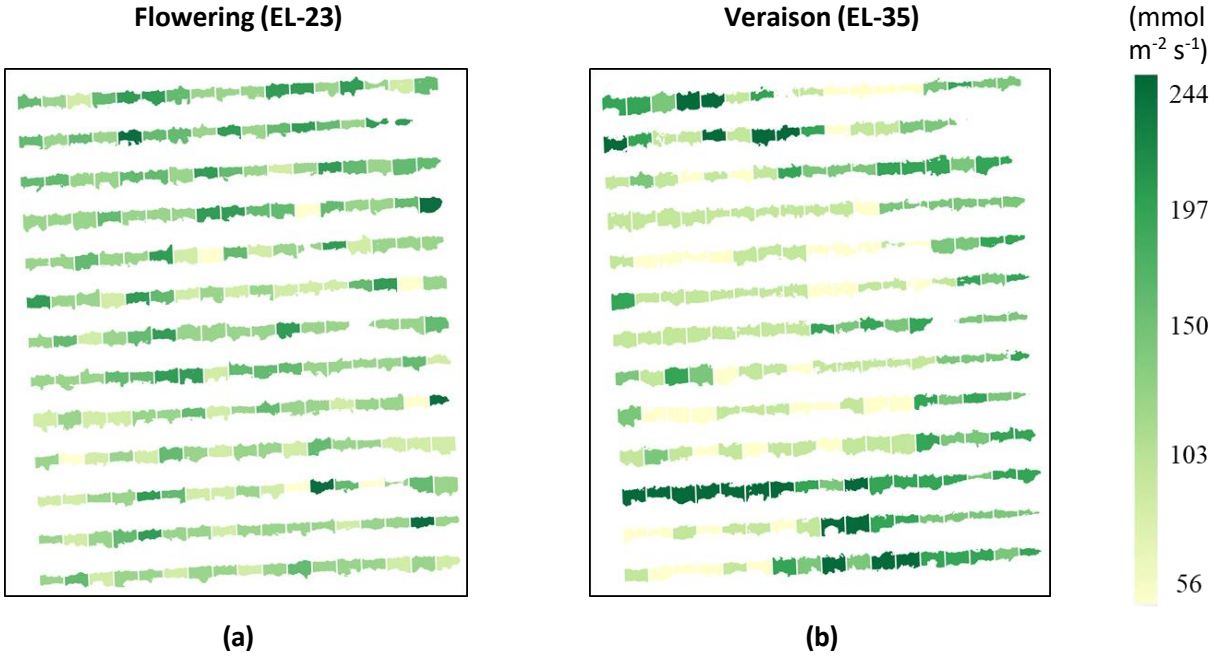



*Figure 47: Spatial and temporal prediction of canopy conductance, $g_c$, in KAT-SHI during flowering (a) and véraison (b). Values for $g_c$ are shown in mmol $H_2O$ $m^{-2}$ $s^{-1}$. Single vine level data is presented for the entire mapping area of the vineyard beyond the sentinel vines.*

Remote sensing-based model predictions of spatial canopy conductance through multispectral and thermal high-resolution imagery, indicated that, at flowering, $g_c$ ranged from 56 to ~200 mmol $H_2O$ $m^{-2}$ $s^{-1}$, with no clear spatial structure in the data (lack of defined zones). By véraison, these values ranged from 56 to 244 mmol $H_2O$ $m^{-2}$ $s^{-1}$, with significantly more vines at the higher $g_c$ values compared to at flowering. At this later stage, there appeared to be a separation between the central rows (with lower $g_c$) and the sides of the block (with higher $g_c$), which provide guidance on where to implement precision irrigation through irrigation zoning. This pattern was consistent with the spatiotemporal trends of both pre-dawn and stem water potentials (Figs. 43, 44), but not $K_c$ (Fig. 45).

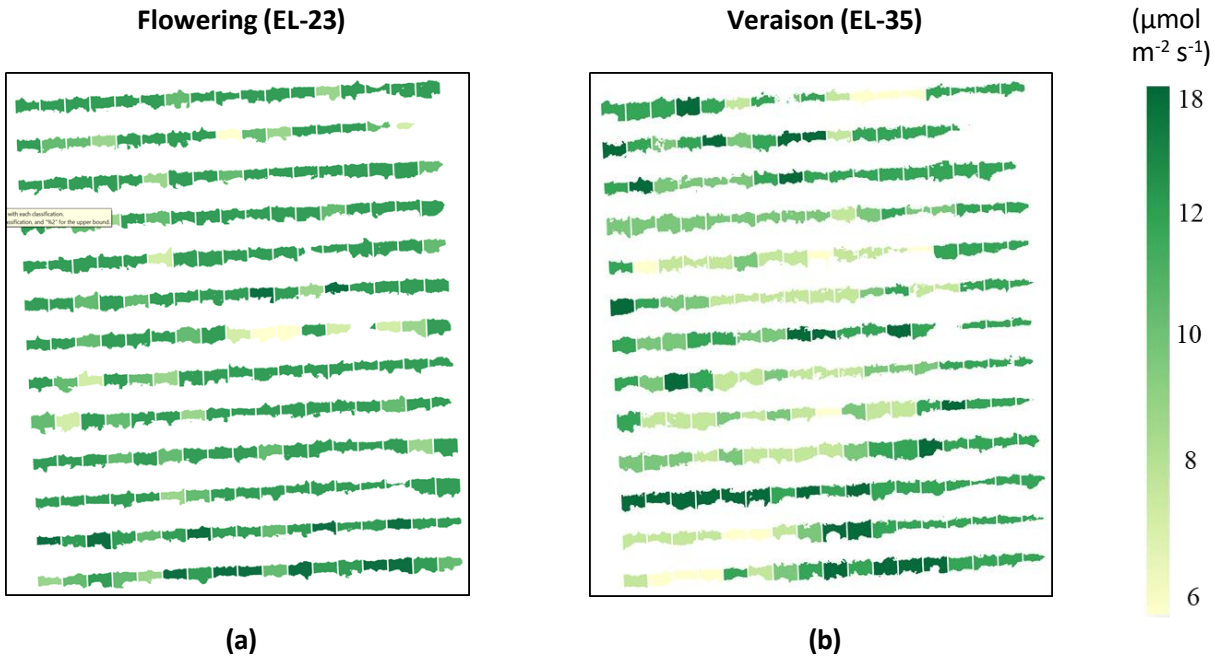



*Figure 48: Spatial and temporal prediction of canopy net photosynthesis, $A_n$, in KAT-SHI during flowering (a) and véraison (b). Values for $A_n$ are shown in µmol $CO_2$ $m^{-2}$ $s^{-1}$. Single vine level data are presented for the entire mapping area of the vineyard beyond the sentinel vines.*

Canopy net photosynthesis rates predicted at the single vine level via HR-RS indicated a range of 8-12 µmol $CO_2$ $m^{-2}$ $s^{-1}$ during flowering, rising to 10-18 µmol $CO_2$ $m^{-2}$ $s^{-1}$ by véraison. The Shiraz block showed spatial structure between these two phenological stages; the upper and lower portions of the block had higher values of $P_n$, consistent with $g_c$, and soil and vine water status spatial trends.

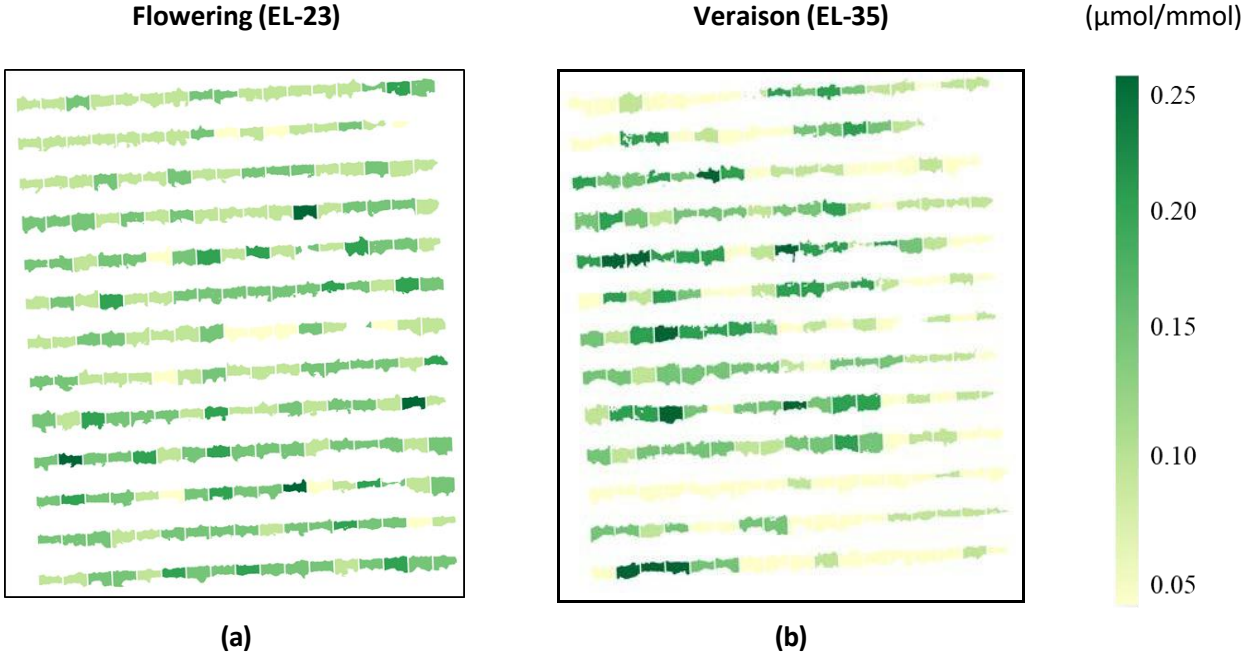



*Figure 49: Spatial and temporal prediction of leaf intrinsic water use efficiency ($WUE_i = A_n/g_s$) in KAT-SHI during flowering (a) and véraison (b). Values for $WUE_i$ are shown in µmol $CO_2$ $mmol^{-1}$ $H_2O$. Single vine level data are presented for the entire mapping area of the vineyard beyond the sentinel vines.*

Using the spatial and temporal $A_n$ and $g_s$ information in Figs. 47-48, the spatial and temporal patterns of leaf intrinsic water use efficiency ($WUE_i$) were obtained for the Shiraz vineyard during the 2021/22 season (Fig. 49). During the early season, around flowering, $WUE_i$ values ranged from 0.05 to 0.2 across the block, while later in the season, around véraison, those value shifted higher in the centre of the block to around 0.2-0.25. The

two north-south edges of the block clearly had low $WUE_i$ ; this could be attributed to the larger canopies in those regions (high Kc values, Fig. 45) using more water due to their relatively higher $g_s$ values (Fig. 47) that was not matched by the increase in $A_n$ (Fig. 48). This is another opportunity to implement precision irrigation by zoning the two ends of the vineyard and applying water at lower rates to decrease the $g_s$ relative to $A_n$. The central rows are clearly quite efficient in their water use patterns, showing high $WUE_i$.

## 5.5 Yield components and pruning weights

As shown in the Table 9, total yield per vine did not change dramatically with different irrigation treatments in both Alex88-east and Alex88-west during 2018/19 (S1) and 2019/20 (S2) seasons. However, in the 2020/21 season, total yield of CONV+ vines was significantly higher relative to SWS vines due to increased average berry weight. Even though yield per unit length (kg $m^{-1}$) seemed to be constant in Alex88-east during all three seasons despite of different irrigation scheduling strategy, in Alex88-west CONV vines displayed significantly higher yield per metre relative to PWS vines in S2.

*Table 9: Yield components for all irrigation treatments in Alex88-east and Alex88-west and experimental season (2018/19, 2019/20 and 2020/21). Means (n = 4 – 8) are presented. Interactions between irrigation treatments are reported both within a soil type and between soil types.*

| | Season | S1 | | S2 | | S3 | | ANOVA | | | | |
|---|---|---|---|---|---|---|---|---|---|---|---|---|
| | Treatment | AX88-E | AX88-W | AX88-E | AX88-W | AX88-E | AX88-W | T | ST | S | T×ST | S×ST |
| Yield (kg vine$^{-1}$) | CONV | 7.33 | 7.12 | 3.85 | 4.20 | - | - | ** | *** | *** | ns | ns |
| | PWS | 7.19 | 5.24 | 4.59 | 3.04 | 6.53 ab | 5.30 | | | | | |
| | ET | - | - | 5.80 | 3.33 | 7.02 ab | 6.67 | | | | | |
| | SWS | - | - | 4.97 | 3.10 | 4.88 b | 4.73 | | | | | |
| | CONV+ | - | - | - | - | 8.71 a | 7.48 | | | | | |
| Yield (kg m$^{-1}$) | CONV | 2.22 | 2.28 | 1.14 | 1.35 a | - | - | * | ** | *** | ** | * |
| | PWS | 2.16 | 1.38 | 1.36 | 0.81 b | 1.94 | 1.60 | | | | | |
| | ET | - | - | 1.56 | 0.96 ab | 1.80 | 1.92 | | | | | |
| | SWS | - | - | 1.51 | 0.89 ab | 1.47 | 1.37 | | | | | |
| | CONV+ | - | - | - | - | 1.91 | 2.12 | | | | | |
| Bunch count (bunches m$^{-1}$) | CONV | 43.4 | 51.2 a | 29.6 | 32.7 | - | - | * | * | *** | ns | ns |
| | PWS | 41.3 | 34.4 b | 30.8 | 25.3 | 42.2 | 34.8 | | | | | |
| | ET | - | - | 36.5 | 22.8 | 39.6 | 39.8 | | | | | |
| | SWS | - | - | 39.2 | 24.7 | 36.2 | 35.8 | | | | | |
| | CONV+ | - | - | - | - | 49.2 | 52.1 | | | | | |
| Berries per bunch | CONV | 55.8 | 54.0 | 40.5 | 51.3 | - | - | ns | * | *** | ns | ** |
| | PWS | 60.1 | 47.8 | 46.1 | 43.3 | 53.3 | 44.1 ab | | | | | |
| | ET | - | - | 44.9 | 46.9 | 51.9 | 49.6 a | | | | | |
| | SWS | - | - | 41.2 | 45.1 | 49.0 | 41.0 b | | | | | |

| | | | | | | | | | | | | |
|---|---|---|---|---|---|---|---|---|---|---|---|---|
| | CONV + | - | - | - | - | 54.2 | 45.4 ab | | | | | |
| Average berry weight (g) | CONV | 0.92 | 0.83 | 0.95 | 0.84 | - | - | ** | *** | ns | ns | *** |
| | PWS | 0.86 | 0.85 | 1.00 | 0.78 | 0.88 b | 0.97 | | | | | |
| | ET | - | - | 0.98 | 0.90 | 0.85 b | 0.98 | | | | | |
| | SWS | - | - | 0.96 | 0.82 | 0.85 b | 0.92 | | | | | |
| | CONV + | - | - | - | - | 0.98 a | 1.02 | | | | | |
| Average bunch weight (g) | CONV | 51.1 | 44.6 | 38.3 | 41.6 | - | - | * | *** | *** | * | ns |
| | PWS | 51.9 | 40.7 | 46.3 | 32.6 | 46.8 | 42.6 ab | | | | | |
| | ET | - | - | 44.3 | 42.0 | 44.5 | 48.5 a | | | | | |
| | SWS | - | - | 39.2 | 36.2 | 41.5 | 37.4 b | | | | | |
| | CONV + | - | - | - | - | 53.2 | 44.3 ab | | | | | |
| Pruning weight (kg $m^{-1}$) | CONV | 0.66 | 0.57 | 0.73 | 0.45 | - | - | ns | *** | ** | ns | *** |
| | PWS | 0.67 | 0.46 | 0.84 | 0.56 | 0.51 | 0.42 | | | | | |
| | ET | - | - | 0.83 | 0.49 | 0.53 | 0.52 | | | | | |
| | SWS | - | - | 0.86 | 0.42 | 0.53 | 0.52 | | | | | |
| | CONV + | - | - | - | - | 0.44 | 0.64 | | | | | |
| Ravaz Index (kg $kg^{-1}$) | CONV | 3.62 | 4.44 | 1.66 | 3.11 a | - | - | ns | ns | *** | ns | ns |
| | PWS | 3.26 | 3.74 | 1.73 | 1.57 b | 3.77 | 3.52 | | | | | |
| | ET | - | - | 2.08 | 2.31 ab | 3.52 | 3.92 | | | | | |
| | SWS | - | - | 1.90 | 2.18 ab | 2.84 | 2.77 | | | | | |
| | CONV + | - | - | - | - | 4.62 | 3.65 | | | | | |

It was consistently observed across three seasons that the total yield of SHI in the Prodigy block was significantly lower relative to all trial SHI vines at Katnook. For instance, in S1 and S3, PWS1 and SWS vines showed significantly higher yield relative to Prodigy vines, whereas in the 2021/22 season, all irrigation treatments produced significantly higher yield compared to Prodigy vines. Yield reduction in Prodigy can be attributed to significantly lower berries per bunch as well as average bunch weight.

*Table 10: Yield components for all irrigation treatments in Katnook during four experimental seasons (2018/19, 2019/20, 2020/21 and 2021/22). Means (n = 4 – 8) are presented. Prod=Prodigy block. Interactions between irrigation treatments are reported.*

| | Season | S1 | S2 | S3 | S4 | T | S | T× S |
|---|---|---|---|---|---|---|---|---|
| Yield (kg vine$^{-1}$) | CONV | 5.3 ab | 1.9 ns | - | 7.5 a | ** | *** | ns |
| | CONV + | - | - | 9.9 a | 8.4 a | | | |
| | ET | 5.2 ab | 1.3 | 8.7 ab | 6.2 a | | | |
| | PWS1 | 5.9 a | 2.1 | 10.4 a | 6.2 a | | | |
| | PWS2 | - | - | - | 6.4 a | | | |
| | SWS | 6.0 a | 1.6 | 9.7 a | 5.9 a | | | |
| | Prod-CONV | 3.5 b | - | 4.8 b | 3.0 b | | | |
| Yield (kg vine$^{-1}$) | CONV | 3.0 ns | 1.1 ns | - | 4.6 ns | ns | ns | ns |
| | CONV + | - | - | 5.7 ns | 4.2 | | | |
| | ET | 3.0 | 0.74 | 5.0 | 3.5 | | | |
| | PWS1 | 3.4 | 1.2 | 5.9 | 3.5 | | | |
| | PWS2 | - | - | - | 3.6 | | | |
| | SWS | 3.4 | 0.94 | 5.6 | 3.3 | | | |
| | Prod-CONV | - | - | - | 3.4 | | | |
| Bunch count (bunches m$^{-1}$) | CONV | 18.14 a | 17.1 ns | - | 26.1 b | * | *** | * |
| | CONV + | - | - | 32.8 ns | 25 b | | | |
| | ET | 5.0 b | 11.4 | 36.7 | 24 b | | | |
| | PWS1 | 5.9 b | 17.9 | 42.4 | 22.1 b | | | |
| | PWS2 | - | - | - | 24.1 b | | | |
| | SWS | 5.6 b | 14.3 | 38.1 | 23.5 b | | | |
| | Prod-CONV | - | - | - | 42.2 a | | | |
| Berries per bunch | CONV | 131.4 b | 44.2 ns | - | 121 a | ** | *** | * |
| | CONV + | - | - | 113.6 a | 102 a | | | |
| | ET | 126 b | 49.2 | 113.6 a | 109 a | | | |
| | PWS1 | 124 b | 50.1 | 104.4 a | 111 a | | | |
| | PWS2 | - | - | - | 115 a | | | |
| | SWS | 128 b | 49.4 | 125.7 a | 120 a | | | |
| | Prod-CONV | 194 a | - | 70.0 b | 41 b | | | |
| Average berry | CONV | 1.13 ns | 1.36 ns | | 1.5 ab | ** | ** | * |
| | CONV + | - | - | 1.54 a | 1.6 a | | | |
| | ET | 1.15 | 1.35 | 1.20 b | 1.3 bc | | | |

| | | | | | | |
|---|---|---|---|---|---|---|
| | PWS1 | 1.20 | 1.37 | 1.31 b | 1.4 bc | |
| | PWS2 | - | - | - | 1.4 bc | |
| | SWS | 1.16 | 1.33 | 1.15 b | 1.3 c | |
| | Prod-CONV | 1.1 | - | - | 1.3 bc | |
| Average bunch weight (g) | CONV | 148.0 b | 59.8 ns | - | 178 a | * *** * |
| | CONV + | - | - | 174 a | 168 ab | |
| | ET | 145.3 b | 64.5 | 134.6 b | 145 b | |
| | PWS1 | 148.0 b | 66.4 | 136.2 b | 150 ab | |
| | PWS2 | - | - | - | 155 ab | |
| | SWS | 147.8 b | 65.7 | 143.9 b | 151 ab | |
| | Prod-CONV | 203.4 a | - | 86.2 c | 53 c | |
| Pruning weight (kg m−1) | CONV | 0.80 ns | - | 1.0 ns | | ns ns ns |
| | CONV + | - | - | - | | |
| | ET | 0.91 | - | 0.84 | | |
| | PWS1 | 0.95 | - | 1.10 | | |
| | PWS2 | - | - | - | | |
| | SWS | 0.81 | - | 1.00 | | |
| | Prod-CONV | - | - | - | | |
| Ravaz Index (kg $kg^{-1}$) | CONV | 3.9 ns | - | 5.6 ns | | ns ns ns |
| | CONV + | - | - | - | | |
| | ET | 3.5 | - | 6.0 | | |
| | PWS1 | 4.5 | - | 5.9 | | |
| | PWS2 | - | - | - | | |
| | SWS | 4.2 | - | 5.7 | | |
| | Prod-CONV | 5.2 | - | - | | |

## 5.6 Water use efficiency

### 5.6.1 Crop water use efficiency

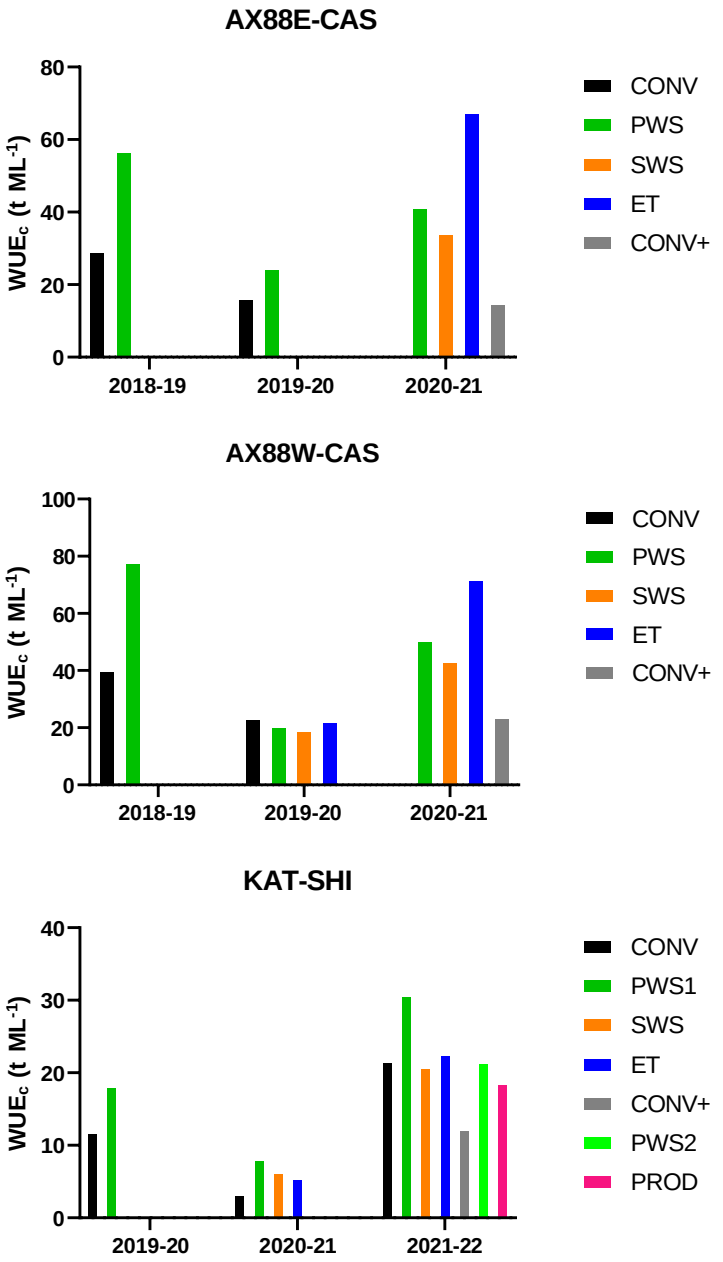



*Figure 50: Crop water use efficiency (WUEc, t/ML) for the AX88E (CAS), AX88W (CAS) and KAT (SHI) vineyards during the three seasons. Water application volumes do not include rainfall during the growing season.*

Crop water use efficiency ($WUE_c$) metrics derived from yield and irrigation data, also known as Irrigation Water Productivity, were calculated for each of the three seasons of the trial in the CAS and SHI vineyards. The 2019/20 season notwithstanding, $WUE_c$ values in CAS were highest in the PWS and ET treatments, followed by the SWS treatment. These data-driven treatments were significantly higher than the CONV, by 3-6 fold (300-600%) in the final season. This is strong evidence that using data to drive irrigation decisions, regardless of the approach, is beneficial to improve WUE, even in premium vineyards that are routinely deficit irrigated to increase grape/wine quality. In SHI, similar trends were observed; while there was only a slight increase in $WUE_c$ in the first season using the PWS treatment, by the second season, all data-driven approaches were over

double the $WUE_c$ of the CONV group. In the final season, 2021/22, the PWS1 treatment based on the proximal IR sensors appeared to have the highest $WUE_c$ of the group, which were not different from each other or versus CONV or the Prodigy block (PROD). The only outlier in this group was the CONV+ treatment, which received double the CONV irrigation volume; clearly this did not translate to a proportional yield increase, thereby decreasing its WUEc (relative to CONV).

Unlike many warm climate vineyards, it seems that in a cooler region with smaller vines, higher irrigation volumes may not benefit growers seeking to increase yields in mid-grade SHI blocks that are already yielding upwards of 13 t/ha as in the case of KAT. A similar observation was made in AX88E-CAS on Terra rossa; in the final season, 2020/21, increased irrigation from 0.4 ML/ha (PWS) to 1 ML/ha (CONV+) did not alter yield; both groups had yields of ~15 t/ha. The heavier Rendzina vineyard, AX88W, did, however, benefit from increased irrigation in the CONV+ group; yield in this group was ~33% higher than the data-driven groups receiving less irrigation, but this yield increase (in CONV+) required an irrigation increase from 0.25 ML/ha to 0.7 ML/ha, i.e. approximately 80% higher than the data-driven groups, PWS and ET. The marginal yield benefit (increased yield per unit increase of water application) is therefore quite low and not favouring high irrigation rates.

### 5.6.2 Berry carbon isotopes

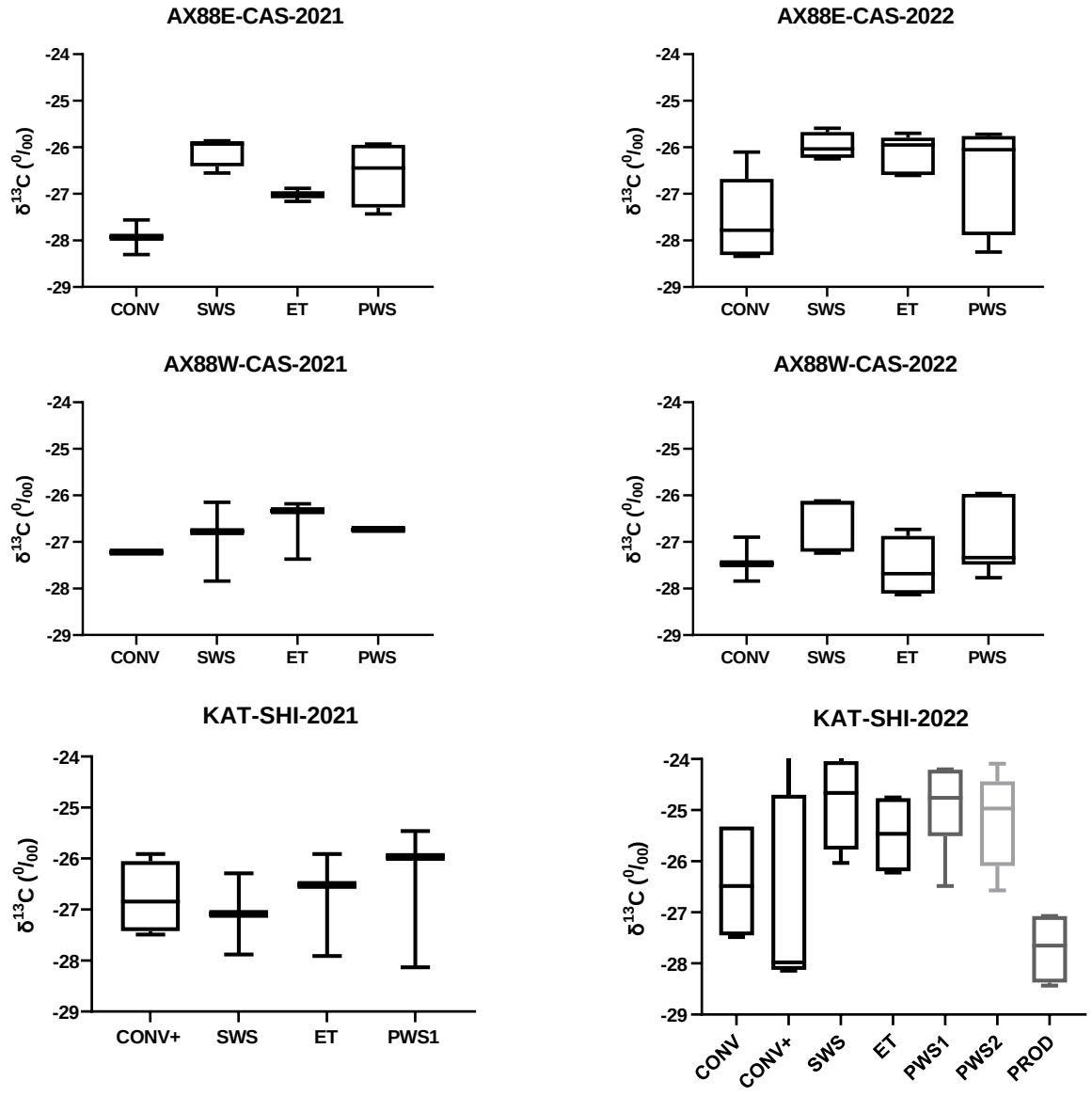



*Figure 51: Carbon isotope ($\delta^{13}C$) analysis of SHI and CAS grape berries. Boxplots show median value (horizontal line inside the box), minimum and maximum values (lower and upper edges of box) and SE (whiskers).*

Carbon isotope analysis was used as an estimate of the seasonal water use efficiency (WUE) of the vines as there is a high correlation between the $\delta^{13}C$ value and leaf-level instantaneous WUE (or Transpiration Efficiency, TE) as reported in several published studies. In AX88E-CAS (on Terra rossa), the highest (least negative) $\delta^{13}C$ values were found in the data-driven treatments, indicating higher WUE than the CONV in both seasons. The CAS vines on Rendzina soils (at AX88W) had fewer differences even though the same trend held in 2021. Amongst the data-driven treatments in CAS-Terra rossa, the PWS and SWS treatments had the highest $\delta^{13}C$ values in the first season.

For SHI grapevines on Terra rossa, ET and PWS had the highest $\delta^{13}C$ values in the first season, with no differences between the CONV+ and SWS treatments. In the second season, 2021/22, all the data-driven treatments were significantly higher than the CONV, CONV+ and PROD vines, indicative of their high WUE. Comparing these data-driven groups, the highest $\delta^{13}C$ values were observed in the SWS, PWS1 and PWS2 treatments, consistent with the $WUE_i$ values obtained from leaf gas exchange (Figure 38b).

## 5.7 Berry and juice composition

It was consistently observed that juice quality of CAS in both Alex88-east and Alex88-west vineyards did not significantly vary in response to different irrigation treatments across the first two seasons. However, berry quality attributes (colour, total phenolics and tannin concentrations) were significantly lower in SWS vines in the S1 relative to CONV vines.

In the 2020/21 season in both Alex88-east and Alex88-west, berry quality and most of the juice quality parameters remained unchanged. However, in Alex88-east, both PWS and SWS vines showed significantly lower pH and TA relative to CONV+ (Table 11).

*Table 11: Variations in berry and juice composition in Alex88-east and Alex88-west during three experimental seasons (2018/19, 2019/20 and 2020/21) in response to different irrigation treatments. Means (n = 4 – 8) are presented. Interactions between irrigation treatments are reported.*

| | Season | S1 | | S2 | | S3 | |
|---|---|---|---|---|---|---|---|
| | | Alex88-E | Alex88-W | Alex88-E | Alex88-W | Alex88-E | Alex88-W |
| pH | CONV | - | - | 4.2 ns | 3.6 ns | - | - |
| | CONV+ | - | - | - | - | 6.3 a | 4.1 ab |
| | ET | - | - | 4.2 | 3.7 | 5.9 ab | 4.1 ab |
| | PWS | - | - | 4.2 | 3.5 | 5.3 bc | 5.0 a |
| | SWS | - | - | 4.2 | 3.1 | 5.1 c | 3.8 b |
| TA | CONV | - | | 3.0 ns | 3.6 ns | - | - |
| | CONV+ | - | - | - | - | 6.3 a | 4.1 ab |
| | ET | - | - | 3.2 | 3.7 | 5.9 ab | 4.4 ab |
| | PWS | - | - | 3.3 | 3.5 | 5.3 bc | 5.0 a |
| | SWS | - | - | 2.9 | 3.1 | 5.1 c | 3.8 b |
| TSS | CONV | - | - | 25.2 ns | 26.3 a | - | - |
| | CONV+ | - | - | - | - | 26.2 ab | 26.8 ns |
| | ET | - | - | 25.5 | 25.2 b | 26.0 b | 26.9 |
| | PWS | - | - | 25.7 | 25.7 ab | 27.4 a | 26.7 |
| | SWS | - | - | 25.7 | 25.7 ab | 27.2 a | 26.9 |
| Colour per berry (mg anthocyanins per berry) | CONV | 3.5 ns | 3.5 ns | 1.8 ab | 1.5 ns | - | - |
| | CONV+ | - | - | - | - | 2.2 ns | 2.6 ns |
| | ET | 3.5 | 3.4 | 2.2 a | 1.6 | 2.3 | 2.6 |
| | PWS | 3.4 | 3.7 | 1.8 ab | 1.6 | 2.3 | 2.6 |
| | SWS | 3.0 | 3.7 | 1.7 b | 1.6 | 2.2 | 2.5 |
| Colour per gram berry weight (mg anthocyanins per | CONV | 4.2 a | 4.2 ns | 1.9 ns | 1.8 ns | - | - |
| | CONV+ | - | - | - | - | 2.4 ns | 2.7 ns |
| | ET | 3.8 ab | 3.8 | 2.3 | 1.8 | 2.4 | 2.6 |
| | PWS | 3.9 ab | 4.3 | 1.8 | 1.9 | 2.6 | 2.7 |
| | SWS | 3.2 b | 4.2 | 1.9 | 1.9 | 2.6 | 2.8 |

| | Season | S1 | S2 | S3 | | | |
|---|---|---|---|---|---|---|---|
| | | Alex88-E | Alex88-W | Alex88-E | Alex88-W | Alex88-E | Alex88-W |
| Total phenolics per berry (absorbance units (au) per | CONV | 2.5 ns | 2.5 ns | 1.8 ns | 1.5 ns | - | - |
| | CONV+ | - | - | - | - | 2.0ns | 2.2 ns |
| | ET | 2.5 | 2.4 | 1.8 | 1.7 | 2.1 | 2.3 |
| | PWS | 2.4 | 2.5 | 1.8 | 1.6 | 2.0 | 2.3 |
| | SWS | 2.2 | 2.6 | 1.7 | 1.6 | 1.9 | 2.2 |
| Total phenolics per gram berry weight (absorbance units (au) per gram berry | CONV | 3.0 a | 3.0 ns | 1.9 ns | 1.8 ns | - | - |
| | CONV+ | - | - | - | - | 2.2 ns | 2.3 ns |
| | ET | 2.7 ab | 2.7 | 1.9 | 1.8 | 2.2 | 2.3 |
| | PWS | 2.8 ab | 3.0 | 1.8 | 1.9 | 2.3 | 2.4 |
| | SWS | 2.4 b | 2.9 | 1.9 | 2.0 | 2.5 | 2.4 |
| Tannin concentration in homogenate (mg/g) | CONV | 8.2 ab | 7.0 ns | 5.3 ns | 5.2 ns | - | - |
| | CONV+ | - | - | - | - | 5.9 ns | 5.4 ns |
| | ET | 9.4 a | 7.2 | 4.9 | 5.4 | 5.2 | 5.1 |
| | PWS | 8.7 ab | 8.6 | 4.7 | 5.3 | 5.4 | 5.6 |
| | SWS | 4.9 b | 4.4 | 4.6 | 5.5 | 5.7 | 5.3 |
| Colour density | CONV | - | - | 3.9 ns | 4.4 ns | - | - |
| | CONV+ | - | - | - | - | 4.7 ns | 4.5 ns |
| | ET | - | - | 3.9 | 4.4 | 4.7 | 4.5 |
| | PWS | - | - | 3.8 | 4.4 | 4.7 | 4.7 |
| | SWS | - | - | 4.2 | 4.3 | 4.8 | 4.6 |
| Hue | CONV | - | - | 1.1 ns | 1.0 ns | - | - |
| | CONV+ | - | - | - | - | 1.0 ns | 1.0 ns |
| | ET | - | - | 1.1 | 1.0 | 1.0 | 1.0 |
| | PWS | - | - | 1.1 | 1.0 | 1.0 | 1.0 |
| | SWS | - | - | 1.1 | 1.0 | 1.0 | 1.0 |
| Total anthocyanins (mg/L) | CONV | - | - | 176 ab | 220 ns | - | - |
| | CONV+ | - | - | - | - | 400 ns | 327 ns |
| | ET | - | - | 162 b | 203 | 382 | 310 |
| | PWS | - | - | 170 ab | 234 | 409 | 307 |
| | SWS | - | - | 203 a | 215 | 425 | 310 |
| Total phenolics | CONV | - | - | 2.2 ns | 1.7 ns | 3.2 ns | 1.7 ns |
| | CONV+ | - | - | - | - | - | - |
| | ET | - | - | 1.7 | 1.8 | 2.9 | 2.4 |
| | PWS | - | - | 2.0 | 1.7 | 3.2 | 1.9 |
| | SWS | - | - | 1.7 | 1.7 | 3.8 | 2.5 |

In the 2018/19 season, irrigation scheduling did not significantly affect berry anthocyanin, phenolic and tannin concentrations in SHI in Katnook (Table 12). In the 2019/20, 2020/21 and 2021/22 seasons, juice quality parameters such as pH, TA, TSS, hue and total phenolics were also did not change in response to different irrigation treatments in SHI in Katnook. However, statistically significant differences were observed between Prodigy vines and SHI in Katnook. For instance, in S4, Prodigy vines showed significantly lower juice

quality parameters (pH and TSS) and higher TA and total phenolics relative to SHI vines in Katnook.

*Table 12: Variations in berry and juice composition in Katnook during four experimental seasons (2018/19, 2019/20, 2020/21 and 2021/22) in response to different irrigation treatments. Means (n = 4 – 8) are presented. Interactions between irrigation treatments are reported.*

| | Season | S1 | S2 | S3 | S4 | T | S | T×S |
|---|---|---|---|---|---|---|---|---|
| pH | CONV | - | 4.3 ns | - | 3.6 a | ** | *** | * |
| | CONV+ | - | - | 3.4 ns | 3.6 a | | | |
| | ET | - | 4.3 | 3.3 | 3.7 a | | | |
| | PWS1 | - | 4.3 | 3.4 | 3.7 a | | | |
| | PWS2 | - | - | - | 3.6 a | | | |
| | SWS | - | 4.3 | 3.3 | 3.6 a | | | |
| | Prod-CONV | - | - | 3.3 | 3.0 b | | | |
| TA | CONV | - | 5.5 ns | 7.0 ns | 5.3 bcd | * | *** | ** |
| | CONV+ | - | - | - | 5.9 b | | | |
| | ET | - | 5.6 | 7.0 | 5.1 d | | | |
| | PWS1 | - | 5.6 | 6.7 | 5.1 d | | | |
| | PWS2 | - | - | - | 5.1 d | | | |
| | SWS | - | 5.2 | 7.0 | 5.1 d | | | |
| | Prod-CONV | - | - | 7.4 | 8.6 a | | | |
| TSS | CONV | - | 27.8 ns | - | 25.5 a | * | *** | * |
| | CONV+ | - | - | 22.9 a | 25.8 a | | | |
| | ET | - | 29.6 | 20.5 b | 26.5 a | | | |
| | PWS1 | - | 28.7 | 20.6 b | 26.7 a | | | |
| | PWS2 | - | - | - | 26.7 a | | | |
| | SWS | - | 28.2 | 20.8 ab | 25.9 a | | | |
| | Prod-CONV | - | - | 22.5 ab | 22.5 b | | | |

| | Season | S1 | S2 | S3 | S4 | T | S | T×S |
|---|---|---|---|---|---|---|---|---|
| Colour per berry (mg anthocyanins per berry) | CONV | 4.4 ns | 2.3 ns | - | 3.0 ab | * | *** | * |
| | CONV+ | - | - | 2.9 a | 3.5 a | | | |
| | ET | 4.9 | 2.4 | 2.3 ab | 2.9 b | | | |
| | PWS1 | 4.8 | 2.7 | 2.5 ab | 3.0 ab | | | |
| | PWS2 | - | - | - | 3.0 ab | | | |
| | SWS | 4.3 | 2.1 | 2.0 bcd | 3.0 ab | | | |
| | Prod-CONV | - | - | 1.5 d | - | | | |
| Color per gram berry weight (mg anthocyanins per gram berry weight) | CONV | 3.6 ns | 2.0 ns | - | 2.1 ns | ** | * | ** |
| | CONV+ | - | - | 1.8 a | 2.1 | | | |
| | ET | 4.2 | 2.1 | 2.0 a | 2.2 | | | |
| | PWS1 | 4.0 | 2.1 | 1.9 a | 2.2 | | | |
| | PWS2 | - | - | - | 2.2 | | | |
| | SWS | 3.6 | 1.7 | 1.8 a | 2.4 | | | |
| | Prod-CONV | - | - | 1.2 b | - | | | |
| Total phenolics per berry (absorbance units (au) per berry) | CONV | 3.2 ns | 2.1 ns | - | 2.8 ab | * | *** | * |
| | CONV+ | - | - | 2.7 a | 3.0 a | | | |
| | ET | 3.4 | 2.3 | 2.4 abc | 2.6 b | | | |
| | PWS1 | 3.3 | 2.3 | 2.6 ab | 2.7 ab | | | |
| | PWS2 | - | - | - | 2.7 ab | | | |
| | SWS | 2.9 | 2.0 | 2.1 bc | 2.6 b | | | |
| | Prod-CONV | - | - | 2.0 c | - | | | |
| Total phenolics per gram berry weight (absorbance units (au) per gram berry weight) | CONV | 2.7 ns | 1.9 ab | - | 1.9 ns | * | ** | ** |
| | CONV+ | - | - | 1.4 ab | 1.9 | | | |
| | ET | 2.9 | 2.0 a | 2.0 a | 1.9 | | | |
| | PWS1 | 2.8 | 1.9 ab | 2.0 a | 2.0 | | | |
| | PWS2 | - | - | - | 2.0 | | | |
| | SWS | 2.4 | 1.6 b | 1.9 ab | 2.0 | | | |
| | Prod-CONV | - | - | 1.6 b | - | | | |

| | Season | S1 | S2 | S3 | S4 | T | S | T×S |
|---|---|---|---|---|---|---|---|---|
| Tannin concentration in homogenate (mg/g) | CONV | 9.3 ns | - | - | 517 ns | * | *** | * |
| | CONV+ | - | - | 2.0 ns | 530 | | | |
| | ET | 9.2 | - | 3.2 | 517 | | | |
| | PWS1 | 10.4 | - | 3.2 | 582 | | | |
| | PWS2 | - | - | - | 568 | | | |
| | SWS | 10.6 | - | 2.9 | 685 | | | |
| | Prod-CONV | - | - | 3.2 | - | | | |
| Colour density | CONV | - | 4.7 ns | - | 3.3 bc | | | |
| | CONV+ | - | - | 3.7 ab | 3.0 c | | | |
| | ET | - | 4.8 | 4.3 a | 4.0 ab | * | *** | * |
| | PWS1 | - | 4.8 | 4.2 a | 4.0 ab | | | |
| | PWS2 | - | - | - | 4.2 a | | | |
| | SWS | - | 4.6 | 4.1 a | 3.7 bc | | | |
| | Prod-CONV | - | - | 3.2 b | 3.8 abc | | | |
| Hue | CONV | - | 1.0 ns | - | 0.82 ns | | | |
| | CONV+ | - | - | 1.0 ns | 0.75 | | | |
| | ET | - | 1.0 | 0.96 | 0.82 | * | *** | * |
| | PWS1 | - | 1.0 | 0.97 | 0.82 | | | |
| | PWS2 | - | - | - | 0.86 | | | |
| | SWS | - | 1.0 | 0.92 | 0.70 | | | |
| | Prod-CONV | - | - | 0.95 | 0.77 | | | |
| Total anthocyanins (mg/L) | CONV | - | 254.2 ns | - | 100.9 ns | | | |
| | CONV+ | - | - | 162.3 ab | 78.82 | | | |
| | ET | - | 237 | 234 a | 105.5 | | | |
| | PWS1 | - | 230 | 230 a | 89.41 | * | *** | * |
| | PWS2 | - | - | - | 76.81 | | | |
| | SWS | - | 222 | 207 a | 83 | | | |
| | Prod-CONV | - | - | 114 b | 69.21 | | | |

| | Season | S1 | S2 | S3 | S4 | T | S | T×S |
|---|---|---|---|---|---|---|---|---|
| Total phenolics (g/L) | CONV | - | 2.5 ns | - | 1.6 b | | | |
| | CONV+ | - | - | 0.9 ns | 1.6 b | | | |
| | ET | - | 2.5 | 1.2 | 1.6 b | | | |
| | PWS1 | - | 2.4 | 1.1 | 1.6 b | * | *** | * |
| | PWS2 | - | - | - | 1.6 b | | | |
| | SWS | - | 2.2 | 0.9 | 1.6 b | | | |
| | Prod-CONV | - | - | 1.1 | 2.0 a | | | |

## 5.8 Wine composition

*Table 13: Wine composition of Coonawarra Cabernet Sauvignon from AX88 East and West vineyards under different irrigation regimes.*

| | Season | Treatment | pH | TA | Colour | Hue | Total Anthocyanins (mg/L) | Total Phenolics (g/L) |
|---|---|---|---|---|---|---|---|---|
| **Alex East** | **2018/19** | CONV | 4.11 | 5.35 | 4.77 | 1.05 | 365.47 | 4.05 |
| | | ET | 4.14 | 5.60 | 4.80 | 1.05 | 326.21 | 3.50 |
| | | PWS | 4.07 | 5.43 | 4.78 | 1.05 | 329.02 | 2.98 |
| | | SWS | 4.12 | 5.27 | 4.79 | 1.05 | 279.02 | 2.77 |
| | **2019/20** | CONV | 3.98 | 6.32 | 4.94 | 1.04 | 378.19 | 2.31 |
| | | ET | 3.94 | 6.90 | 4.93 | 1.04 | 393.54 | 2.47 |
| | | PWS | 3.98 | 6.60 | 4.89 | 1.04 | 392.45 | 2.99 |
| | | SWS | 3.99 | 6.52 | 4.91 | 1.04 | 396.28 | 3.16 |
| | **2020/21** | CONV+ | 4.16 | 5.70 | 4.81 | 1.04 | 308.05 | 3.54 |
| | | ET | 4.24 | 5.53 | 4.81 | 1.04 | 291.56 | 3.84 |
| | | PWS | 4.20 | 5.56 | 4.75 | 1.05 | 295.90 | 3.59 |
| | | SWS | 4.30 | 5.11 | 4.80 | 1.04 | 296.47 | 4.25 |
| **Alex West** | **2018/19** | CONV | 4.05 | 5.31 | 4.77 | 1.05 | 335.54 | 4.94 |
| | | ET | 4.06 | 5.10 | 4.82 | 1.05 | 309.84 | 4.02 |
| | | PWS | 4.03 | 5.33 | 4.80 | 1.05 | 337.97 | 4.63 |
| | | SWS | 4.06 | 5.22 | 4.82 | 1.05 | 309.59 | 4.13 |
| | **2019/20** | CONV | 3.95 | 6.48 | 4.86 | 1.04 | 374.35 | 3.29 |
| | | ET | 3.95 | 6.67 | 4.95 | 1.04 | 382.77 | 3.16 |
| | | PWS | 3.92 | 6.37 | 4.81 | 1.04 | 376.78 | 3.33 |
| | | SWS | 3.94 | 6.51 | 4.77 | 1.04 | 397.09 | 3.34 |
| | **2020/21** | CONV+ | 4.21 | 5.29 | 4.83 | 1.04 | 322.09 | 3.75 |
| | | ET | 4.21 | 5.43 | 4.74 | 1.04 | 283.29 | 3.76 |
| | | PWS | 4.13 | 5.34 | 4.81 | 1.04 | 312.91 | 3.43 |
| | | SWS | 4.21 | 5.23 | 4.84 | 1.04 | 314.93 | 4.26 |

Irrigation scheduling methods did not have a significant effect on basic wine composition parameters, pH and TA, colour and hue in most years. The total anthocyanins in the wine were lower in the ET treatment in most years except 2019/20, with no differences between the other groups. Total phenolics were often higher in the data-driven treatments except in the first season, 2018/19. The higher polyphenolic concentrations were generally related to the extent of vine water stress in the post-véraison period.

*Table 14: Wine composition of Coonawarra Shiraz from Katnook Estate under different irrigation regimes. In 2018/19 and 2019/20, the wines were made categorised by three vine water stress levels, LOW, MEDIUM, HIGH.*

| | Season | Treatment | pH | TA | Colour | Hue | Total Anthocyanins (mg/L) | Total Phenolics (g/L) |
|---|---|---|---|---|---|---|---|---|
| Katnook | 2018/19 | LOW | 4.21 | 4.70 | 4.78 | 1.05 | 354.34 | 4.13 |
| | | MEDIUM | 4.13 | 4.79 | 4.79 | 1.05 | 350.51 | 3.46 |
| | | HIGH | 4.14 | 4.78 | 4.77 | 1.05 | 339.76 | 4.63 |
| | 2019/20 | LOW | 4.34 | 7.15 | 4.84 | 1.04 | 367.51 | 2.40 |
| | | MEDIUM | 4.34 | 7.04 | 4.94 | 1.04 | 299.74 | 2.15 |
| | | HIGH | 4.32 | 6.94 | 4.88 | 1.04 | 372.50 | 2.44 |
| | 2020/21 | CONV+ | 4.17 | 5.24 | 4.74 | 1.05 | 265.52 | 1.99 |
| | | ET | 3.90 | 5.47 | 4.64 | 1.02 | 258.54 | 2.53 |
| | | PWS | 4.08 | 5.13 | 4.72 | 1.03 | 260.71 | 1.86 |
| | | SWS | 4.00 | 5.45 | 4.69 | 1.03 | 256.11 | 2.18 |
| | 2021/22 | CONV | 4.09 | 6.30 | 4.88 | 1.03 | 226.90 | 1.39 |
| | | ET | 4.05 | 6.08 | 4.84 | 1.04 | 293.15 | 1.78 |
| | | PWS | 4.08 | 6.19 | 4.94 | 1.04 | 252.56 | 1.55 |
| | | SWS | 4.07 | 6.05 | 4.87 | 1.04 | 308.22 | 1.65 |

In Shiraz grapevines, TA, pH, colour and hue were in a narrow range between treatments and did not differ significantly in any of the seasons. When the wines were grouped based on vine water stress levels in the first two seasons, the highest anthocyanin levels were observed in the low and high water stress levels, particularly in the 2019/20 season when the differences were significant. Phenolics followed a similar pattern in those years. When the different irrigation treatments were applied starting in the 2020/21 season, the ET treatment had higher phenolics in both seasons, but there were few differences in anthocyanins (except for SWS in the 2021/22 season).

## 5.9 Financial analysis

Investment and operational costs for each irrigation treatment are shown in Table 15.

*Table 15: Approximate investment and operational costs for each irrigation scheduling strategy investigated in this study. Operational costs for the GROW and ET treatments were calculated on a per season basis, whereas PWS and SWS operational costs were considered over a year as data subscription plans occur in 12-month cycles. Costs were considered for a 15 ha vineyard considering an 18-week irrigation period.*

| | Investment concept | Initial cost ($) | Lifespan (years) | Operational concept | Yearly operational cost ($) | Benefits |
|---|---|---|---|---|---|---|
| **GROW** | Experienced vineyard manager and one soil moisture sensor | 3,453 | 10 | Cost of wages involved in making decisions, ongoing maintenance of soil moisture probe | 479 | Minimal equipment requirements and interpretation of complex data |
| **ET** | Paso panel and labour required to establish crop factor values over one season | 1,172 | 10 | Cost of wages required to calculate $ET_c$ | 440 | Ability to numerically calculate irrigation needs |
| **PWS** | Thermography towers (thermal camera, gateway, waterproof outdoor boxes, pole, self-installation) | 6,000 | 5 | Data subscription each month, ongoing annual maintenance, cost of wages to analyse data | 580 | Integrates data from the whole canopy with measurements directly related to vine transpiration |
| **SWS** | Multiple depth capacitance probe (probes, installation cost and software) | 13,577 | 10 | Data subscription each month, ongoing maintenance of soil moisture probe, cost of wages to analyse data | 357 | Well-established methodology with a high degree of support for troubleshooting equipment and data problems |

The primary assumptions for the implementation of various sensors to obtain data relate to sensor density (i.e., number of sensors per ha), sensor prices and lifespan.

The following financial metrics were calculated for three seasons per cultivar (2018-2021 for CAS; 2019-2022 for SHI):

- Economic Productivity (EP)
- Economic Water Productivity (EWP)
- Unit production cost
- Total operational cost
- Income
- Cash flow
- Net Present Value (NPV)
- Internal Rate of Return (IRR)
- Pay-back Period (PB)
- Total margin

Results are presented in Tables 16-18 in the following pages.

### 5.9.1 Cabernet Sauvignon – Terra rossa

*Table 16: Financial indicators of various non-data and data-driven irrigation scheduling approaches for Cabernet Sauvignon grapevines grown on Terra rossa soil in Coonawarra.*

| | 2018/19 | | | | 2019/20 | | | | 2020/21 | | | | |
|---|---|---|---|---|---|---|---|---|---|---|---|---|---|
| | GROW | ET | PWS | SWS | GROW | ET | PWS | SWS | GROW+ | GROW | ET | PWS | SWS |
| Gross margin ($ ha$^{-1}$) | 20,001 | 19,925 | 18,203 | 20,221 | 7,635 | 14,936 | 9,893 | 10,775 | 23,373 a | 18,082 ab | 19,040 ab | 18,668 ab | 10,445 b |
| Economic water productivity ($ ML$^{-1}$) | 32,764 b | 61,914 a | 60,774 ab | 33,310 b | 13,032 b | 34,613 a | 22,311 ab | 20,026 ab | 18,385 c | 29,361 bc | 86,353 a | 61,549 ab | 29,524 bc |
| Breakeven point ($ t$^{-1}$) | 1,305 | 1,337 | 1,439 | 1,309 | 2,313 | 1,654 | 1,970 | 1,976 | 1,214 a | 1,341 a | 1,400 ab | 1,451 ab | 1,897 b |
| NPV ($ ha$^{-1}$) | 121,171 | 120,719 | 102,000 | 122,077 | -4,622 | 69,987 | 17,492 | 26,003 | 155,499 | 101,603 | 111,708 | 106,735 | 22,630 |

One-way ANOVA and Tukey's multiple comparison test ($\alpha = 0.05$) was used to compare treatments

In Terra rossa soils, the gross margin of CAS varied quite significantly from season to season; the anomalous year was 2019/20 where the margin was half or less than the other two seasons. The highest margins were found for the GROW treatment (GROW+ in the last year), whereas the lowest values were in the PWS. The EWP was highest in the data-driven treatments, particularly ET and PWS, and was consistent across seasons. These numbers were high due to the low price (or no cost) of water in Coonawarra. In areas where water prices have to be factored into the model, the EWP numbers would be considerably lower, particularly in dry years. These numbers are consistent with the NPV – the highest NPVs are associated with the ET and PWS treatments. In the case where excess irrigation was applied, GROW+, there was a strong yield response translating to the highest NPV values of the group. To evaluate which of the irrigation strategies were economically feasible, the breakeven point was determined. The BP values were around $1300-$1500 per tonne of grapes, which reflects the minimum price that has

to be received by growers if selling their crop. Lower BP values were observed in GROW treatment (except in 2019/20) likely due to the low investment costs associated with the sensor infrastructure. However, this is a scenario specific to Coonawarra where water prices are not a factor and could be quite different in areas like the inland regions along the Murray River, where water is a real cost to production and yields are substantially higher for a given amount of water applied i.e. higher gains in water use efficiency are expected to decrease the BP relative to GROW/GROW+. These strategies may then have very different feasibilities.

### 5.9.2 Cabernet Sauvignon – Rendzina

*Table 17: Financial indicators of various non-data and data-driven irrigation scheduling approaches for Cabernet Sauvignon grapevines grown on Rendzina soil in Coonawarra.*

| | 2018/19 | | | | 2019/20 | | | | 2020/21 | | | | |
|---|---|---|---|---|---|---|---|---|---|---|---|---|---|
| | GROW | ET | PWS | SWS | GROW | ET | PWS | SWS | GROW+ | GROW | ET | PWS | SWS |
| Gross margin ($ ha$^{-1}$) | 19,401 | 18,922 | 11,889 | 22,900 | 7,705 | 4,995 | 4,485 | 3,542 | 20,802 | 18,118 | 17,645 | 13,234 | 9,841 |
| Economic water productivity ($ ML$^{-1}$) | 43,110 b | 119,149 a | 70,049 ab | 48,511 b | 16,452 | 14,934 | 13,846 | 9,539 | 29,387 b | 51,108 ab | 81,666 a | 58,935 ab | 39,004 b |
| Breakeven point ($ t$^{-1}$) | 1,375 | 1,629 | 1,954 | 1,200 | 2,346 | 3,334 | 3,483 | 3,168 | 1,380 | 1,336 | 1,406 | 2,416 | 2,176 |
| NPV ($ ha$^{-1}$) | 115,053 | 110,508 | 37,774 | 149,318 | -3,884 | -38,553 | -51,700 | -49,992 | 122,641 | 101,940 | 97,522 | 40,365 | 16,484 |

One-way ANOVA and Tukey's multiple comparison test ($\alpha = 0.05$) was used to compare treatments

In the heavier Rendzina soils of Coonawarra, CAS gross margins followed a similar trend to the lighter Terra rossa soils – GROW had higher margins due to the low investment in infrastructure, but this was not linked to EWP or NPV. The returns per unit application of water (EWP) was highest in the ET treatment, primarily due to the low investment cost associated with obtaining crop coefficients and calculating $ET_c$. The EWP values were generally higher in Rendzina compared with Terra rossa (except 2019-20), reflecting the marginal benefit of using sensor technology in vineyards with heavier soils, possibly due to the greater disconnect between water content in the soil and vine water status that drives yield. The BP values were higher also compared to Terra rossa by nearly $500 per tonne reflecting how critical it is to manage irrigation prudently in heavier soils that have a higher clay content. While NPV values were generally highest in the GROW/GROW+ treatments, the data-driven treatments were only slightly lower due to the investment costs associated with the infrastructure as well as slightly lower yields. With water prices factored in (in other regions), these numbers are likely to tip in favour of the data-driven treatments.

### 5.9.3 Shiraz – Terra rossa

*Table 18: Financial indicators of various non-data and data-driven irrigation scheduling approaches for Shiraz grapevines grown on Terra rossa soil in Coonawarra.*

| | 2019/20 | | | | 2020/21 | | | | | 2021/22 | | | | | |
|---|---|---|---|---|---|---|---|---|---|---|---|---|---|---|---|
| | **GROW** | **ET** | **PWS** | **SWS** | **GROW+** | **GROW** | **ET** | **PWS** | **SWS** | **GROW+** | **GROW** | **ET** | **PWS1** | **PWS2** | **SWS** |
| **Gross margin ($ ha$^{-1}$)** | 5,271 | 2,610 | 4,047 | 2,425 | 42,154 a | 15,827 b | 36,116 ab | 44,777 a | 41,522 a | 29,588 ab | 31,168 a | 23,228 ab | 19,779 b | 24,265 ab | 22,887 ab |
| **Economic water productivity ($ ML$^{-1}$)** | 5,632 | 3,885 | 6,022 | 4,393 | 21,077 b | 15,827 b | 83,992 a | 81,412 a | 86,505 a | 15,096 b | 25,136 a | 21,310 ab | 17,199 ab | 21,665 ab | 24,092 a |
| **Breakeven point ($ t$^{-1}$)** | 3,310 | 5,026 | 2,686 | 2,893 | 471 a | 917 b | 561 b | 492 b | 490 b | 616 ab | 576 a | 753 ab | 842 b | 699 ab | 749 ab |
| **NPV ($ ha$^{-1}$)** | -72,524 | -105,041 | -62,701 | -87,233 | 359,906 | 85,220 | 297,118 | 386,263 | 351,842 | 228,841 | 226,375 | 162,756 | 125,594 | 129,137 | 157,521 |

One-way ANOVA and Tukey's multiple comparison test ($\alpha = 0.05$) was used to compare treatments

The Shiraz grapevines on Terra rossa soils had similar financial trends to the CAS. The highest gross margins were attained in the GROW treatment while the lowest were in the data-driven treatments. The benefit of using sensor driven technology was apparent when looking at the EWP: the PWS and ET treatments were amongst the highest in the group while the GROW/GROW+ were the lowest. The breakeven points for SHI were considerably lower than for CAS although the trends were the same; the lowest BPs were in the GROW treatment due to the low investment required, while the ET treatment was amongst the lowest in the data-driven group for the same reasons. The plant sensor-based treatments had the lowest BP and highest NPV of the group, so, in the long term, this strategy represents a prudent financial decision for SHI.

## 5.10 Irrigation Practices Survey

The Limestone Coast irrigation survey was launched on 14 July 2021 and it was closed on 23 August 2021. Thirty-five grapevine growers participated in the survey. The irrigation survey and responses are in the Appendix. The survey results were disseminated to the industry in September 2021 and one random respondent to Part 3 of the survey was selected to win a $100 gift card. The number of survey respondents was 32.

Aggregated results of the irrigation practices survey data are provided in the Appendix. The highlights of the survey responses include:

- Most organisations surveyed had a total vineyard area between 20-500 ha with average yields between 3-9 t/ha.
- The majority (~90%) of vineyards were irrigated using above-ground drip irrigation.
- Most (72%) irrigation decisions were made based on historical experience of the block(s).
- Most irrigators used weather forecasts to make irrigation decisions; less than 30% of the respondents used ET to schedule irrigation using historical or published crop coefficients.
- Two-thirds of the respondents used soil moisture monitoring; only two growers used plant-based sensors (sap flow, canopy temperature)
- The greatest barriers to adoption of new technology (for irrigation scheduling) were a lack of understanding of the technology, uncertainty of its value and high cost.
- Approximately half of the respondents plan to invest in new or additional irrigation technology within three years.

# 6 Other related outputs

Three scientific (peer-reviewed) manuscripts have been published as a part of this project:

- Gautam et al. (2021) Estimation of grapevine crop coefficient using a multispectral camera on an unmanned aerial vehicle. *Remote Sensing* 13: 2639.
- Gautam et al. (2020) A review of current and potential applications of remote sensing to study the water status of horticultural crops. *Agronomy* 10: 140.
- Pagay, V. (2021) Evaluating a novel microtensiometer for continuous trunk water potential measurements in field-grown irrigated grapevines. *Irrigation Science* 40: 45-54.

Two additional papers are in preparation:

- Schlank, R. et al. Evaluating different irrigation scheduling strategies in Cabernet Sauvignon grapevines according to soil type and water use efficiency metrics in a Mediterranean climate.
- Schlank, R. et al. Financial analysis of implementing different irrigation scheduling strategies in premium Cabernet Sauvignon grapevine in a cool climate Australian vineyard.

The findings of this research project were presented or will be presented at the following events.

- Pagay, V. (invited) Innovative technologies for precision irrigation in vineyards. 2021. American Society for Enology and Viticulture (ASEV) Precision Viticulture Symposium. (22 June 2021)
- Schlank, R. Evaluating different irrigation scheduling strategies in Cabernet Sauvignon grapevines according to soil type and water use efficiency metrics in a Mediterranean climate. Crush 2021-the grape and wine science symposium. Adelaide. 16 June 2021
- Presentations to industry collaborators
    - WA bilateral project updates. Treasury Wine Estates. (27 August 2021)
    - WA bilateral project updates. Katnook Estate. (1 September 2021)
- ASVO podcast on irrigation strategies in vineyards (31 August 2021)
- AWRI webinar on optimising irrigation in vineyards (November 2021)
- AWRI Irrigation Roadshows (several in 2022)
- AWITC 2022 Workshop on Water Use Efficiency (oral presentation, 26 June 2022)
- Abstract submitted to the ISHS 10th International Symposium on Irrigation of Horticultural Crops, Stellenbosch, South Africa (January-February 2023).

# 7 Concluding remarks

Irrigation strategies based on data-driven techniques enabled the saving of water without compromising vine physiological performance, yield or grape composition.

A key finding of this trial was that in premium vineyards under deficit irrigation, seasonal irrigation volumes only partly account for variable yields. Irrigation schedules play a vitally important role in this regard and managing irrigation based on data, whether soil moisture, plant water status or ETc, can greatly benefit water use efficiency and, importantly, without sacrificing grape/wine quality.

We validated two new commercial crop water status sensors as part of the trial – microtensiometers (Florapulse) and TranspIR (Athena IR-Tech). Both were found to strongly correlate with conventional vine water status metrics such as stem water potential and stomatal conductance.

High resolution remote sensing from UAVs was shown to be valuable for: (i) assessing spatial variations in water status and canopy performance; and (ii) developing predictive models of these parameters over space and time. Together, these are essential for precision irrigation, informing the placement of crop-based sensors as well as zoning of irrigation blocks into sub-blocks.

Together, these techniques have the potential to increase water use efficiency in grapevine and other crops that are similarly irrigated.

Our choice of the two vineyards for Shiraz and Cabernet Sauvignon that were contrasting in their variability highlighted the importance of understanding spatial variability to improve management practices, including irrigation scheduling.

The use of continuous crop water status sensors provided near real-time (or daily) data to inform the temporal management of irrigation to achieve greater efficiencies in water management in Australian vineyards.

## 8 Acknowledgements

The authors and the PIs would like to acknowledge all the involved industry, industry personnel, researchers and many students who were involved over the years. Special thanks to Wynns Coonawarra Estate, Katnook Estate, Dr Catherine Kidman, Chris Brodie, Gavin Blacker, Dr Deepak Gautam, Felipe Canela, Rochelle Schlank, Dr Dilrukshi Nagahatenna, Hans Loder, Zac Han Chow, Do Mai Chi, Ockert Le Roux, Heidi Eldridge (Coonawarra Vignerons), Kerry DeGaris, Ulrich-Grey-Smith (LCGWC) for their involvement and assistance at various stages of the project.

# 9 References


Australia, W. (2022) *Australian wine sector at a glance*, Available: https://www.wineaustralia.com/market-insights/australian-wine-sector-at-a-glance [Accessed 20/08/2022.

AWRI (2019) *Vineyard and winery practices survey*, Available: https://www.awri.com.au/wp-content/uploads/2019/05/AWRI_Practices_Survey_Final_Report.pdf [Accessed 20/08/2022.

Caravia, L., Pagay, V., Collins, C. and Tyerman, S. (2017) Application of sprinkler cooling within the bunch zone during ripening of Cabernet Sauvignon berries to reduce the impact of high temperature. *Australian Journal of Grape and Wine Research* **23**, 48-57.

Cifre, J., Bota, J., Escalona, J. M., Medrano, H. and Flexas, J. (2005) Physiological tools for irrigation scheduling in grapevine (*Vitis vinifera* L.) An open gate to improve water-use efficiency? *Agriculture Ecosystems & Environment* **106**, 159-170.

Collins, M. and Loveys, B. (2010) Optimising irrigation for different cultivars. *Final report to Grape and Wine Research & Development Corporation. Project Number CSP* **5**.

Dry, P. R., Loveys, B. R., McCarthy, M. G. and Stoll, M. (2001) Strategic irrigation management in Australian vineyards. *OENO One* **35**, 129-139.

Fereres, E. and Soriano, M. A. (2006) Deficit irrigation for reducing agricultural water use. *Journal of Experimental Botany* **58**, 147-159.

Fernandez, J. E. (2017) Plant-based methods for irrigation scheduling of woody crops. *Horticulturae* **3**.

Fraga, H., Malheiro, A. C., Moutinho-Pereira, J. and Santos, J. A. (2012) An overview of climate change impacts on European viticulture. *Food and Energy Security* **1**, 94-110.

Green, G. and Pannell, A. (2020) *Guide to climate projections for risk assessment and planning in South Australia.* Adelaide, SA.

Jones, G. V. and Goodrich, G. B. (2008) Influence of climate variability on wine regions in the western USA and on wine quality in the Napa Valley. *Climate Research* **35**, 241-254.

Jones, G. V. and Webb, L. B. (2010) Climate change, viticulture, and wine: challenges and opportunities. *Journal of Wine Research* **21**, 103-106.

Jones, G. V., White, M. A. and Cooper, O. (2004) Climate change and global wine quality. *Bulletin of the American Meteorological Society* **85**, 504-+.

Jones, G. V., White, M. A., Cooper, O. R. and Storchmann, K. (2005) Climate change and global wine quality. *Climatic Change* **73**, 319-343.

Lebon, E., Dumas, V., Pieri, P. and Schultz, H. R. (2003) Modelling the seasonal dynamics of the soil water balance of vineyards. *Functional Plant Biology* **30**, 699-710.

Marks, J., Lines, T., Penfold, C. and Cavagnaro, T. (2022) Cover crops and carbon stocks: How under-vine management influences SOC inputs and turnover in two vineyards. *Science of The Total Environment* **831**, 154800.

Miras-Avalos, J. M. and Araujo, E. S. (2021) Optimization of vineyard water management: challenges, strategies, and perspectives. *Water* **13**.

Muñoz-Carpena, R. (2004) Field devices for monitoring soil water content: BUL343/AE266, 7/2004. *EDIS* **2004**.

Pagay, V. (2018) *Using in-canopy misters to mitigate the negative effects of heatwaves in grapevines*. Wine Australia Project UA 1502.

Rienth, M. and Scholasch, T. (2019) State-of-the-art of tools and methods to assess vine water status. *OENO One* **53**.

Romero, P., Navarro, J. M. and Ordaz, P. B. (2022) Towards a sustainable viticulture: The combination of deficit irrigation strategies and agroecological practices in Mediterranean vineyards. A review and update. *Agricultural Water Management* **259**, 107216.

Santos, J. A., Fraga, H., Malheiro, A. C., Moutinho-Pereira, J., Dinis, L.-T., Correia, C., Moriondo, M., Leolini, L., Dibari, C., Costafreda-Aumedes, S., Kartschall, T., Menz, C., Molitor, D., Junk, J., Beyer, M. and Schultz, H. R. (2020) A review of the potential climate change impacts and adaptation options for European viticulture. *Applied Sciences* **10**, 3092.

Schultz, H. R. and Stoll, M. (2010) Some critical issues in environmental physiology of grapevines: future challenges and current limitations. *Australian Journal of Grape and Wine Research* **16**, 4-24.

Shackel, K. (2011) A plant-based approach to deficit irrigation in trees and vines. *HortScience* **46**, 173-177.

Webb, L., Whetton, P. and Barlow, E. W. R. (2007) Future climate change impacts on Australian viticulture. In: Paper presented to the Actes du colloque "Réchauffement climatique, quels impacts probables sur les vignobles.

Williams, L. E. (2013) Physiological tools to assess vine water status for use in vineyard irrigation management: review and update. In: Paper presented to the 9th International Symposium on Grapevine Physiology and Biotechnology, La Serena, Chile.

# 10 Appendix: Limestone Coast Vineyard Irrigation Survey

**Industry Experience and Operation**

1. What is your age range?
    a. 18 – 25
    b. 26 – 35
    c. 36 – 45
    d. 46 - 55
    e. 55+

2. What is your main occupation in the wine industry? (Please circle all that apply)
    a. Grape grower
    b. Viticulturist
    c. Winemaker (not winery owner)
    d. Winery owner

3. How long have you been involved in the grape and wine sector? _____

    How many of these have you been growing or managing grapes for? _____

    Of these years, how many have been in the Limestone Coast region? _____

4. Which region(s) of the Limestone Coast are you based or operating in?

5. What is the total vineyard size in which you operate? (for all varieties grown in the Limestone Coast region)
    a. <20 ha
    b. 20-49 ha
    c. 50-99 ha
    d. 100 - 500 ha
    e. >500 ha

6. What is a typical annual yield range from your operations? (total tonnes for all red winegrape varieties grown in the Limestone Coast region)

    _____

7. Do you typically dry farm or irrigate your grapevines?
    a. Irrigated
    b. Rainfed/dry grown

8. If you irrigate, how do you deliver irrigation? (circle all relevant)
    a. Above ground drip irrigation
    b. Subsurface drip irrigation
    c. Micro sprinklers
    d. Overhead sprinklers
    e. Other (please describe)

**Irrigation Scheduling**

1. How much time do you devote towards making irrigation decisions during an average week?
    a. Less than 5 minutes

b. 5 to 20 minutes
c. 20+ minutes

2. How do you carry out irrigation scheduling in established vineyards (mature, > 5 years old)? (Please select options within each of a, b, c, d. More than one can be selected)

   a. Historical irrigation levels

   b. Regular visual assessments of vine canopies for signs of water stress

   c. Weather forecasts

   d. Soil moisture monitoring (sensor-based)
      - Soil water tension (e.g. gypsum blocks, tensiometers)
        - How many do you have across all your red winegrape vineyards? _____
      - Volumetric water content (e.g. capacitance probes)
        - How many do you have across all your red winegrape vineyards? _____

   e. Evapotranspiration (ET)-driven
      - How do you obtain your reference ET? _____
      - How do you obtain your crop factors (crop coefficients, $K_c$)? _____
      - Which weather station do you use? _____

   f. Plant water status
      What type of sensor(s) do you use? (include make and model) _____
      - How many do you have across all your red winegrape vineyards? _____

   g. Other
      - Remote sensing
        - UAVs/Drones
        - Fixed wing aircraft
        - Satellite

        What specific dataset or indices are you looking at? _____
      - Not listed (if circled, please describe) _____

3. If you use historical irrigation practices and/or weather forecast data, are there any specific barriers that have prevented you from adopting/considering other sensor-based (e.g. soil or plant sensors) technologies listed? Check one or more boxes from the list below:
   a. High cost
   b. Unsure of value of technology / lack of understanding

4. Why did you choose the specific irrigation scheduling approach you are currently using? What motivated this decision? You can circle more than one:
    a. Familiarity/previous experience
    b. Recommended by colleagues
    c. Availability (e.g. sensor hardware, data access/visualization)
    d. Convenience (or sensors already in place), ease of use
    e. Reliability
    f. Maintenance (if sensors used)
    g. Price
    h. Other: _____

5. What are your concerns about your current irrigation practices?
    a. No concerns
    b. High energy cost
    c. Maintenance of irrigation infrastructure
    d. Low irrigation system efficiency
    e. Uncertainty about plant and/or soil moisture levels
    f. Inadequate information to make prudent irrigation decisions
    g. Other: _____

6. What are your future plans in terms of investment/adoption of technologies to aid in irrigation scheduling? Please describe according to the criteria mentioned below:
    a. Timeframe for investment: _____
    b. Infrastructure/sensors(s): _____
    c. Budget: _____
    d. No current plans to invest in irrigation technology

**Thank you for your participation**. If you would like to receive a copy of the aggregated survey results of the region, please fill in your contact details.

**BOX to allow participants to fill in name, email address, phone number (optional)**

You may optionally continue to the next page to provide some cultivar specific information for a chance to win a $50 gift card/voucher. Please remember to enter your contact details above before you proceed to the next page.

**Cultivar-specific irrigation**

Please fill in all relevant information for the varieties you typically grow focusing on only one specific block per cultivar during growing season (not including frost protection). Please fill in as much as you are comfortable providing information about.

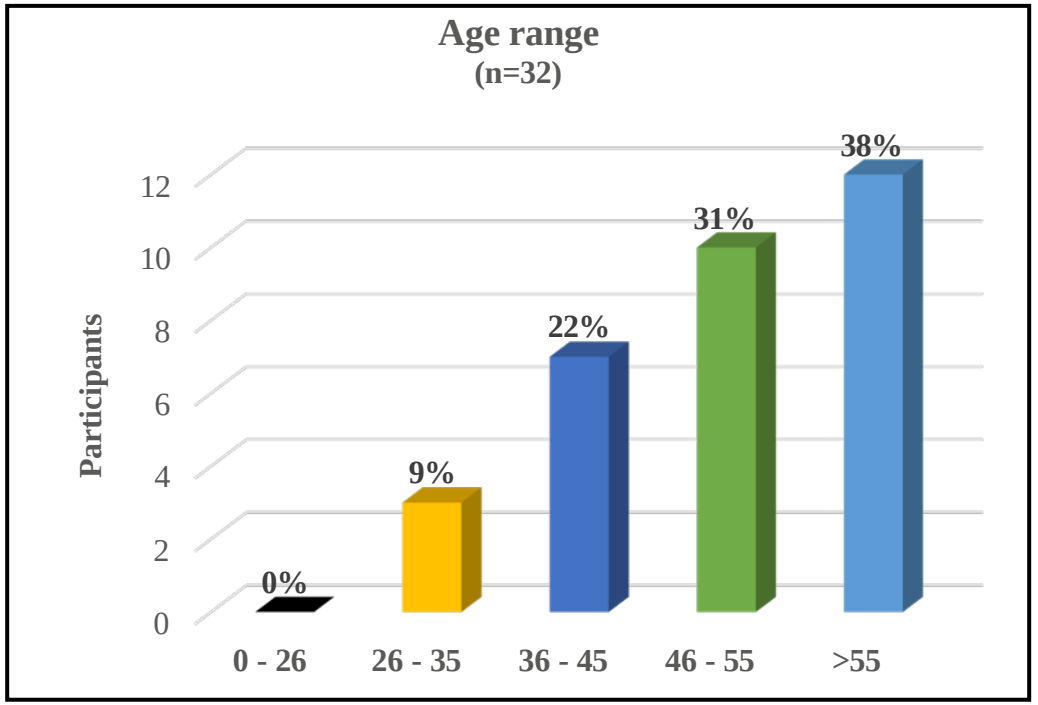
| | Size and soil type of plantings (Ha) | Region within Limestone Coast | Vine age (mature, more than 5 years old) | Vine density (vine/ha) | Is this block deficit irrigated, and if so what regime? (RDI* or SDI*, other) | Typical irrigation regime (mm per week) | Number of irrigation applications per week | Total seasonal irrigation ML/ha (typical ranges, max and min) | Yield (t/Ha) (2020 and 2016 vintage) | Average farm gate value for grapes ($/tonne)<br>a. <$500<br>b. $500 - $1200<br>c. $1200 - $2000<br>d. $2000+ |
|---|---|---|---|---|---|---|---|---|---|---|
| Barbera | | | | | | | | | | |
| Cabernet Franc | | | | | | | | | | |
| Cabernet Sauvignon | | | | | | | | | | |
| Malbec | | | | | | | | | | |
| Merlot | | | | | | | | | | |
| Nebbiolo | | | | | | | | | | |
| Petit Verdot | | | | | | | | | | |
| Pinot Meunier | | | | | | | | | | |
| Pinot Noir | | | | | | | | | | |
| Shiraz | | | | | | | | | | |
| Tempranillo | | | | | | | | | | |
| Other red: | | | | | | | | | | |
| Chardonnay | | | | | | | | | | |
| Gewürztraminer | | | | | | | | | | |
| Pinot Gris/Grigio | | | | | | | | | | |
| Riesling | | | | | | | | | | |
| Sauvignon Blanc | | | | | | | | | | |
| Semillon | | | | | | | | | | |
| Other white: | | | | | | | | | | |

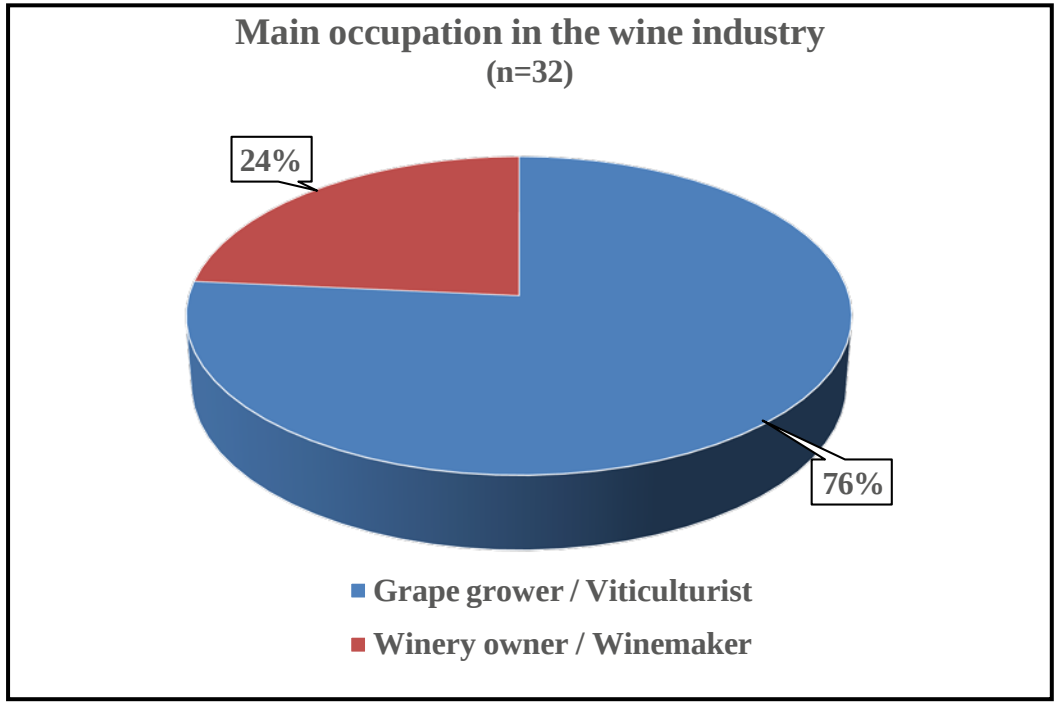
*RDI: Regulated deficit irrigation *SDI: Sustained deficit irrigation

# Vineyard Irrigation Practices Survey
# Limestone Coast Region (SA)

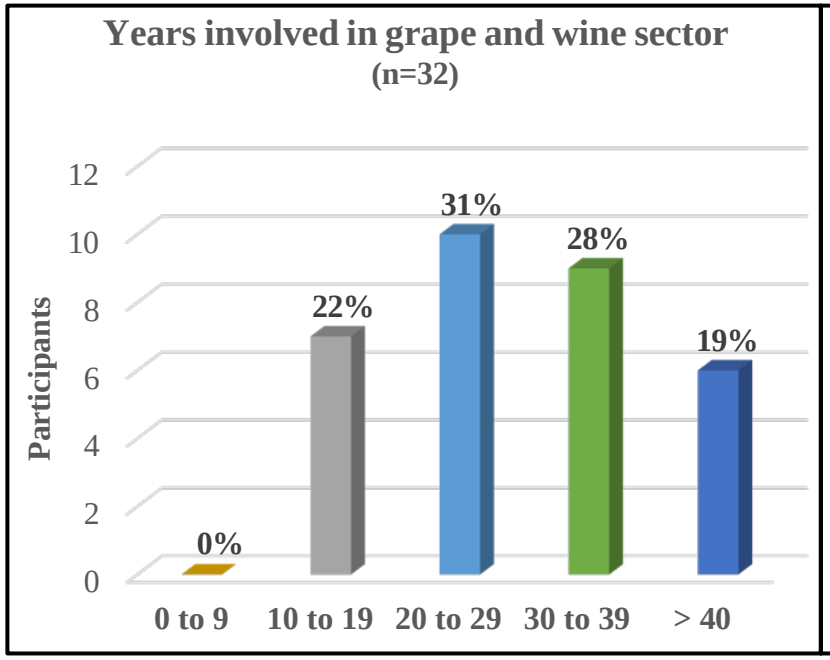
- **Date of Survey: July-August 2021**
- **Number of respondents: 32 (17 completed all three sections)**
- **Survey conducted by Dr Vinay Pagay, University of Adelaide (vinay.pagay@adelaide.edu.au)**

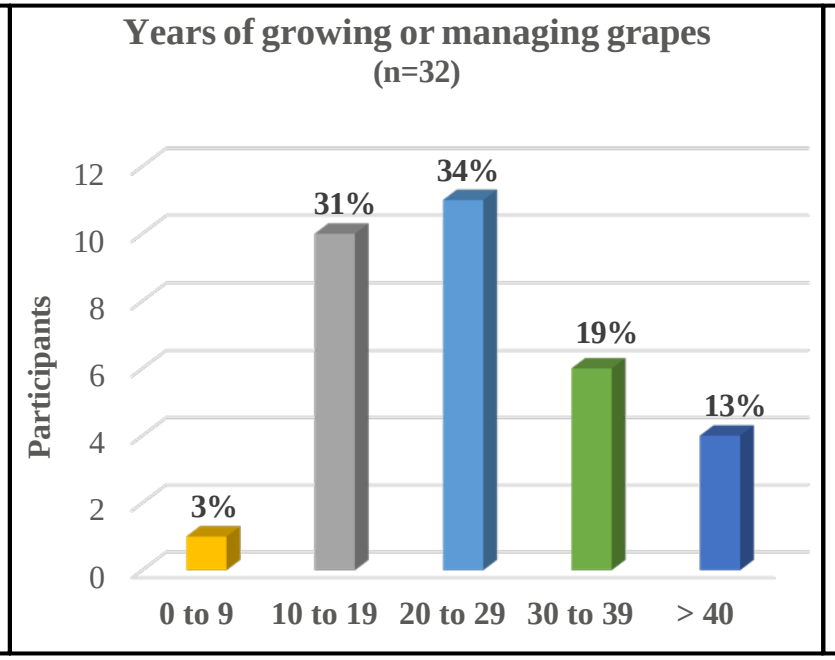
# Age and occupation

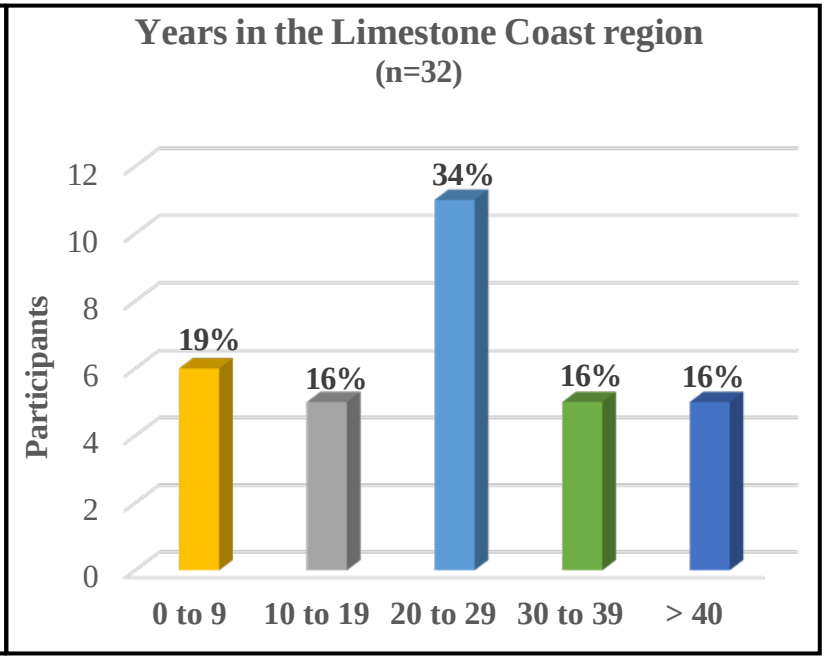


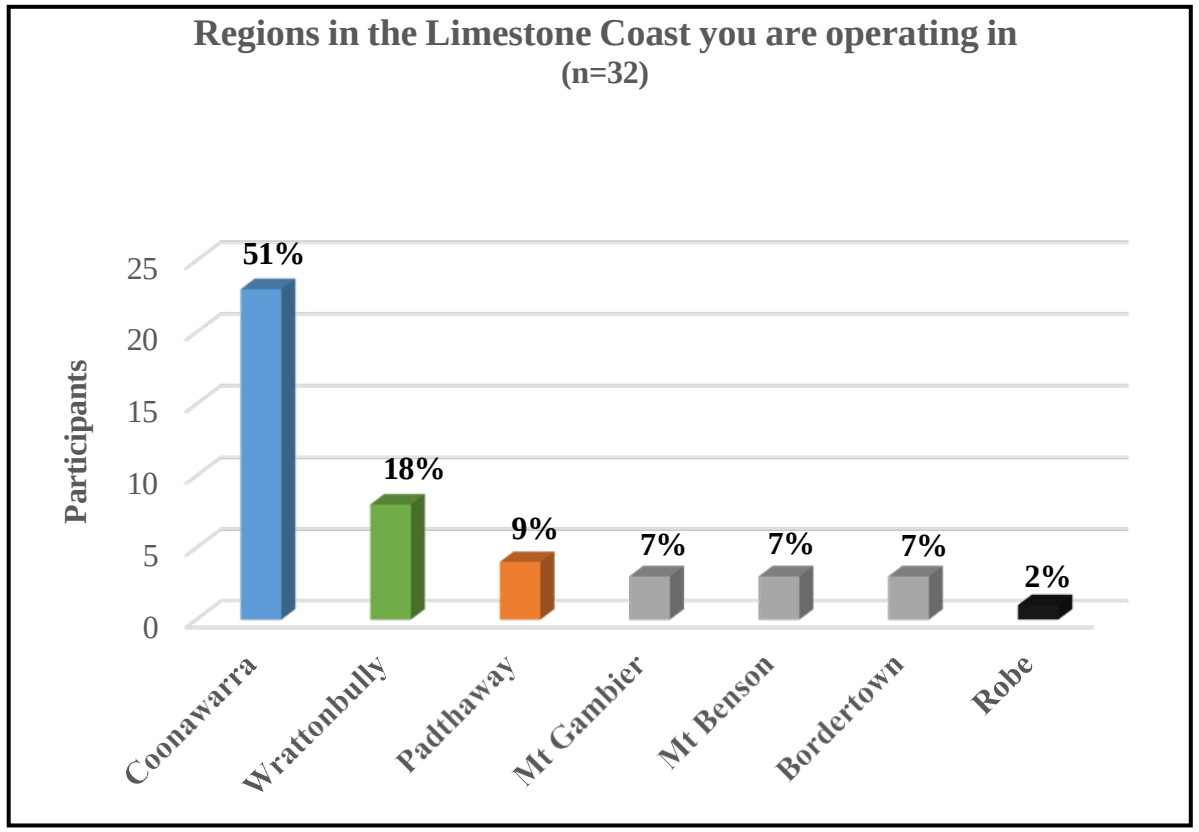
# Background/experience

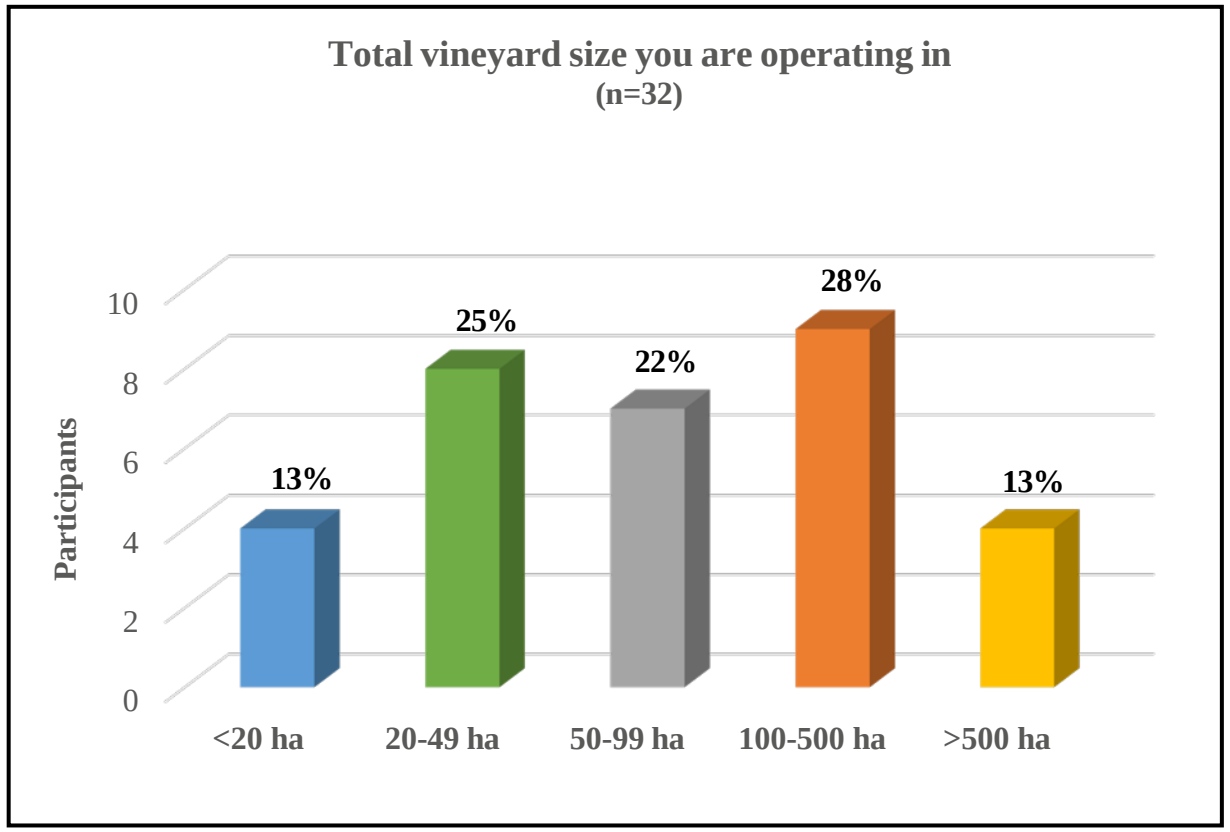


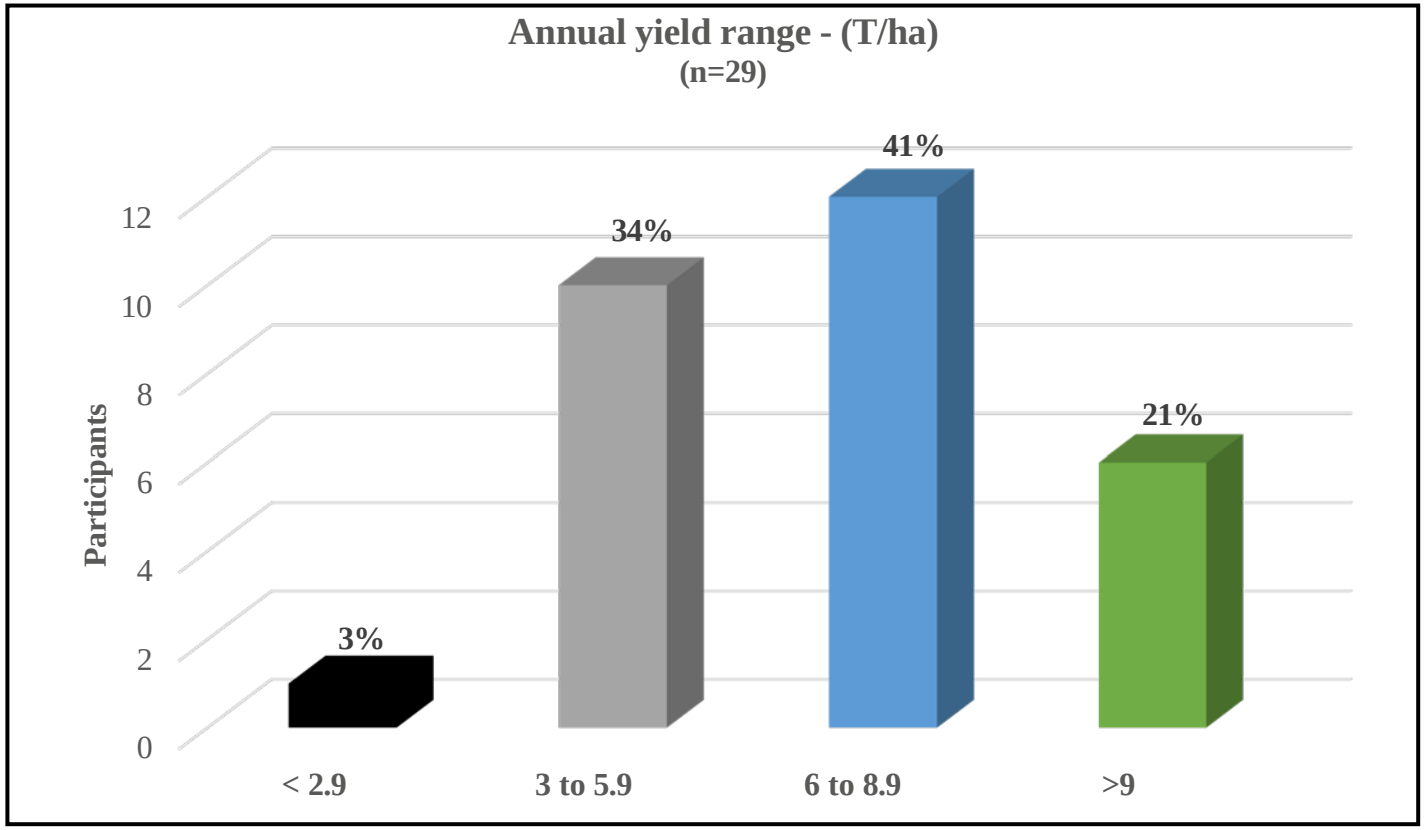



# Operation location(s) (sub-regions), Vineyard size



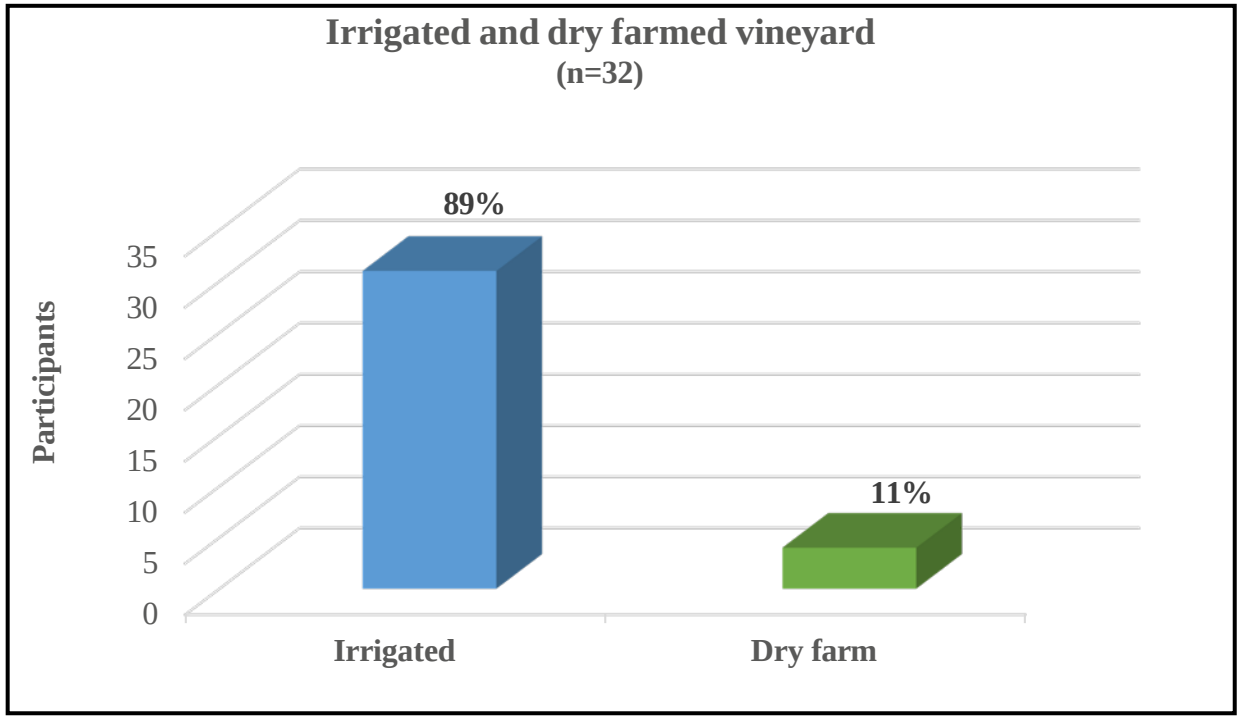



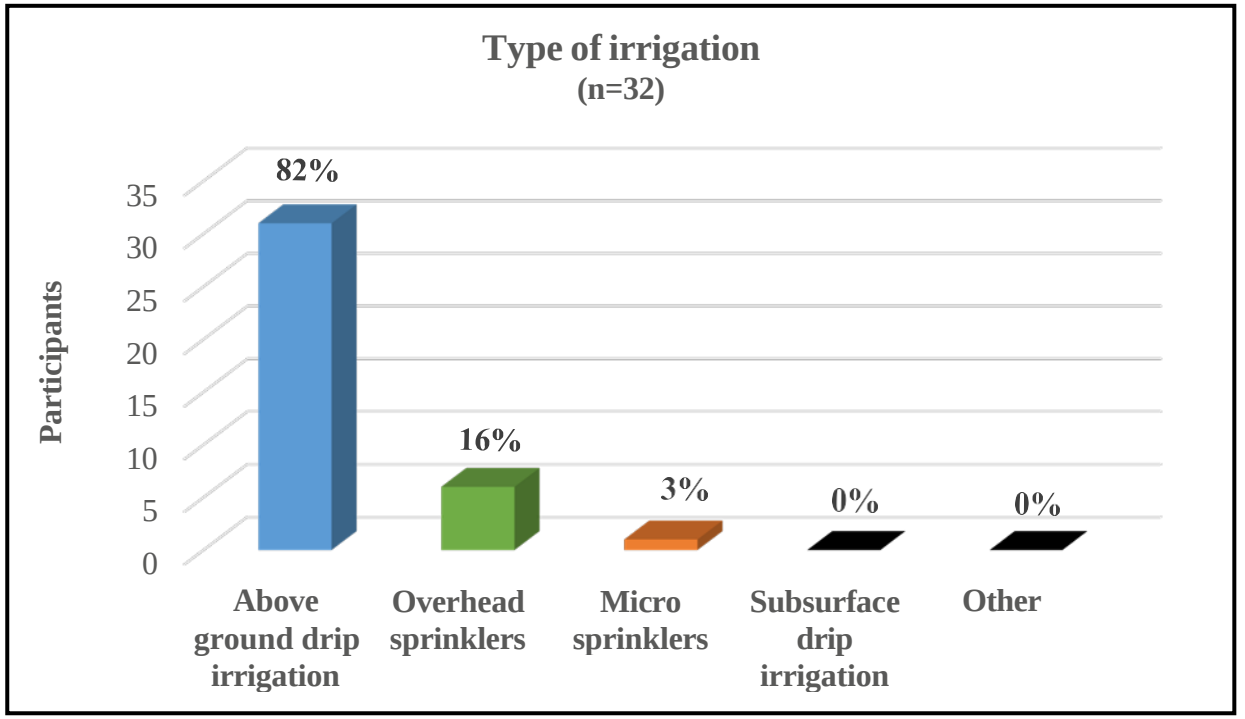
# Annual Yields



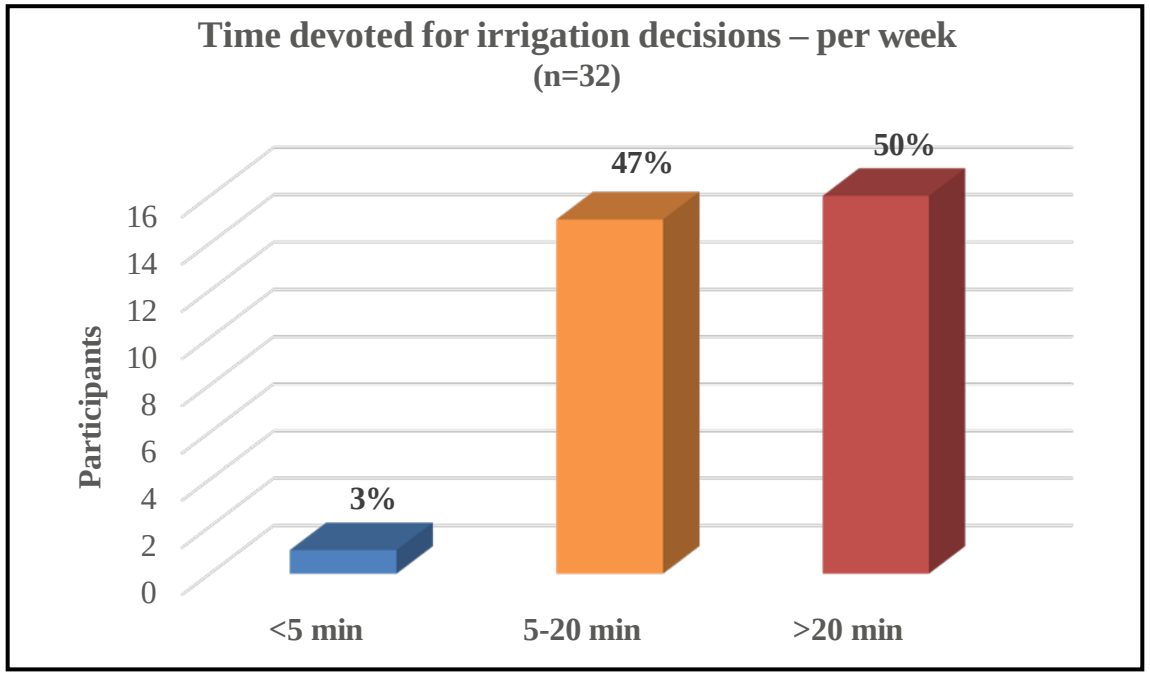

**Bordertown** and **Padthaway** are **not** included into the graph.
**Median:** 9 T/ha

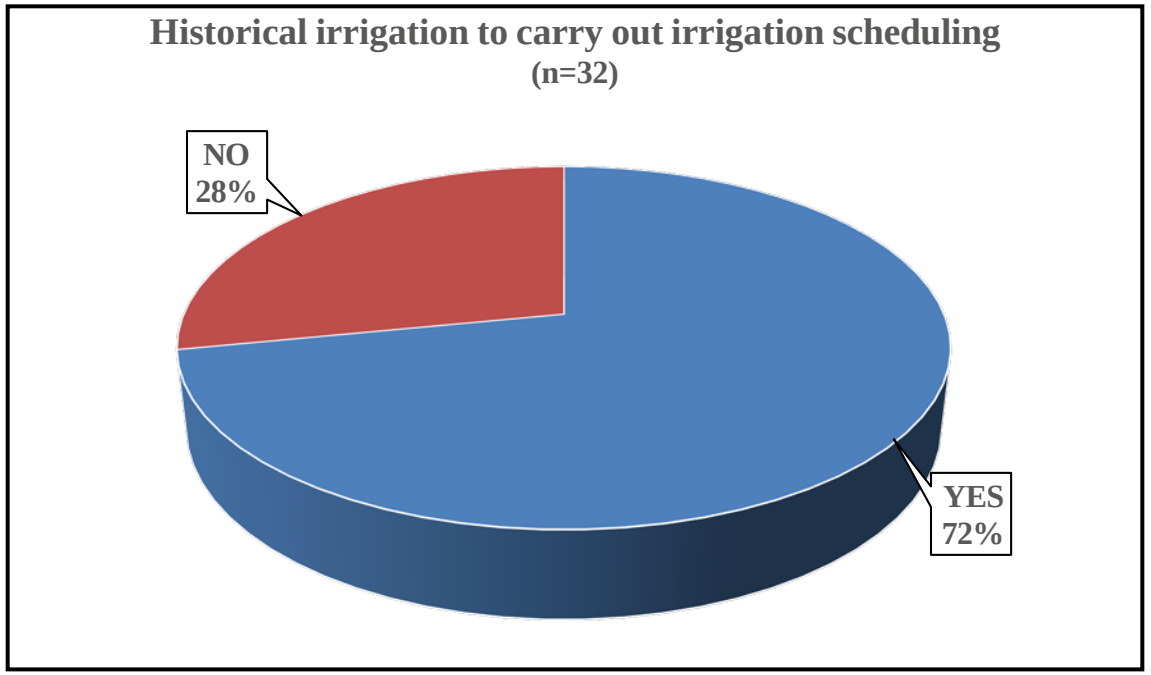
# Irrigation system type



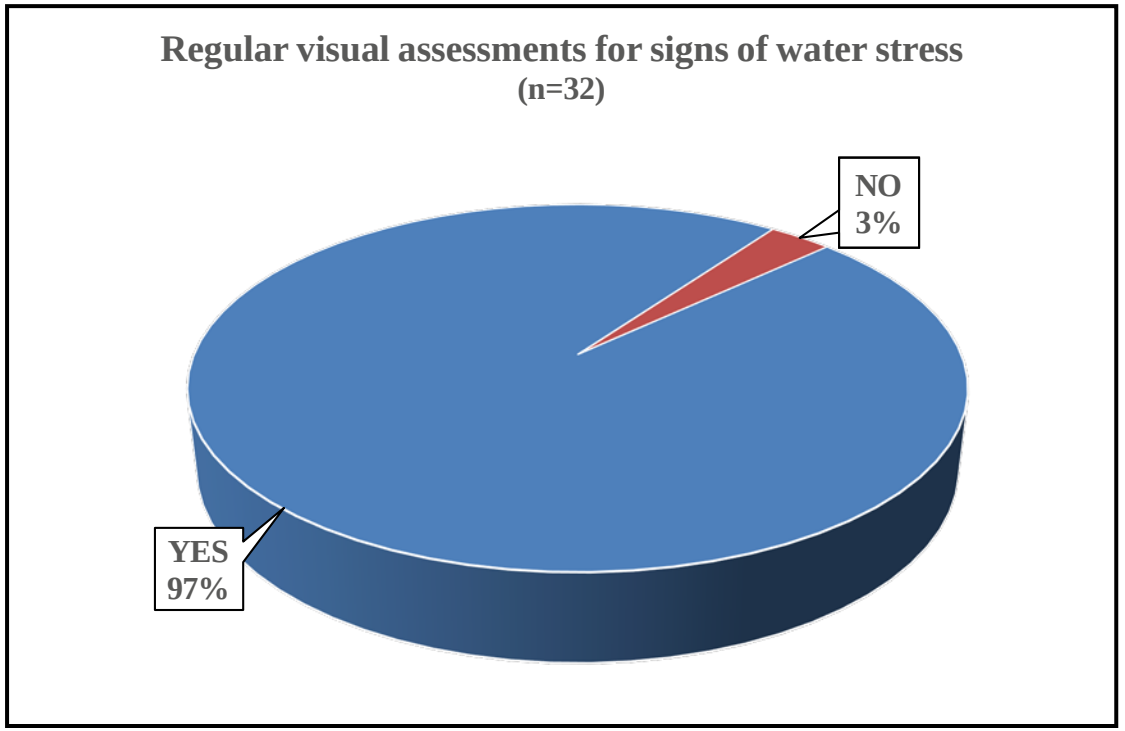



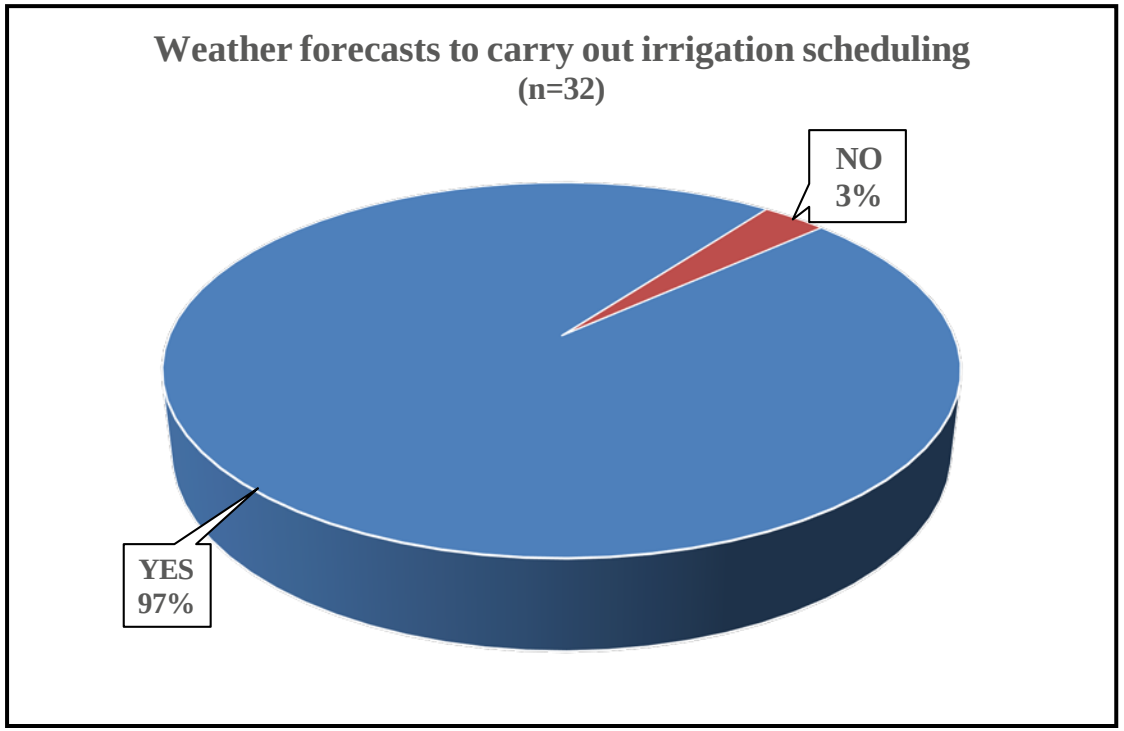
# Irrigation Decision-making (time, method)



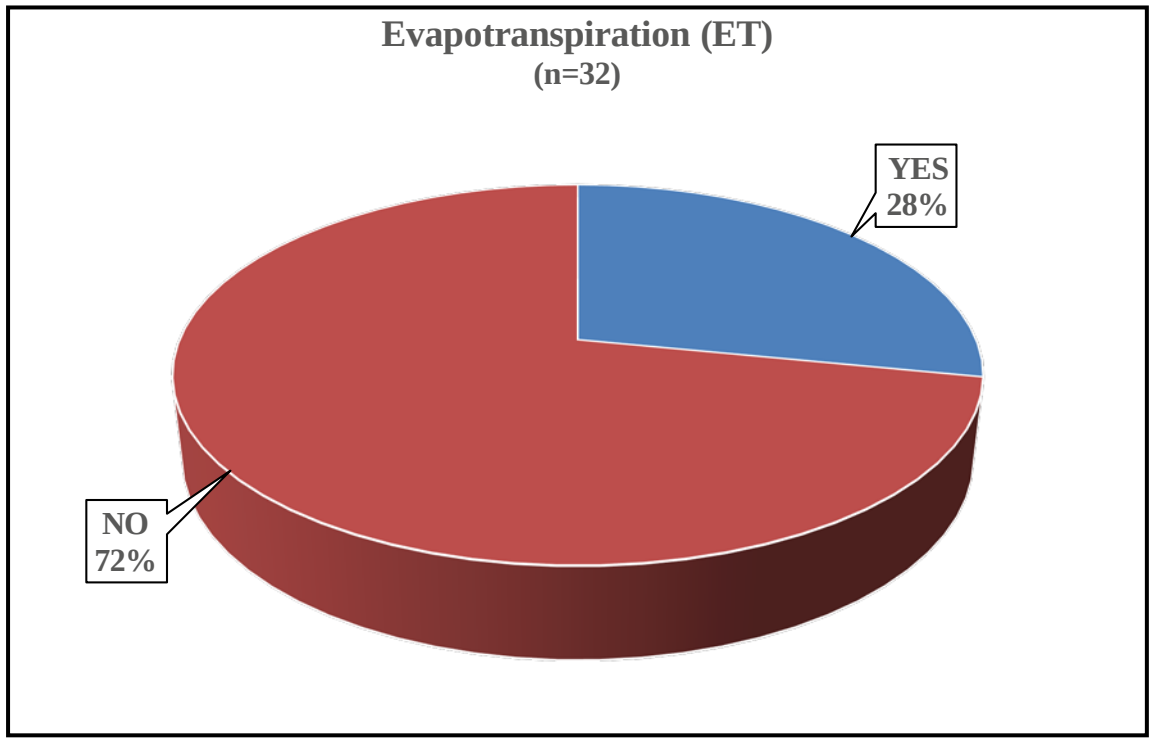



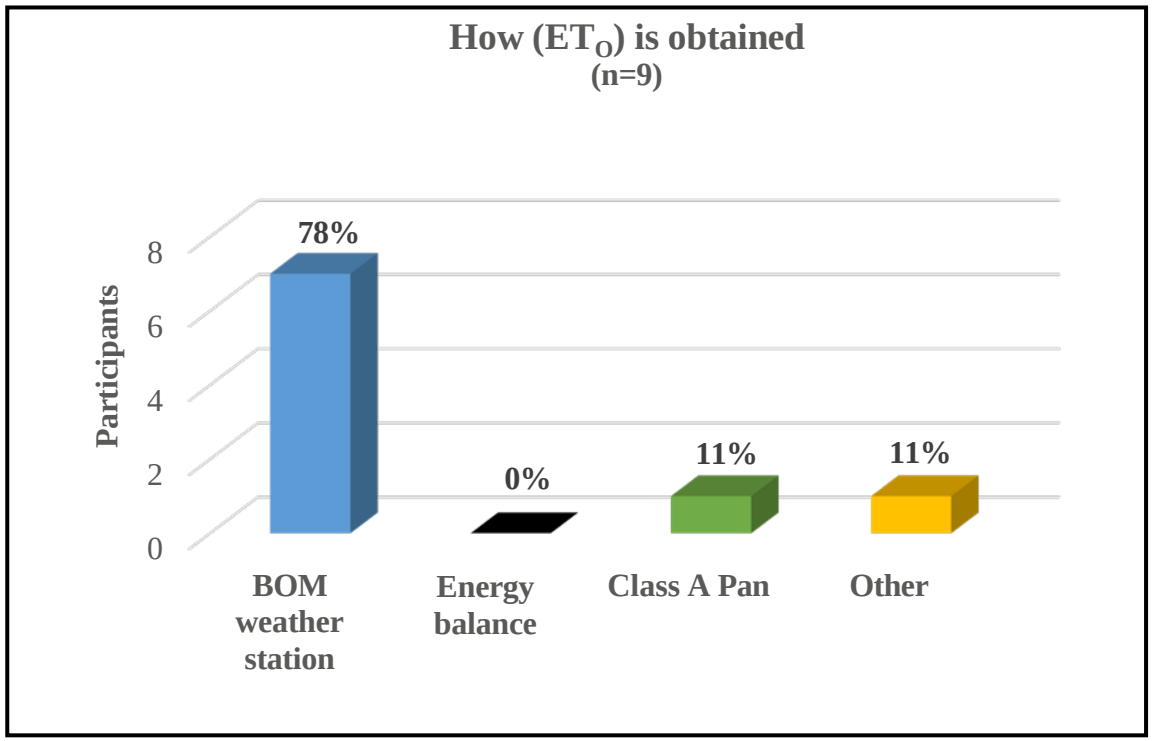
# Irrigation Scheduling
## Use of Soil moisture and weather forecasts



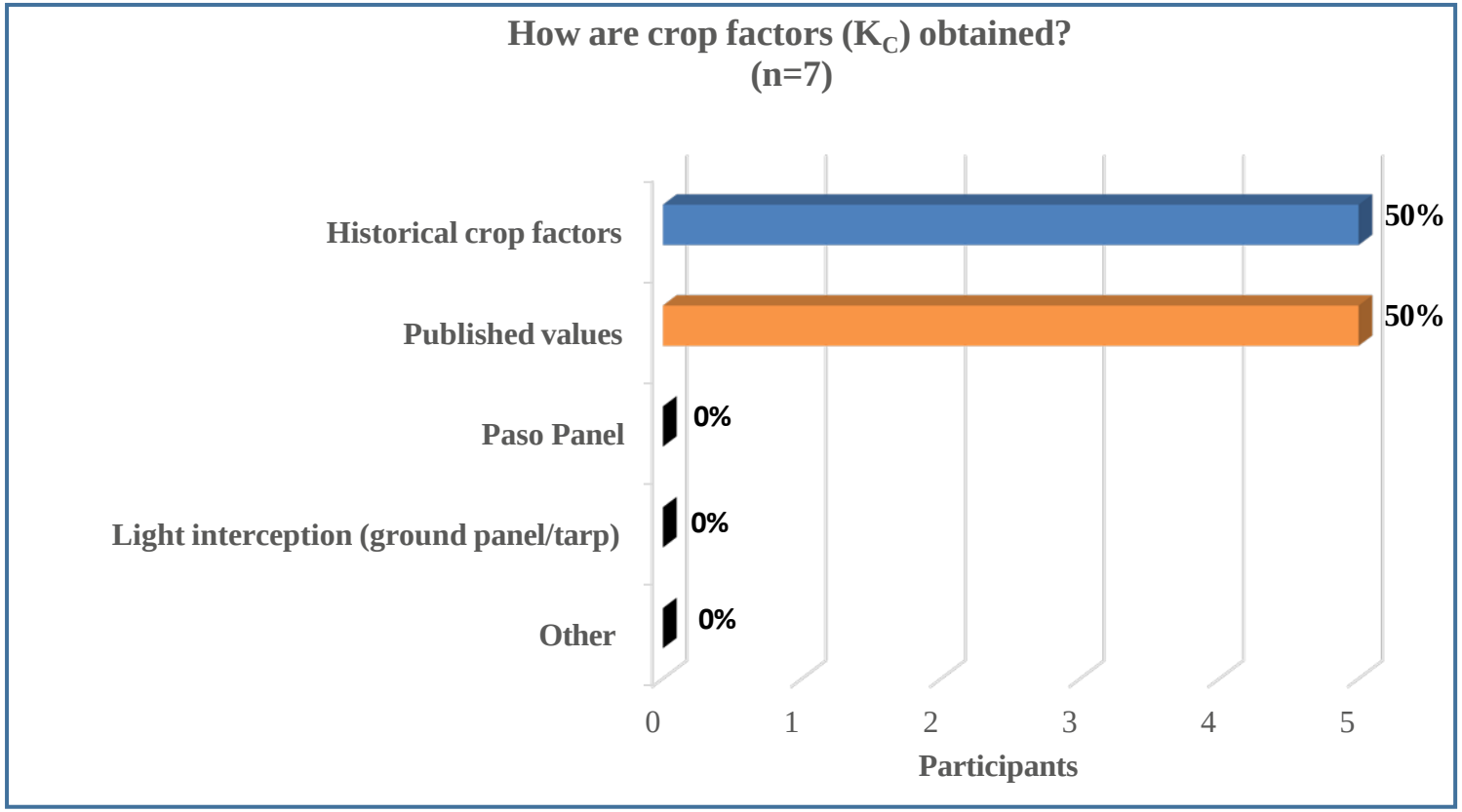



# Irrigation Scheduling
# Use of Evapotranspiration - ET

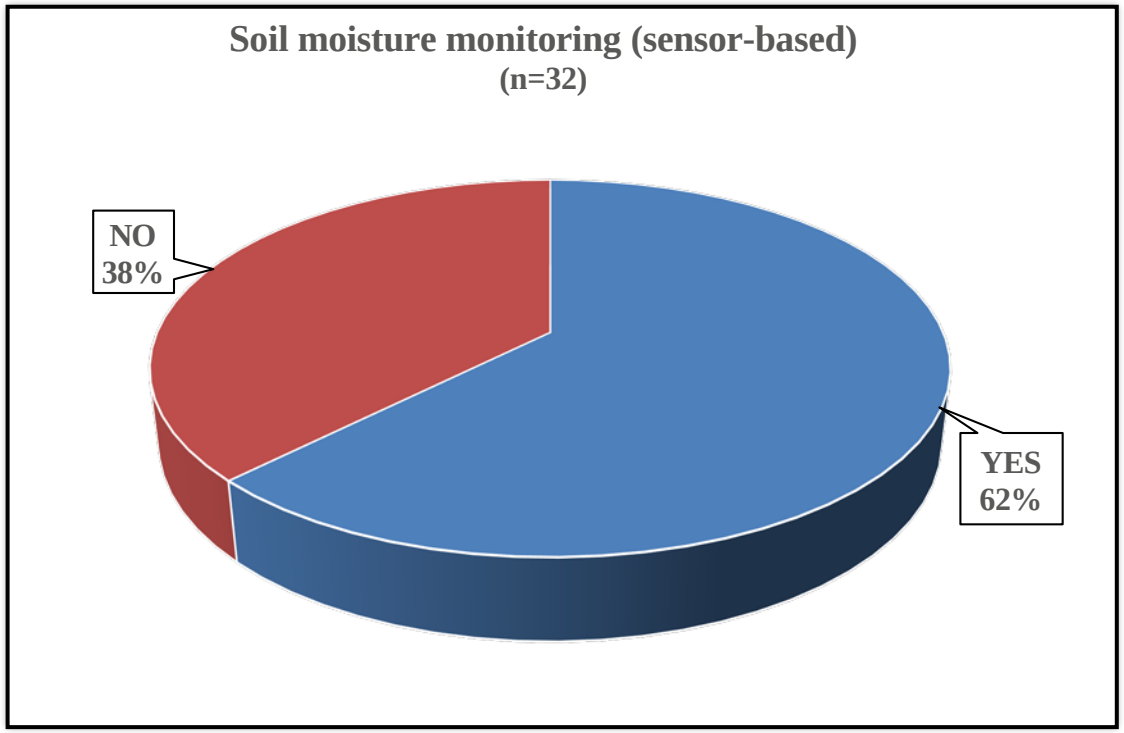


# Irrigation Scheduling
# Use of Evapotranspiration – ET – Crop Factors

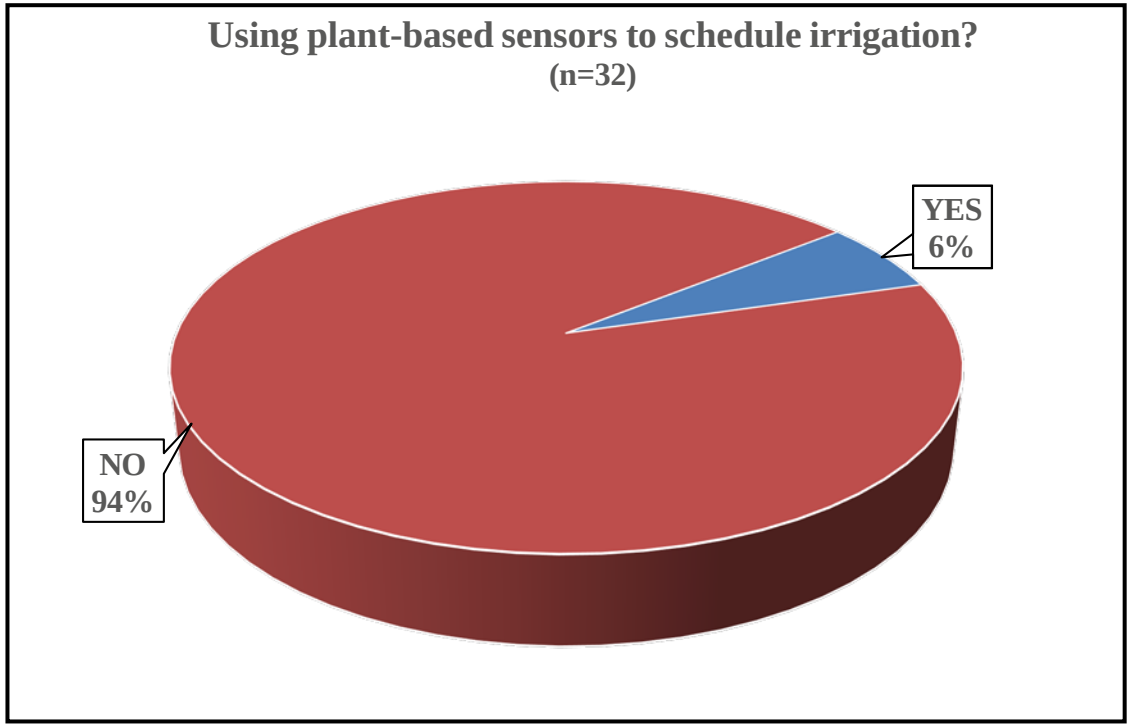


# Irrigation Scheduling
# Use of Soil moisture sensors



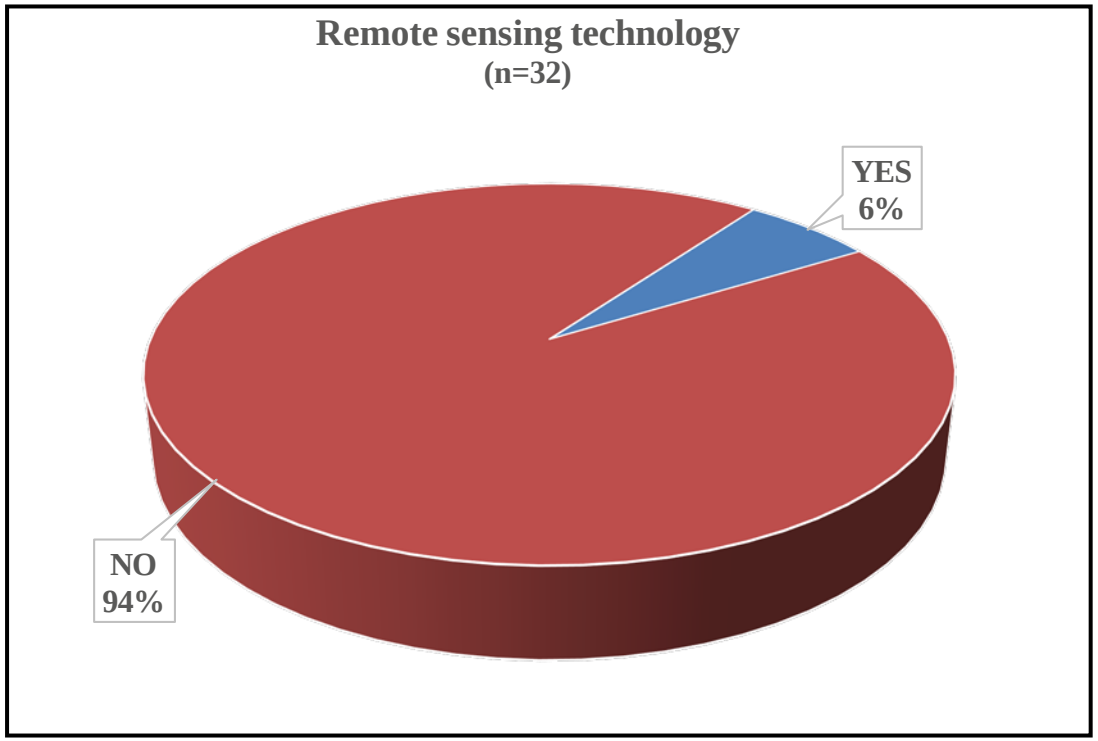

- **From 62% using soil moisture (n=20);**
  **51 sensors:** Soil water tension (e.g. gypsum blocks, tensiometers) **(n=3)**
  **133 sensors:** Volumetric water content (e.g. capacitance probes) **(n=17)**

# Irrigation Scheduling
# Use of plant-based sensors



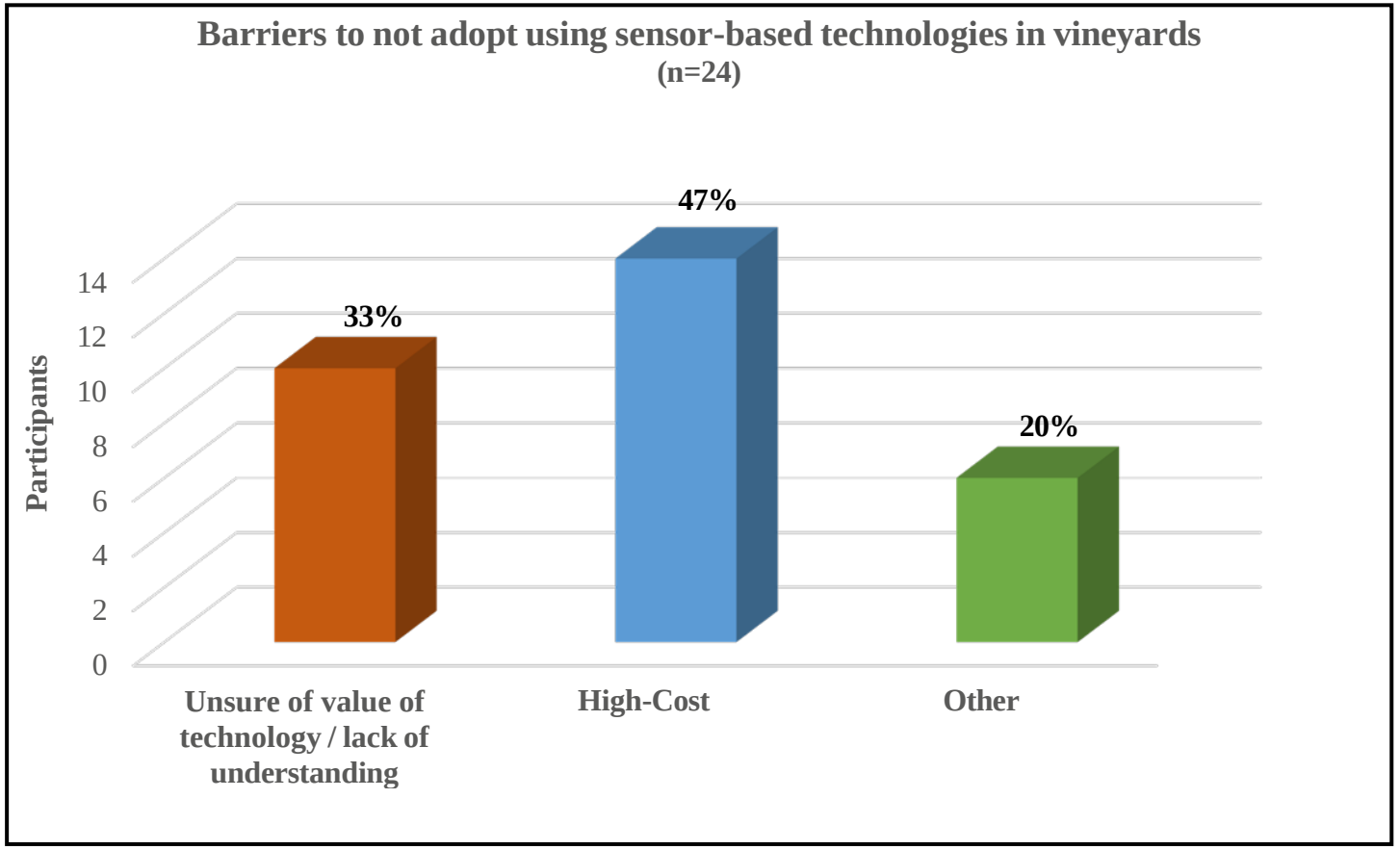

- **1 grower** using leaf/canopy temperature sensor for PWS
- **1 grower** using sapflow sensors for PWS

# Irrigation Scheduling
# Use of Remote Sensing



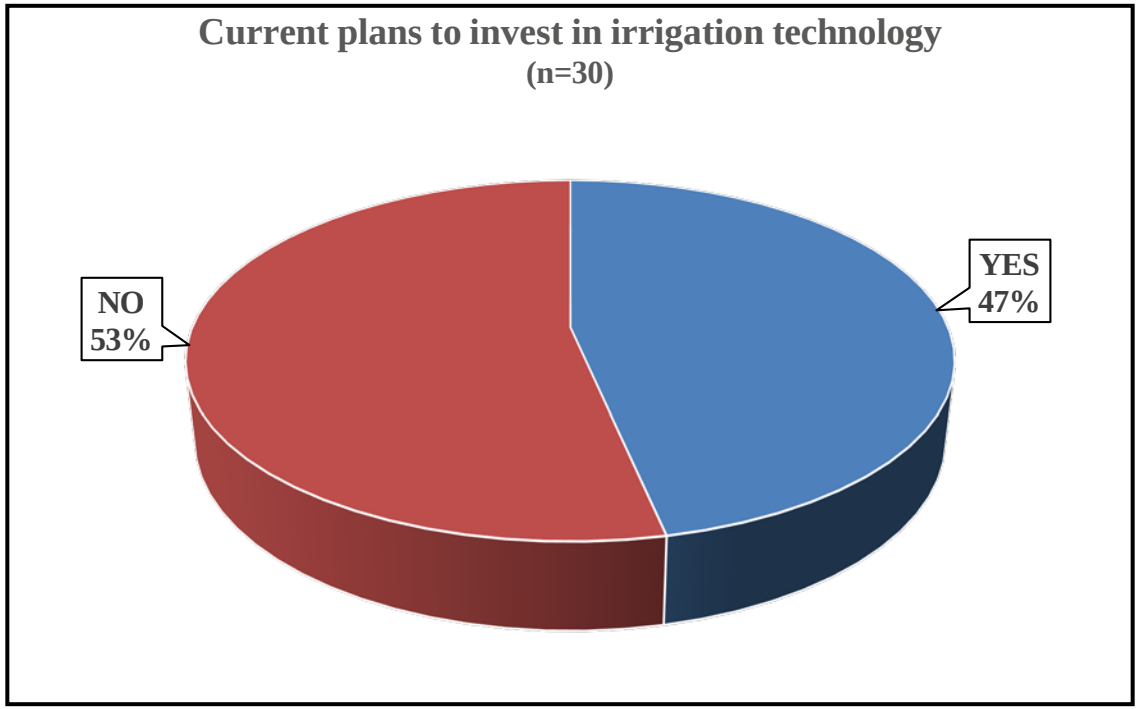

- **2 growers** using satellites

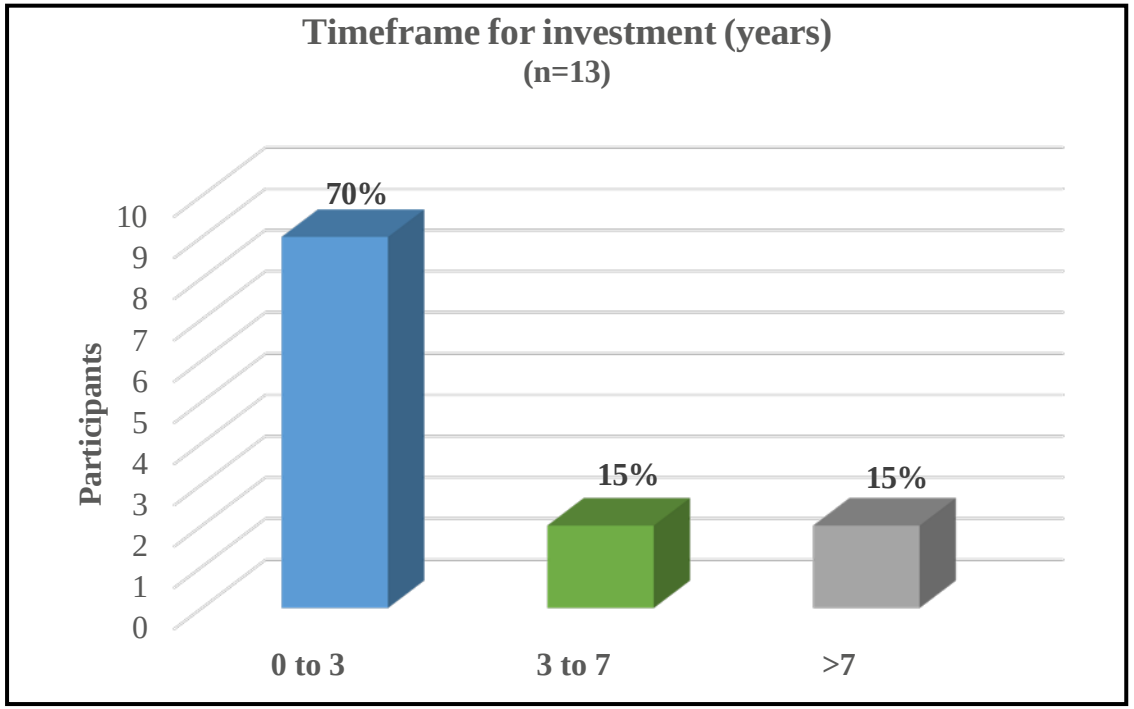
# Adoption of AgTech - Barriers



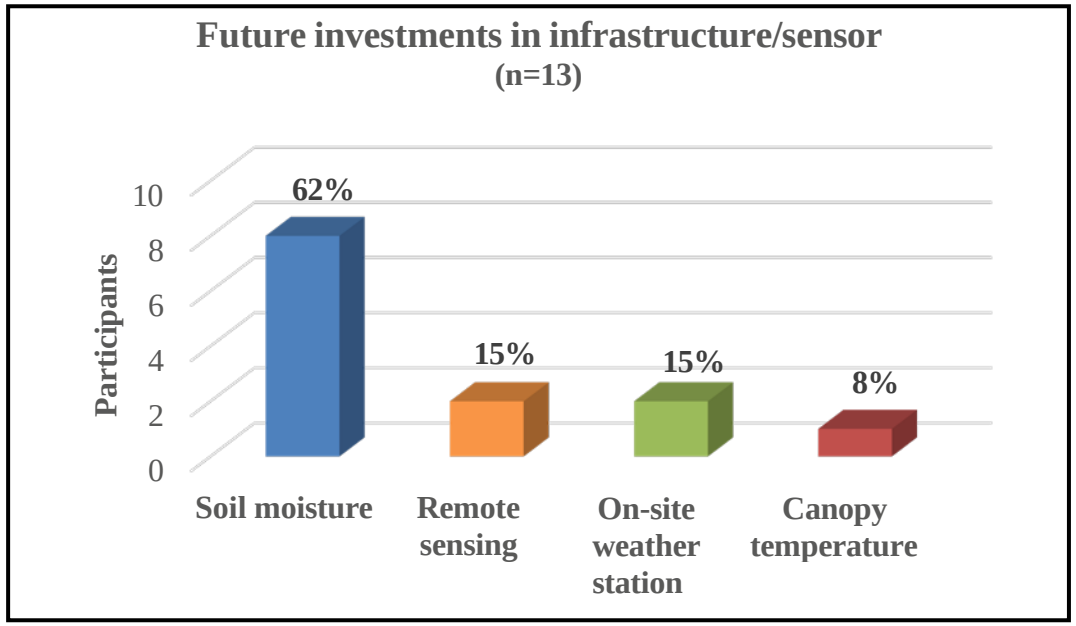

***Other/Comments:** **"**Use in combination with other devices", "Easy to find information", "Nothing replaces feet in the vineyard", "Use of shovel and boot".

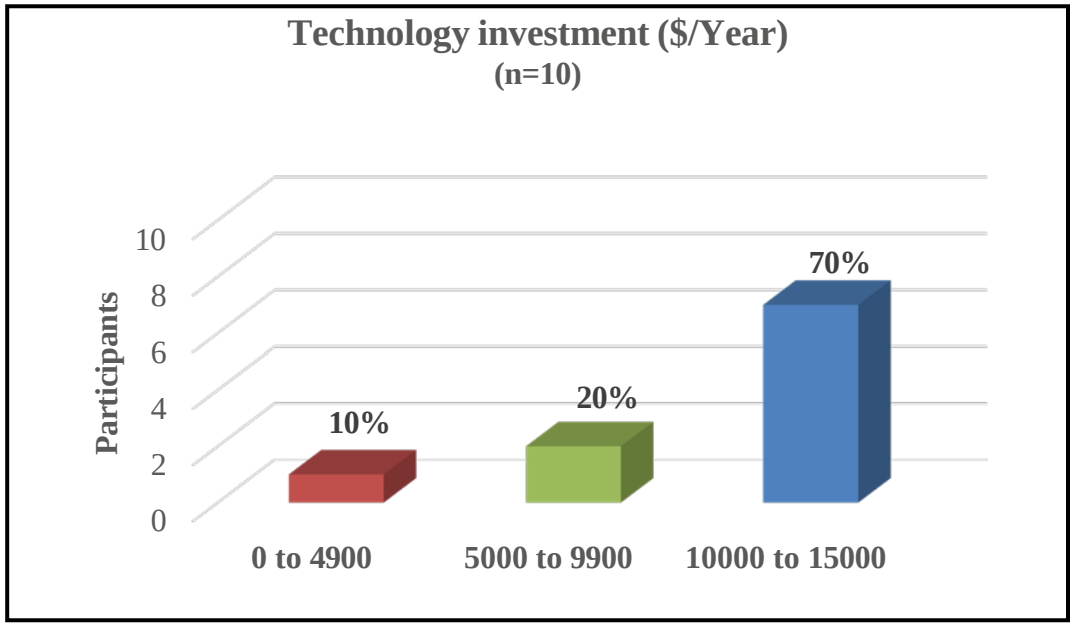
# Adoption of AgTech – Investment Plans



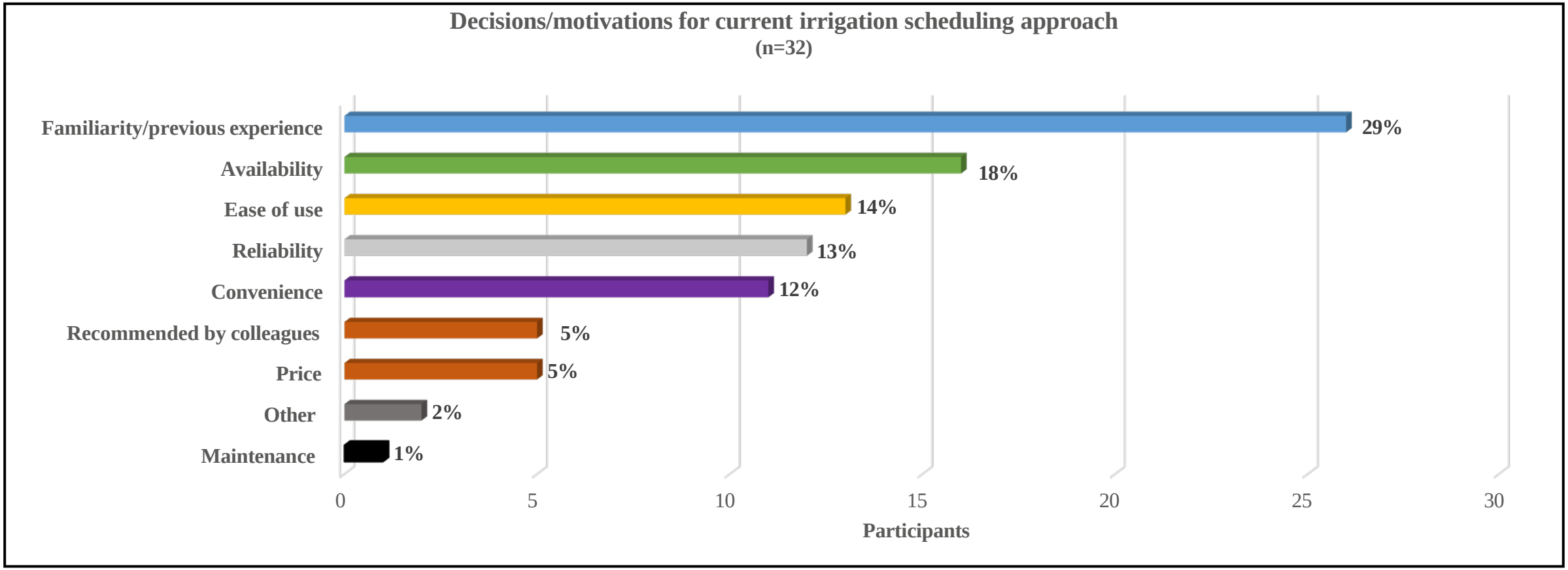



# Adoption of AgTech – Future Plans



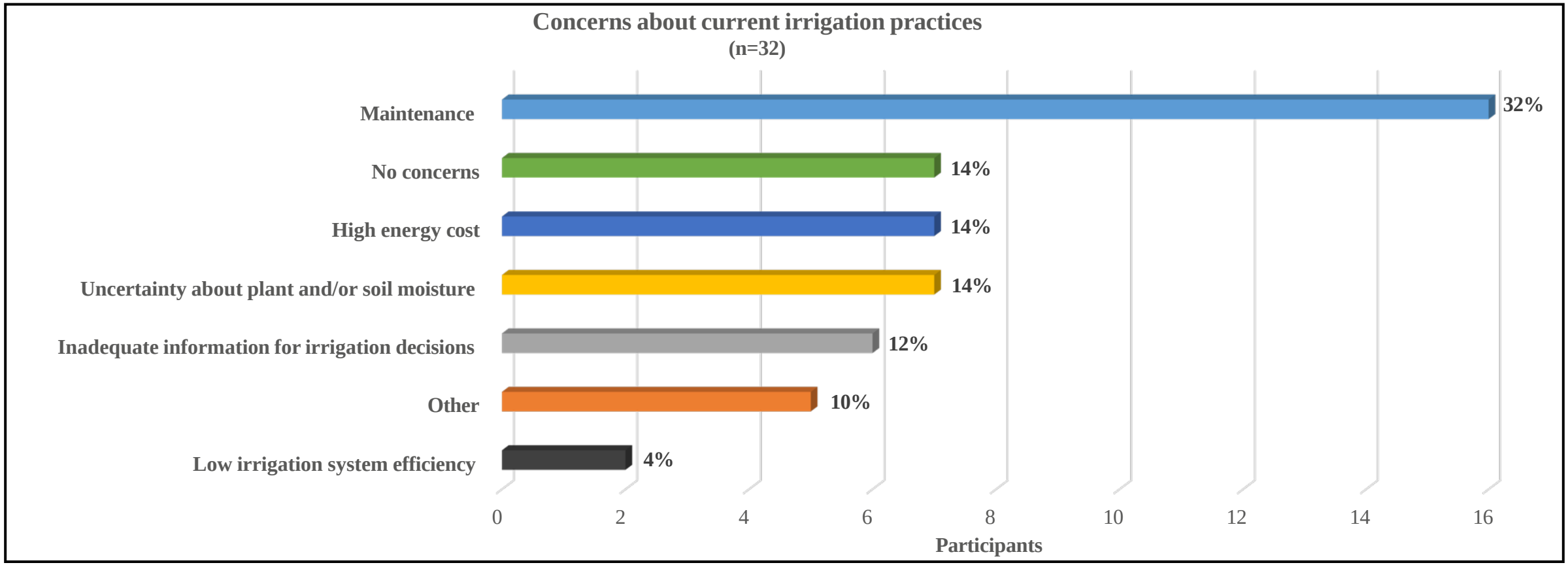



# Motivation to continue current irrigation approach



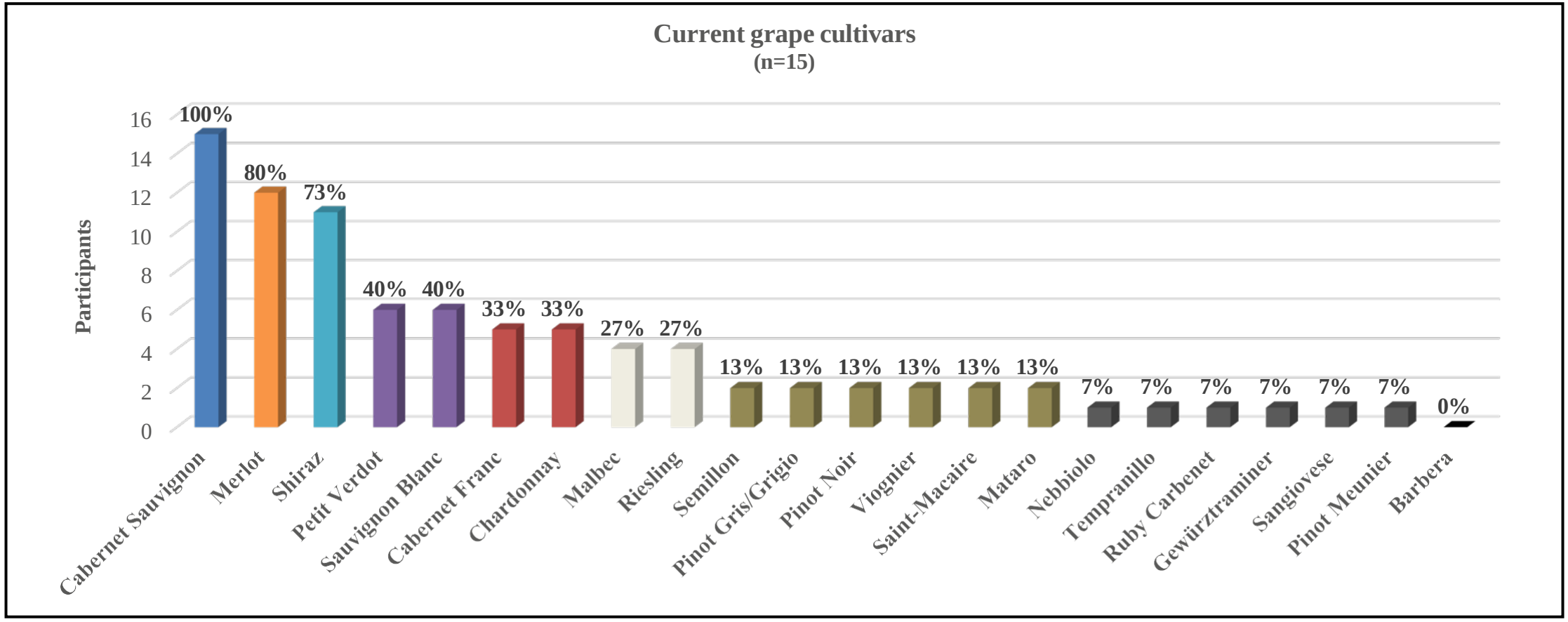

**Other/Comments:** "It was what was here when we purchased 6 years ago", "Employ a water monitoring company to do the scheduling recommendations"

# Irrigation Scheduling – Concerns




***Other/Comments:** "Sensors often getting damaged or failing", "We feel the monitoring is sometimes giving us information which may be pushed towards the high end of the vine's needs", "Employing a water monitoring company is quite costly", "Looking to maximise water use efficiency while trying to minimise actual volume used", "Salinity & water availability in a changing climate", "We run high stress levels , there is a fine line in running high stress levels if the weather pattern is unstable".

# Limestone Coast – Cultivars (from survey responses)



# Additional responses received for Coonawarra and Mount Benson

- **Variety:** Cabernet Sauvignon, Merlot, Shiraz and Chardonnay
- **Median size area:** 7.75 ha **Range:** 0.1 to 45 ha
- **Soil type**: Terra rossa and Rendzina
- **Regions:** Coonawarra and Mount Benson
- **Median vine age:** 24 years **Range:** 7 to 35 years
- **Average vine density:** 1908 vines/ha **Range:** 1580 to 2424 vines/ha
- **82%** do not use deficit irrigation regimes, **18%** using RDI regimes for deficit irrigation **No SDI used**
- **Median irrigation volumes:** 12.5 mm/week **Range**: 6 to 16 mm/week
- **Irrigation frequency:** 1 to 4 per week
- **Seasonal irrigation applied:** 0.2 to 3.0 ML/ha (Mount Benson average 2.75 ML/ha)
- **Annual farmgate value of winegrapes ($/tonne):** approx $2000 **Range:** $1100 to $5000

# Ground, Proximal and Remote Sensing Techniques for Precision Irrigation of Vineyards

Deepak Gautam [1], Vinay Pagay [1], Catherine Kidman [2], Stephen Tyerman [1], Bertram Ostendorf [3], Chris Brodie [4], Richard Muhlack [1], Kerry Wilkinson [1] and David Jeffery [1]

[1] School of Agriculture, Food and Wine , Waite Campus, the University of Adelaide, SA., [2] Treasury Wine Estates, Wynns Coonawarra Estate, Coonawarra, SA., [3] School of Biological Sciences, North Terrace Campus, the University of Adelaide., [4] Wingara Wine Group Pty Ltd, Katnook Coonawarra Estate, Coonawarra, SA.

Australian Government
Wine Australia

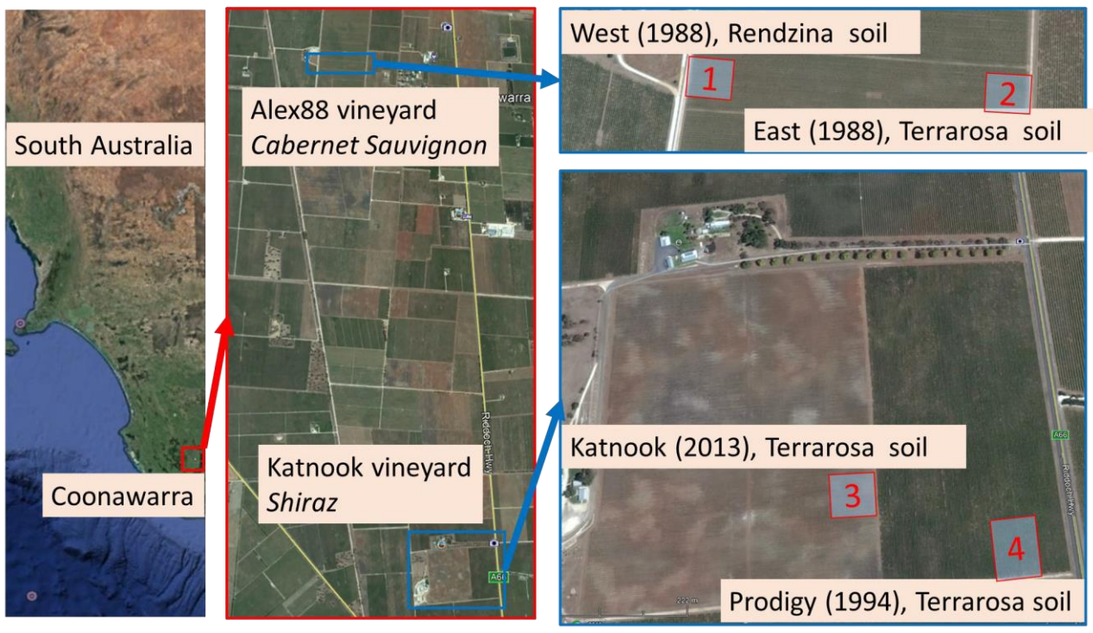
## Introduction

Precision irrigation to save water, make better wine, and increase the profitability of vineyards.



## Test sites

Cabernet Sauvignon and Shiraz at Coonawarra, the premium wine region of South Australia, are studied.




## Experimental design

Each test site includes four irrigation treatments with two replication blocks.

**Precision irrigation experimental design**

| Rows | | Replication block #1 | | | | | | | | Replication block #2 | | | | | | | |
|---|---|---|---|---|---|---|---|---|---|---|---|---|---|---|---|---|---|
| 1 | | | | | | | | | | | | | | | | | |
| 2 | | W | * | M | M | M | M | | | | | M | M | M | M | | |
| 3 | | | | | | | | | | | | | | | | | |
| 4 | | | | | | | | | | | | | | | | | |
| 5 | | | | | | | | | | | | | | | | | |
| 6 | | W | * | M | M | M | M | | | | | M | M | M | M | | |
| 7 | | | | | | | | | | | | | | | | | |
| 8 | | | | | | | | | | | | | | | | | |
| 9 | | | | | | | | | | | | | | | | | |
| 10 | | W | * | M | M | M | M | | | | | M | M | M | M | | |
| 11 | | | | | | | | | | | | | | | | | |
| 12 | | | | | | | | | | | | | | | | | |
| 13 | | | | | | | | | | | | | | | | | |
| 14 | | W | * | M | M | M | M | | | | | M | M | M | M | | |
| 15 | | | | | | | | | | | | | | | | | |
| Vines-> | 1 | 2 | 3 | 4 | 5 | 6 | 7 | 8 | 9 | 10 | 11 | 12 | 13 | 14 | 15 | 16 | 17 |

M Measurement/sentinel vine
W Water meter
* Soil moisture sensor
Conventional treatment
Evapotranspiration treatment
Plant water status treatment
Soil water status treatment



The terrarossa soil type

## Proximal and ground sensing

Using proximal and ground sensors, following measurements are made throughout the season: pre-dawn leaf water potential ($\psi_{pd}$), mid-day stem water potential ($\psi_{stem}$), canopy conductance ($g_s$), net photosynthesis ($p_n$), soil moisture, leaf area index (LAI), crop coefficient ($k_c$), porosity, canopy temperature, in bunch temperature, and meteorological data (daily temperature, humidity, precipitation, wind, solar radiation), etc.

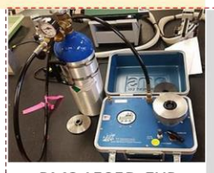
**Plant water status**



*LI-COR LI-6400XT Portable Photosynthesis System ($g_s$, $p_n$, F)*



*Decagon SC-1 leaf porometer ($g_s$)*



*PMS 1505D-EXP Pressure chamber ($\Psi_{stem}$, $\Psi_{soil}$)*



*Soil moisture probe*

Soil water status

**Light measurement**



*AccuPAR LP-80 ceptometer (porosity)*

*Paso panel (LAI, $k_c$)*

**Network of proximal sensors**



*Ground network of thermography towers via LoRaWAN gateway for cloud-based monitoring (RH%, Ambient T, Shade T)*

**Meteorological**



*Weather station (T, RH%, PAR, rain, wind)*




*Tinytag (RH%, T)*

## Remote sensing

Remote thermal and multispectral (including visible) data is acquired at critical phenology stages of the plant.

**Platforms**



DJI Matrice 600 Pro

**Remote sensors**



Sony Alpha 7R III



MicaSense RedEdge-M



FLIR Tau2 640

**Map georeferencing**



Custom GCPs



Surveying pegs

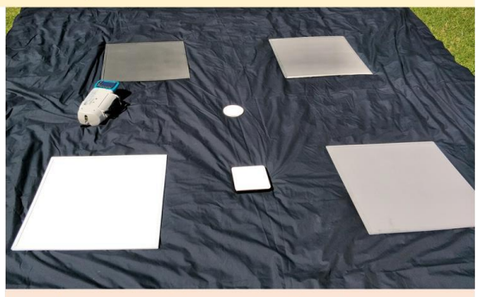
**Multispectral/Thermal calibration**



FFC blackbody



FLIR Fluke gun



Multispectral/thermal calibration panels, spectralon and spectroradiometer

## Data collection stages



1. Flowering



2. Peppercorn



3. Pea size



4. Pre-veraison



5. Veraison



6. Post-veraison#1

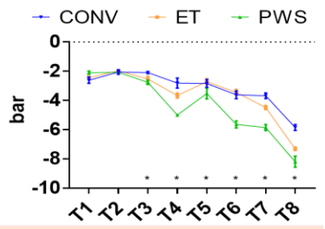


7. Post-veraison#2

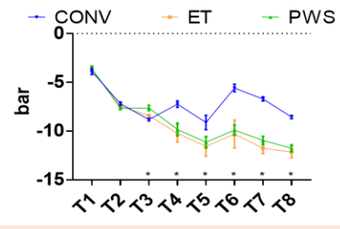


8. Pre-harvest

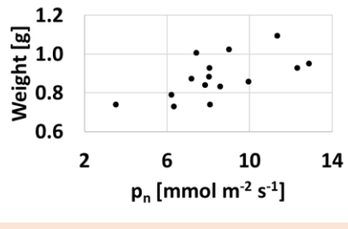
## Preliminary results (season 1)



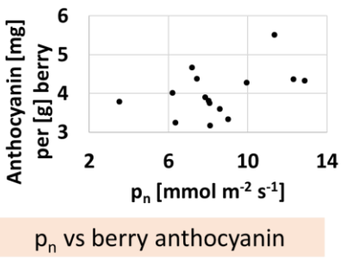

Seasonal pre-dawn $\psi_{leaf}$



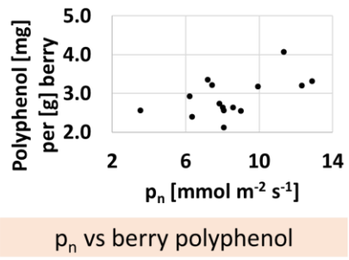

Seasonal mid-day $\psi_{stem}$



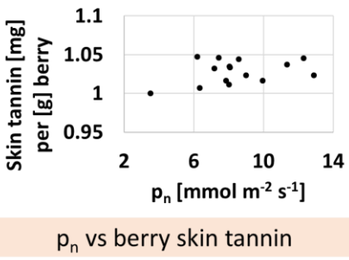

$p_n$ vs berry weight




$p_n$ vs berry anthocyanin




$p_n$ vs berry polyphenol




$p_n$ vs berry skin tannin

## Conclusion and future work

- The irrigation treatment appears to stand out at later season.
- The post-veraison net photosynthesis appears to be strong covariate of berry size and berry quality parameters.
- Thermal and multispectral remote sensing will be used to predict the water status, yield, and wine quality parameters
- Mechanistic and/or machine learning models will be incorporated with remote sensing for spatial/temporal prediction.

## Get in touch

*Dr Deepak Gautam*
*Email: Deepak.Gautam@adelaide.edu.au*

References

1. Bellvert, J., Zarco-Tejada, P.J., Marsal, J., Girona, J., González-Dugo, V. and Fereres, E., 2016. Vineyard irrigation scheduling based on airborne thermal imagery and water potential thresholds. *Australian Journal of Grape and Wine Research*, *22*(2), pp.307-315.
2. Espinoza, C.Z., Khot, L.R., Sankaran, S. and Jacoby, P.W., 2017. High resolution multispectral and thermal remote sensing-based water stress assessment in subsurface irrigated grapevines. *Remote Sensing*, *9*(9), p.961.